# Modeling and Analyzing the Effects of Operating Constraints on Pricing Signals in the Competitive Electricity Market

by

Chaminda Amarasinghe

A dissertation submitted to the Faculty of Graduate Studies in partial fulfillment of the requirements for the degree of

Doctor of Philosophy

The Department of Electrical and Computer Engineering

The University of Manitoba

Winnipeg, Manitoba, Canada

THE UNIVERSITY OF MANITOBA

FACULTY OF GRADUATE STUDIES

*****

COPYRIGHT PERMISSION

# Modeling and Analyzing the Effects of Operating Constraints on Pricing Signals in the Competitive Electricity Market

BY

Chaminda Amarasinghe

A Thesis/Practicum submitted to the Faculty of Graduate Studies of The University of

Manitoba in partial fulfillment of the requirement of the degree

Of

Doctor of Philosophy

To my parents

## Acknowledgements

I would like to express my deep appreciation and gratitude to Dr. Udaya Annakkage for his continuous advice, guidance and encouragement throughout the research work. It has always been a pleasure working under his guidance. I greatly appreciate the advice and assistance received from Dr. Ani Gole. I am also grateful to Dr. Alan Wang of Manitoba HVDC Research Center for useful inputs. I must also thank the technical staff at the Department of Electrical and Computer Engineering, especially Mr. Erwin Dirks for his support.

Conducting this work would have not been possible without the financial support received from Manitoba Hydro, Manitoba HVDC Research Center, Faculty of Graduate Studies at the University of Manitoba, and National Science and Engineering Research Council.

I must also express my gratitude to the management of the Manitoba HVDC Research Center, specially to the managing director Mr. Paul Wilson, for providing their facilities to carry out a part of this research, in addition to the financial support. Also, I would like to thank all my friends in the Power Tower and the staff of the Department of Electrical and Computer Engineering for their continuous encouragement and for making my years at the University of Manitoba a pleasant one.

This acknowledgement would not complete without thanking my family. I extend my heartfelt gratitude to my parents for their support and encouragement throughout my life. A very special thank to my sister for all the love and support over the years. Last but not least I would thank my wife for guiding me to achieve my goals, and my little son for keeping me happy all the time.

Chaminda Amarasinghe

December 2007

# Abstract

In a competitive electricity market, market signals are the main driving forces or the incentives for the market participants to make their operational and investment decisions. Locational Marginal Prices (LMP) are the only prevailing market signals, and are determined using an Optimal Power Flow (OPF) program.

The present practice is mainly focus on real power dispatch by solving a LP-OPF together with LMP based settlement. Acquiring the required reactive power & other ancillary services, and ensuring the security (both static and dynamic) are performed subsequently, which may result in curtailments to the already agreed optimal real power dispatch. With such a dispatch mechanism, the resulting market signals are also impaired. Thus, correct market signals can only be analyzed, if the related constraints are suitably modeled in the OPF.

This thesis analyzes market signals after incorporating two such important constraints; reactive power and security issues into market dispatch. First, a reactive power model is proposed to suit the requirements of the competitive electricity market and is incorporated into the OPF. The recently proposed transient stability boundary is then used as a constraint in the OPF to ensure the secure operation of the system.

In determining market signals, the recently proposed method of analysis of LMP components is first presented. The network rental, which is the surplus collected by the system operator due to LMP based settlement of transactions, is then proposed as a method in market signal analysis by decomposing the network rental. The key advantage is that network rental components show how each consumer has actually overpaid due to each binding constraint and losses in a detailed manner, which is argued to be a supplementary pricing signal especially from the consumer's perspective.

Finally, implementation of a software tool using $C^{++}$ to solve the OPF and extend it to incorporate the above market signal analysis methods is achieved. This allows market signals to be readily available along with the optimal dispatch. The potential of the proposed components of network rental in market signal analysis together with

the suitability of the proposed models in market dispatch are evaluated for different case studies using the developed software tool.

# List of Principal Symbols

All notations and most of the terms used in the thesis are described in this section. The remaining terms are explained as they first appear in the text for the convenience in understanding.

| | |
|---|---|
| $i$, $j$ | node (bus) number |
| $k$ | generator bid number |
| $P$ | real power |
| $Q$ | reactive power |
| $g$ | generation |
| $D$ | demand |
| $P_{gi}$ | real power generation at bus $i$ |
| $Q_{gi}$ | reactive power generation at bus $i$ |
| $P_{Di}$ | real power demand at bus $i$ |
| $Q_{Di}$ | reactive power demand at bus $i$ |
| $B$ | bid |
| $B_i$ | set of all bids at bus $i$ |
| $P_{ik}^{B}$ | real power bid quantity of the $k^{th}$ real power bid at bus $i$ |
| $P_{ik}$ | real power dispatched from the $k^{th}$ bid at bus $i$ |
| $S$ | price |
| $S_{ik}^{B}$ | bid price of the $k^{th}$ real power bid at bus $i$ |
| $S_{i}^{Q}$ | reactive power cost of generator at bus $i$ |
| $I$ | set of all buses |
| $B_i$ | set of all bids at bus $i$ |
| $P_i$ | real power injection at bus $i$ |
| $Q_i$ | reactive power injection at bus $i$ |
| $Q_{g1i}$ | Block 1 (i.e., free) reactive power from the generator at bus $i$ |
| $Q_{g2i}$ | Block 2 (i.e., non-free) reactive power from the generator at bus $i$ |

| | |
|---|---|
| $Q_{gi}^{max}$ | maximum reactive power from the generator at bus $i$ |
| $Q_{gi}^{min}$ | minimum reactive power from the generator at bus $i$ |
| $T$ | set of all transmission lines |
| $T_i$ | set of all transmission lines connecting to bus $i$ |
| $t$ | transmission line |
| $V_i$ | voltage magnitude of $i^{th}$ bus |
| $\theta_i$ | voltage angle of $i^{th}$ bus |
| $\theta_{ij}$ | voltage angle difference between voltages of buses $i$ and $j$ |
| $g_{ij}$ | conductance of the line connected between buses $i$ and $j$ |
| $b_{ij}$ | susceptance of the line connected between buses $i$ and $j$ |
| $PF_{ij}$ | real power flow along the line connected buses $i$ and $j$ |
| $PF_{ij}^{L}$ | real power loss along the line connected buses $i$ and $j$ |
| $P^L$ | real power loss in the system |
| $Q^L$ | real power loss in the system |
| $L$ | Lagrangian equation |
| $max$ | maximum limit |
| $min$ | minimum limit |

| | |
|---|---|
| $\lambda$ | real power LMP at the reference bus |
| $\sigma$ | reactive power LMP at the reference bus |
| $\lambda_i$ | real power LMP at bus $i$ |
| $\sigma_i$ | reactive power LMP at bus $i$ |

The Greek symbols $\mu$, $\beta$, $\alpha$, $\gamma$, $\phi$, $\psi$ and $\eta$ with suitable subscripts are used to denote the Lagrange multipliers associated with the equality and inequality constraints of the Optimal Power Flow problem.

# Table of Contents

# List of Figures

# List of Tables

# Chapter 1

# Introduction

Electricity industry restructuring during the last two decades has made drastic changes to the traditional electricity structure and will continue for the next several decades. In the past, the electric power industry has been either a government-controlled or a government-regulated industry (i.e., single owner), which existed as a monopoly where the overall authority in generation, transmission, and distribution of power are within its domain of operation. Everyone including household, businesses, and industries were required to purchase their electricity from their local monopolistic power company. This was not only a legal requirement, but also the only source they had to rely on to fulfill their day to day requirements.

The restructuring has led the traditional electricity industry to become a competitive electricity market. The main driving forces for these reforms are due to economic inefficiencies and consumer dissatisfaction associated with the single owned electricity industry. Since electricity is an essential source of energy for everyone and due to its unique characteristics such as un-storability and lack of flexibility in controlling the power flow in transmission lines, the whole process of restructuring is a challenging and complex task [1].

Over the past two decades, however, countries have begun to split up these monopolies in favor of competitive markets to introduce commercial incentives in generation, transmission, and distribution. The main goals under a competitive market design are

efficient and reliable operation of the power system together with market incentives for all the participants [2]. This is done by creating competition between participants in the electricity market with open access.

## 1.1 Characteristics of Electricity Markets

The process of restructuring that led to electricity markets are not the same in all countries due to economic, political, and other local differences [3]. As a result, newly formed markets have taken different forms to suit their individual requirements. In some markets, competition is only among suppliers while in others both suppliers and consumers compete. Some markets are compulsory and others are voluntary. Some markets only trade real power and some trade reserves, reactive power and other ancillary services, with real power. Some markets use pool-based systems and others use bilateral contracts. While some markets use full nodal pricing, and others use zonal pricing arrangements, some use uniform prices. In some markets, settlement is only based on a real time market, whereas some others use forward markets in addition to the real time market.

However, there is a common basis and some similar characteristics that can be found in all competitive electricity markets. Generally, generation, transmission, and distribution services are the responsibilities of different companies in order to create the competition. Normally, the wholesale market is pool-based in nature with the provision for bilateral contracts. This means that all suppliers (i.e., generators) sell energy to a pool and consumers buy energy from that pool by bidding to the market (bid/quantity pairs). Furthermore, there can be financial contracts between participants outside the electricity market on long-term basis. Such long-term contracts are agreements between participants to mitigate or share the risk associated with price volatility due to the change in supply and demand conditions [4]. While generation and demand sides are competitive, the transmission remains a monopoly. The huge cost of investing in the transmission network as well as geographical reasons do not

allow the transformation of this service into a competitive market. In order to ensure open and fair access, the grid and the wholesale energy market are operated by an independent entity with no direct interests in the energy business. This entity is commonly known as the Independent System Operator (ISO) and is responsible to achieve the above-mentioned goals while maintaining the security and the quality of the supply.

One of the key concerns to any restructured market is the ability to operate the transmission system in a manner that is fair to all participants. In USA, the Federal Energy Regulatory Commission (FERC) oversees issues involving the transmission system. FERC presently believes that the only way in which everyone will be on a competitive environment is to create open access to all the participants. As stated in its white paper [5] on Standard Market Design (SMD), participants in wholesale power markets will have non-discriminatory open access to the transmission system. Further, it proposes Locational Marginal Pricing (LMP) as a way of settling the transactions between the participants. This is further insisted upon in their recent documents, subsequent to the SMD white paper [6], [7]. This pricing scheme is also called "nodal pricing" and the concept of nodal pricing was proposed in [8] long before the restructuring of the electricity industry started. LMP is the marginal cost of supplying the next increment of a quantity at a specific bus, considering marginal cost of generation and physical aspects of the transmission system. Due to operating the power system at limiting values of the constraints imposed by the physical and operational limits, which are commonly known as 'binding constraints', and due to the transmission losses, there exist different LMPs across the transmission network which provide a precise, market-based method for pricing energy that includes the cost of constraints and transmission losses.

An Optimal Power Flow (OPF) program is commonly used to obtain the optimal generation dispatch [9]. The present practice is based on solving a Linear Programming based OPF (LP-OPF), which has the advantage of simplicity and robustness

in the solution algorithm compared to Nonlinear Programming based OPF (NLP-OPF). Mathematically, LMPs are the dual variables of the power balance equations associated with the OPF. Therefore, once the OPF is solved, LMPs can be easily determined.

The state-of-the-art OPF is nonlinear in nature. The LP-OPF is a linear approximation of this standard NLP-OPF, which only requires linear network models commonly known as dc power flow models. Hence, transmission losses, reactive power related issues and security issues are not modeled in the LP-OPF. However, due to the fact that it does consider the line flow constraints, which has the most impact on real power dispatch, and due to the simplicity associated with the solution algorithms, LP-OPF is still dominating in all electricity markets.

The system losses, however, cause significant impact on generation dispatch depending on the topology of the power system network [10]. Therefore, in some electricity markets losses are incorporated into the LP-OPF with a piece-wise linear approximation for losses [11]. Alternatively, some markets use loss factors to represent the effects of the system losses [12]. All these methods are, however, based on approximations, and therefore do not accurately represent the transmission losses.

For the successful operation of the system, the ISO needs to procure some essential services other than real power, such as reactive power, spinning reserve, regulation, and black start capability, which are commonly known as ancillary services [13]. With the current practice, these ancillary services are not included in the dispatch algorithms, and are accrued in other ways such as long term contracts or having a separate auction similar to real power.

The system security is another crucial issue to be addressed in market dispatch. Unlike in single owner electricity industries, where the system operations are carried out in a carefully planned and cooperative manner, in a competitive electricity market no attention is paid by the market participants to the system security. This is because, each market participant has own interests to maximize its benefits. Thus, the ISO

has a key role in maintaining the system security by incorporating the security related constraints into market dispatch.

The success of a competitive electricity market relies on the competition between the participants. Market signals are the main driving force for the participants in achieving this objective. Correct market signals provide a clear and accurate indication of the price of electricity at every location on the grid. These signals in turn reveal the value of locating new generation, upgrading transmission, alleviating the constraints, increasing the competition, and improving the systems ability to meet power demand.

## 1.2 Motivation Behind the Research

In order to achieve the goals of restructuring, many outstanding engineering problems need to be investigated. Most of the tools used in single owner electricity industry are no longer valid and new tools need to be created. Most importantly, these related issues should be addressed early in the restructuring process.

One such pertaining issue is how to determine the correct market signals for the market participants. Unlike in the single owner electricity industry, participants in the restructured electricity market seek market signals for their operational and investment decisions, which eventually lead to a successful operation of the electricity market. These signals indicate the effects on the price of electricity at each location due to various factors such as system losses and binding constraints. For instance, new generation companies will have an incentive to locate their new generators at high priced locations, while new consumers will prefer low priced locations. On the other hand, the ISO can use these market signals to enhance the performance of the electricity market.

The present practice of market dispatch is based on solving a LP-OPF, where very little attention is given to the procurement of reactive power and other ancillary services, and ensuring the security (both static and the dynamic) of the system.

Typically, these related constraints are not used in the conventional OPF, and are procured or ensured in different ways after solving the OPF. This two-step approach, however, does not guarantee the optimal procurement of real and reactive power due to the subsequent adjustments made to the real power dispatch. Thus, to analyze the correct market signals, those underlying constraints must be correctly incorporated in the OPF.

The main advantage of including these constraints is that both technical and economical aspects related to these constraints are embedded in the OPF. Thus, it represents the actual operation of the network, and hence more accurate market signals can be obtained for the market participants for their operational and investment decisions. Despite the associated complexities due to nonlinear constraints, it could be feasible to solve a NLP-OPF in the future due to the continuous advancement in computing speed [1]. Therefore, how to include these additional constraints into the OPF and what methods should be used in analyzing the resulting market signals are important issues to be investigated.

As mentioned in Section 1.1, the ISO has the responsibility of acquiring the required amount of reactive power from suppliers at appropriate locations of the network. This is done in a sequential manner, where real power is dispatched first and then reactive power is dispatched subsequently as an ancillary service. Different reactive power models have been proposed in the literature for a sequential dispatch of real and reactive power. However, this process may result in adjustments to the already agreed real power dispatch and sometimes this could lead to an infeasible solution. Therefore, there is a need for a good reactive power model that captures both technical and economical aspects to suit the simultaneous dispatch of real and reactive power.

Typically, the Dynamic Security Constraint (DSC) is not used in the traditional OPF, due to the unavailability of such a constraint in the functional form compatible with the OPF. The current industry practice of determining the generation dispatch

that is secure from a dynamic stability point of view is by performing a dynamic stability simulation after solving the OPF [46], [47], or by performing the generation dispatch by some other means. Recently, there has been a motivation towards the development of Dynamic Security Constrained Optimal Power Flow (DSCOPF) programs in which the dispatch is ensured against the security of the system in one step. A novel technique to derive an accurate transient stability boundary is proposed for a given credible contingency in [51]. In this way, a separate DSC can be derived for each credible contingency. This can be used as a constraint in the OPF to obtain dynamically secured generation dispatch.

The LMPs, which represent the price of electricity at each location of the system, are considered to be the key market signals. Even though, LMPs provide valuable information at each location of the system, they do not provide a detailed description in terms of contributions coming from different constraints and marginal generators. Unlike in LP-OPF, where only line flow constraints are considered, with NLP-OPF, several other binding constraints also contribute to the LMP at a given location. The existing method of analyzing LMP components can be used to determine the effects of all the binding constraints explicitly, and hence can be used as better market signals for the participants than LMP itself. However, the effects of transmission losses cannot be seen explicitly from LMP components, which is a drawback of this method.

When LMPs are used for settlement of transactions, there exists a difference between what consumers pay to the ISO and what generators get paid by the ISO [17]. This difference is referred to as network rental in this thesis, and is accumulated with the ISO. Network rental is made up of two components known as the loss rental and the constraint rental. Loss rental is due to the difference in average losses and marginal losses. The constraint rental is due to operating the power system at binding constraints imposed by the OPF. Inclusion of the above additional constraints in the OPF leads to further accumulation of rental with ISO, and therefore, components

of network rental could be used as another way of analyzing market signals. In fact, since the network rental is an overpayment made solely by the consumers, the components of network rental show how each consumer has actually overpaid due to each binding constraint and losses. Therefore, the components of network rental can be considered as consumer oriented market signals. However, the available methods are not sufficient in determining these components separately. Hence, there is a need for a new method to decompose the network rental, so that these components can be effectively used as a tool in market signal analysis.

## 1.3 Main Objectives of the Research

The main objective of this research work is to analyze market signals using both proposed and existing methods, after incorporating two constraints that account for the reactive power and security issues in market dispatch. In this regard, first a reactive power model is proposed to be incorporated in the OPF for a simultaneous dispatch of real and reactive power. This OPF is then extended to incorporate the DSC to ensure the dynamic security of the system in a simultaneous manner.

Having incorporated these constraints, the associated market signals are then analyzed. The existing method of LMP components is first used to analyze market signals. This enables the determination of the effects of marginal generators and all binding constraints explicitly and quantitatively, which in turn can be used as better market signals. However, LMP components do not show the effects of losses explicitly.

Then, a theoretical background related to network rental is presented together with the proposed method to decompose the network rental into contributing components. These components of network rental are then proposed as supplementary market signals, to be used together with LMPs and components of LMPs in determining market signals. Finally, a software tool is developed using $C^{++}$ to implement the OPF to include the above features. Thus, market signals can be determined together with the optimal dispatch.

In meeting the above objectives, the following steps have been accomplished.

1. Investigation of the operation of current electricity markets. This enables the comparison of different electricity markets and the determination of a common market framework for the work presented in this thesis. Further, it gives a better understanding of how reactive power is procured; dynamic security is ensured; and market signals are determined, in existing electricity markets.

2. Proposal of a new reactive power model for a simultaneous dispatch of real and reactive power, by considering the capability of the synchronous generator and the fairness of reactive power supply obligation to suit the competitive electricity market. The opportunity cost of supplying reactive power is implicitly modeled using the rating of the machine as a constraint. Fairness of the reactive power supplying obligation is also ensured by splitting the reactive power supplied by the generator into two components with the first component being proportional to real power dispatch.

3. Incorporation of the Dynamic Security Constraint (DSC) in the OPF, to investigate the effects on generation dispatch due to the DSC. This approach has been enabled by the availability of the DSC in a functional form in terms of nodal voltages and their phase angles.

4. Explanation of the existing method of breaking down of LMP into contributing components. The LMP at a given bus is made up of contributions coming from marginal generators and binding constraints, and therefore, explicit decomposition shows individual contributions due to each of the above factors. Thus, these LMP components serve as better market signals than LMP itself.

5. Explanation of the concept of network rental and proposing a novel technique to decompose the network rental among consumers into contributing components. This enables each rental component paid by each consumer to be quantitatively determined, which in turn can be used as supplementary market signals.

6. Implementation of the OPF in the $C^{++}$ programming language to include the above features. The resulting software can be used as a tool to perform computational experiments to gain insight into the operation of electricity markets, to compare the results with benchmark models and to analyze market signals.

## 1.4 Thesis Overview

The thesis has eight chapters and four appendices, which are organized to allow a progressive discussion of the approach employed to achieve the above objectives.

Chapter 2 provides an overview to operation of the existing electricity markets. This includes historic evolution of electricity markets, analysis of present market structures and procurement methods, and associated problems in the current markets. The OPF program is then presented as it is used to determine the optimal dispatch in the electricity market. Finally, the widely accepted concept of LMP, which is also currently being used in most electricity markets, is presented together with some examples to demonstrate how these LMPs are calculated.

At the beginning of Chapter 3, the present reactive power procurement methods are explained. Then, different ways of modeling reactive power proposed in the literature are presented together with the limitations and the drawbacks of those methods. Finally, a new reactive power model for a simultaneous dispatch of real and reactive power is presented, by considering the capability of the synchronous generator and the fairness of reactive power supply obligation to suit the competitive electricity market. A case study with the proposed reactive power model is also presented to convince the suitability of the proposed model in market dispatch.

Chapter 4 starts with an introduction to the security of the power system and a brief summary of how dynamic security is ensured in the restructured electricity market. This is followed by an explanation to the technique proposed in [51] to derive an accurate transient stability boundary for a given credible contingency, which can be readily used as a constraint in the OPF. Then, the inclusion of DSC in the OPF

is presented together with a case study to determine the effects of DSC on LMPs.

In Chapter 5, different methods to analyze the associated market signals are presented. The chapter begins by presenting the existing method of analyzing components of LMP. Then, a method is proposed to analyze the components of network rental. This includes a novel method of decomposing the network rental among consumers and how these components can be used in analyzing market signals. Finally, some case studies are presented to numerically evaluate these individual components.

Chapter 6 describes the tool developed in $C^{++}$ language that implements the OPF and incorporates the above market signal analysis methods. Based on the analysis of the capabilities of different OPF solving techniques described in the literature survey, Newton method and Sequential Linear Programming (SLP) method are used in this work to implement the OPF. This chapter gives an in-depth analysis and implementation issues of the above two methods and how each method can be extended to incorporate market signal analyzing methods. Finally, the performance and limitations of the developed software tool are presented. A commercially available optimization software tool called the Generalized Algebraic Modeling Systems (GAMS) is used as a benchmark to compare the results of the developed software.

Chapter 7 presents the results of a case study carried out using the developed software. In this study, the reactive power constraints and DSCs are included in the OPF and the resulting LMPs, components of LMPs and components of network rental are analyzed to determine the associated market signals.

Finally, in Chapter 8, conclusions of this research work are drawn. It is concluded that the components of network rental provide consumer oriented market signals, which can be considered as supplementary information, in addition to LMPs and LMP components. A few suggestions are given for future work covering the studied areas which need further research. The appendices introduce the mathematical derivations and details about test systems used in the main chapters of the thesis. References are made to the appendices wherever required.

# Chapter 2

# Electricity Market Overview, Dispatch and Pricing Theory

This chapter presents a brief overview to current electricity market operation. Section 2.1 explains the structure of existing electricity markets in different countries together with historic evolution of market restructuring. This enables the comparison of different electricity market structures and thereby finding a common market framework for the work presented in this thesis. The OPF program, which is used in determining the optimal dispatch in the electricity market is presented in Section 2.2. The concept of LMP used in settling the transactions between market participants is discussed in Section 2.3. An example using a 3 bus system is given to demonstrate how LMPs are calculated and what they physically mean.

## 2.1 Electricity Market Overview

An electricity market is a trading forum where participants compete with each other to buy and sell electricity. Historically, the electricity industry has been a monopoly, and a single owner has had authority over all activities in generation, transmission, and distribution of power within its domain of operation. During this time, there was hardly any competition in the electricity industry and this vertically integrated

monopoly was obliged to provide electricity to everyone within its operating territory. Consumers have had no choice other than purchasing electricity from the local monopoly to fulfill their day-to-day requirements.

However, over the past two decades, power industries worldwide have gone through a process of restructuring to create a clear separation between generation and consumption of electricity, and network operations. The economic inefficiencies and the consumer dissatisfaction associated with the single owned electricity industry were the main driving forces behind this restructuring and as a result single owner electricity industries were replaced by competitive electricity markets. However, due to economic and political reasons, this restructuring was not same in all countries. As a result the newly formed markets have taken different forms to suit their individual requirements. Each market has established their own set of rules for a smooth operation of the electricity market, which are commonly known as market rules [2].

After the Federal Energy Regulatory Commission (FERC) issued its historic Order 888 in 1996, followed by Order 2000 in 1999 [18], containing the foundation required for competitive wholesale electricity power markets, the electricity industry in USA has experienced a wide range of restructuring activities [19]. The Pennsylvania-New Jersey-Maryland (PJM) inter-connection restructured its operation in 1997 by establishing the PJM-ISO, followed by New England (NE-ISO), Midwest (MISO), California (CAISO), New-York (NYISO), and Texas with its Electric Reliability Council of Texas (ERCOT) [12]. These newly formed electricity markets have then undergone further reforms based on FERC recommendations.

One such important recommendation was the Standard Market Design (SMD), which came to the picture through its appearance in FERC publications [5] in late 2001. Many of the underlying principles of the SMD have achieved broad acceptance. The core of the SMD includes;

- LMP scheme to manage the efficient use of the transmission system
- establishment of wholesale power markets

- independent entity to operate the transmission system
- multi-settlement scheme based on a forward market and a real time balancing market
- market monitoring and market power mitigation

These features are now standard guidelines for a successful operation of a restructured electricity market.

In Chile, restructuring was introduced in 1982, where end users were given the right to choose their energy supplier and negotiate the prices [3]. This was later extended to explicit market mechanisms in order to determine the generation dispatch and the wholesale electricity price. New Zealand began the reform of its power sector by setting up both the Electricity Corporation of New Zealand (ECNZ) and the system operator, Transpower, in 1988 [11]. After some years of initial restructuring, a voluntary wholesale electricity market is currently in place in New Zealand.

In neighboring Australia, the Industry Commission recommended reforms to the state-owned electricity industry in 1990. In 1994, a pool market was established in the state of Victoria . The same market form was introduced into New South Wales in 1996. These two markets founded the National Electricity Market of Australia in 1998.

Within the European continent, England started its electricity industry restructuring in 1989 by passing the Electricity Act. The following year, the newly formed electricity market was commenced as a mandatory pool market. In 1994 consumers with a demand of more than 100 MW became eligible to participate in the market and this was extended to all consumers in 1998. The mandatory pool market was replaced in 2001 with a market-based structure under the New Electricity Trading Arrangements (NETA), where bilateral contracts are possible parallel to the voluntary pool market.

In parallel to the restructuring in England and Wales, Norway began its reform

in 1990 by adopting the Energy Act. In 1995, the Swedish market was also reformed and together with the Norwegian electricity market established the Nord-Pool, which was launched in early 1996. This market includes both bilateral and voluntary pool modes. Thereby, it has avoided the non-flexibility of England's initial pool market. Finland became a member of Nord-Pool in 1998 followed by West Denmark in 1999 and finally East Denmark in 2000.

Even though the restructuring process has taken a number of different forms in various countries as explained above, there is a common basis and some similar characteristics that can be found in most newly formed competitive electricity markets. The main characteristic is that the generation, transmission, and distribution services are separated, and are the responsibilities of different entities commonly known as market participants. These market participants compete with each other in the electricity market to buy and sell electricity. While generation and demand sides are competitive, transmission side remains a monopoly. In order to ensure the open and fair access to all the participants in the electricity market, the grid and the wholesale energy market are operated by an independent entity known as the Independent System Operator (ISO).

It is possible to classify the existing market structure into two types; the bilateral contract market and the pool-based market [2]. In the bilateral contract market, generators and consumers have negotiable agreements for power delivery according to their own contracts, independent from the ISO. Thus, in this market structure, the ISO's duties are limited to market operation by verifying whether the preferred transaction can be executed without violating the power flow constraints. Since the participants set their power transactions based on the desired contract terms, this market structure has the minimum intervention from the single owner electricity industry. Alternatively, in the pool-based market, no direct bilateral contracts exist between generators and consumers, instead, both generators and consumers bid into a common pool to buy and sell electricity. However, there can be financial contracts

between participants outside the electricity market. The ISO performs both market administration and system operation to schedule the energy transactions between the participants. This type of market is fully competitive, and therefore, a pool-based market model is considered for the work presented in this thesis.

Another feature common to most electricity markets is that there can be numerous financial contracts between the participants [2]. As electricity prices can be extremely volatile due to the fluctuation in generation and demand, these contracts are essential to hedge against the associated financial risks. A multi-settlement scheme based on a forward market and a real time market, and Financial Transmission Rights (FTRs) are found in most markets to alleviate the participants risk.

Settlements between participants are based on Locational Marginal Pricing, calculated from an OPF. LMP is the marginal cost of supplying the next increment of a quantity at a specific bus, which considers the marginal cost of generation and the physical aspects of the transmission system. Different LMPs exist across the transmission network due to both the constraints imposed by physical and operational limits (commonly known as 'binding constraints') and transmission losses. This provides a precise, market-based method for pricing energy that includes the cost of constraints and transmission losses. These LMPs serve as important pricing signals for the market participants to make their operational and investment decisions.

Another feature common to most markets is that only real power is traded in the market. Other services that are necessary to support the transmission of power while maintaining the security and reliable operation, are acquired subsequently, separate from the real power dispatch. These services are commonly known as ancillary services.

## 2.2 OPF Problem

The Optimal Power Flow (OPF) program has been widely used to determine the optimal generator dispatch of a given power system. This is done by optimizing the

total operating cost of the power system or any other appropriate objective function subjected to a given set of constraints which basically represent the physical and operating capabilities of the power system [20]. The OPF was first introduced in the 1960s and now it has become a standard tool in power system planning and decision making. The recent restructuring process in the electricity industry has broadened the application horizon of the OPF, such that now the OPF is used in making operational decisions as well as investment decisions.

The OPF is modeled as a static problem, in which the time variation of the loads are neglected, by assuming fixed loads at the instant of solving the OPF. In general, OPF is a nonlinear optimization problem and hence the feasible region could be non-convex, leading to a challenging task in solving the OPF [21]. As given in Appendix B, the OPF problem can be written as,

$$\begin{aligned} \text{optimize} \quad & f(x) \\ \text{subject to} \quad & g(x) = 0 \\ & h(x) \leq 0 \end{aligned} \tag{2.1}$$

where $x$ represents the decision variables for which the OPF is being solved; $f(x)$ is the objective function that is being optimized; $g(x)$ are the equality constraints that include the active and reactive power balance equations at each bus; and $h(x)$ are the device limits due to the physical and operating capabilities of the power system.

As mentioned in Chapter 1, current practice focuses on solving a LP-OPF, which has the advantage of simplicity and robustness of the solution algorithm. However, the recent advancement in fast computers enables implementing complex algorithms to solve the OPF. This allows the incorporation of static security limits, dynamic security constraints, reactive power dispatch models, and spinning reserve requirements into the OPF.

The calculation of LMPs is also important during the solution process, even though

it is not directly related to the solution process of the OPF. In fact, LMPs are the Lagrangian multipliers or the dual variables associated with the power balance equations of the OPF. Depending on the OPF solution technique used, there are different ways of calculating the LMPs, which are discussed in Chapter 6 in greater detail.

## 2.3 Locational Marginal Pricing

Locational Marginal Pricing (LMP) or nodal pricing is a method of determining the prices of delivered electricity calculated at every bus in the transmission grid. Each bus represents a physical location in the transmission system, where participants are connected. The LMP at each bus represents the locational value of energy, which includes both cost of the energy and the cost of delivery, by considering the physical aspects of the transmission system. Therefore, LMP at a given bus is nothing more than the cheapest way by which an incremental unit of MW is delivered to that particular bus from the available generators while respecting all the system constraints. These LMPs are thus considered to be key pricing signals for the market participants [2]. The FERC has also advocated using LMP in its Standard Market Design (SMD) as a way to achieve short and long-term efficiency in wholesale electricity markets [5]. This is further insisted upon in their recent documents, subsequent to SMD [6], [7]. The LMP for the reactive power can also be defined in a similar way to that of real power, which is discussed in Chapter 3 in detail.

### 2.3.1 Marginal Pricing Theory

Economic theory states that competition for a commodity could be maximized, if that commodity is sold or purchased at the marginal price [8]. Marginal price is the price of the next increment of the considered commodity. In the case of real power, it is the cost of the next increment MW delivered to a given location of the network. The same is true for the reactive power.

In the electricity market, generators and consumers submit price-quantity bids for

the real power that they are willing to supply or consume at a given time interval. From the generator's perspective, the bid price should only contain the incremental variable cost of generation (i.e., the operational cost and any opportunity cost incurred), which is referred to as their short-run marginal cost (SRMC). The price-quantity bids are derived from the incremental variable cost curve, which is typically a polynomial function of generation as shown in figure 2.1. Generator owners use different bidding strategies to derive the bidding pattern, in order to maximize their own profit [2], [22], [23].

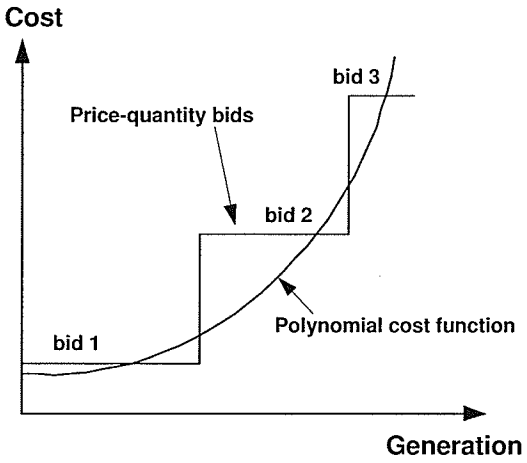


Figure 2.1: Generator bidding to the market

In the long term, generators must also cover fixed operating costs including embedded costs, depreciation, and rate of return [24]. The combined charge of variable and fixed costs is often referred to as the long-run marginal cost (LRMC).

It is important to note that even under pricing based on short-run marginal costs, generators still have the opportunity to recover their fixed costs, as explained below.

Figure 2.2 shows an example with four generator bids and five consumer bids aggregated to a single bus. Generator bids are aggregated in the order of increasing bid price while consumer bids are aggregated in the order of decreasing bid price. The intersection point of the supply and demand curves determines the dispatched quantity and the price, commonly known as the spot quantity and the spot price

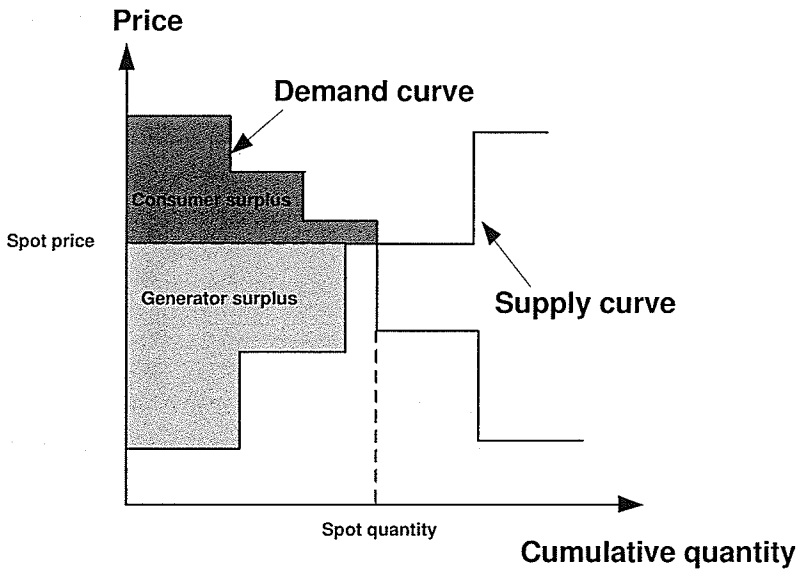


Figure 2.2: Supply-demand curve and market surplus

respectively. This spot price is also known as the Market Clearing Price (MCP) [25]. In general, when there is no transmission network (i.e., no transmission congestion and no transmission losses), MCP is the only existing price. The price of the partly dispatched bid known as the marginal bid sets the MCP. Any generator bid that has a price less than the MCP and any consumer bid that has a price greater than the MCP are fully dispatched.

Therefore, dispatched non-marginal generators earn a surplus, since their marginal cost represented by the bid price is less than the MCP, which is the price paid by the ISO to the generators. This amount in turn can be used to cover their fixed cost. Similarly, dispatched non-marginal consumers also gain a surplus[1]. The dispatch is thus to maximize the total surplus to both generators and consumers.

However, in a practical system with a transmission network, the concept of MCP is no longer valid and more general Locational Marginal Pricing (LMP) has to be used [25]. The next section presents how LMPs are calculated for a multi-bus network.

[1]If consumers are not bidding into the market, the demand curve becomes a straight line resulting in no consumer surplus. In fact, no demand side bidding is considered in the analysis presented in this thesis. Therefore, the loads are known constants for the dispatch.

### 2.3.2 An Example of LMP

The simple 3 bus system shown in figure 2.3 is considered to illustrate the LMPs. For simplicity, the losses are neglected and it is assumed that all the lines have same reactance of 0.25 pu. Further, it is assumed that each generator has placed only one bid. Four cases are considered in the following analysis; in Case 1, line flow limits (i.e., thermal loading of the lines) are ignored; in Case 2, a line limit of 100 MW is applied to line $1-2$; in Case 3, a line limit of 250 MW is applied to line $1-3$; and in Case 4, a line limit of 100 MW is applied to line $2-3$ while shifting the 400 MW load to bus 2.

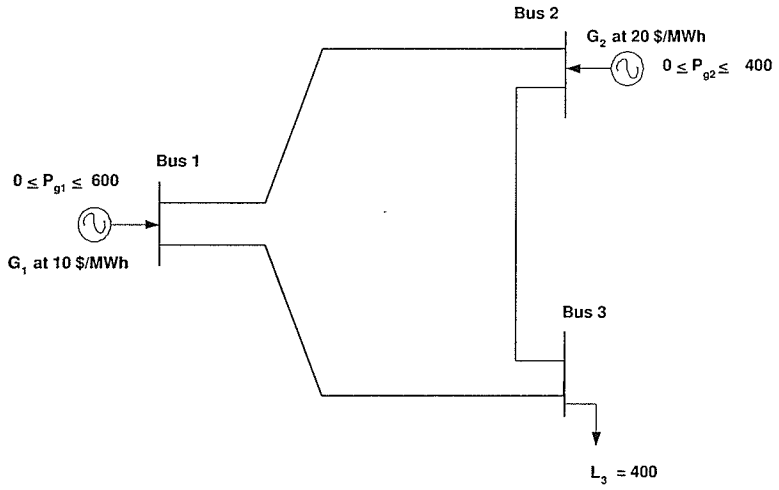


Figure 2.3: 3 bus system

## Case 1: No line flow limits

Without line flow constraints, the cheaper generator $G_1$ is supplied the load at bus 3 and becomes the marginal generator. The expensive generation at $G_2$ is not dispatched at all. Any increase in load at any location will be catered by $G_1$ and therefore, LMPs at all 3 buses are equal to 10 \$/MWh which is the bid price of the generator $G_1$. The generation dispatch, LMPs, and line flows of each line are summarized in figure 2.4.

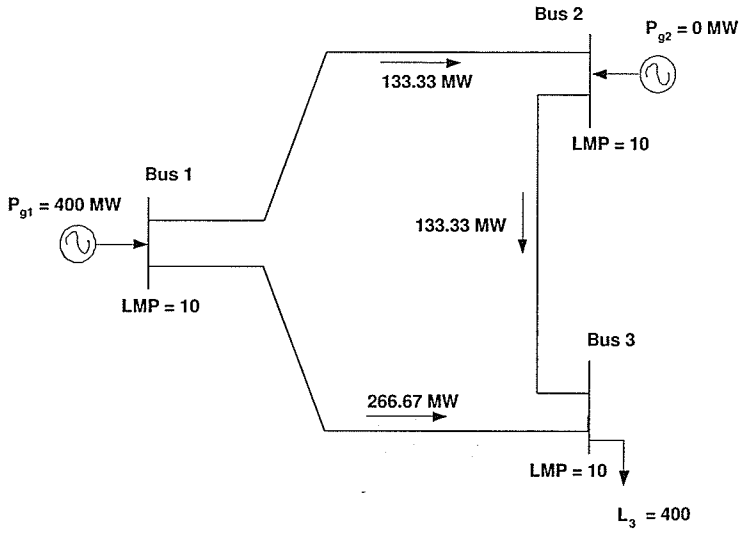


Figure 2.4: LMPs - without line flow limits

## Case 2: 100 MW line limit on line $1-2$

The 100 MW line limit in Case 2 results in line $1-2$ reaching the 100 MW limit. This yields the expensive generation at $G_2$ also partly dispatched. As a result, LMPs are different at each bus and both generators become marginal. The generation dispatch, LMPs, and line flows of each line are shown in figure 2.5.

As in Case 1, LMP at bus 1 is still 10 \$/MWh. This is because any increase in demand at bus 1 can be supplied by $G_1$, despite the line flow constraint on line $1-2$. The LMP at bus 2 is 20 \$/MWh, indicates that any increase in demand at bus 2 is supplied by $G_2$. This is expected because, the line flow constraint on line $1-2$ does not allow any increase in generation from the cheaper generator $G_1$ to cater for any increase in demand at bus 2. Therefore, any increase in demand at bus 2 is entirely supplied by $G_2$.

On the other hand, LMP at bus 3 is neither 10 nor 20, but 15, which is in between the bid prices of the two marginal bids. This can be explained as follows. Due to line flow constraint on line $1-2$, if the demand at bus 3 were to be increased by 1 MW, the total amount would not be completely supplied by $G_1$. Due to the equal

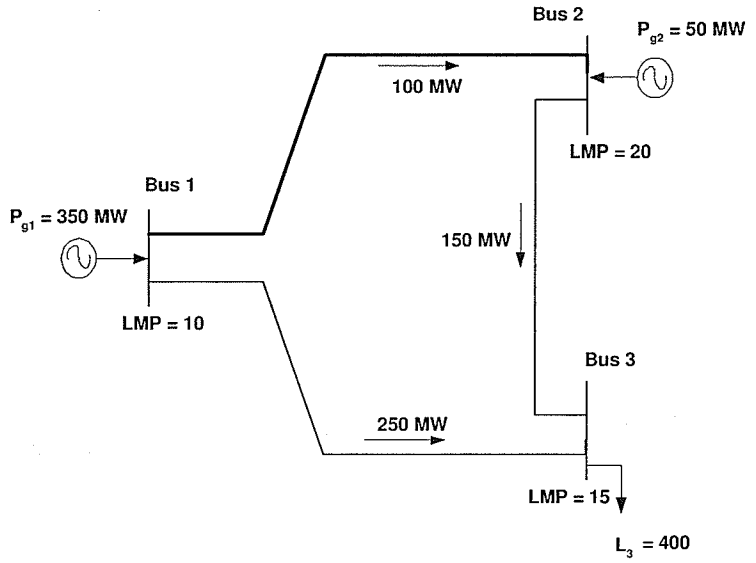


Figure 2.5: LMPs - with 100 MW limit on line $1-2$

reactance of all lines, power flow from $G_1$ to bus 3 would split between lines $1-2$ and $1-3$ in a proportion of 2:1[2]. On the other hand the power flow from $G_2$ to bus 3 would split between lines $2-1$ and $2-3$ to a proportion of 1:2. Since the power flows on line $1-2$ for $G_1$ and $G_2$ are in opposite directions, equal amount of power generated on each generator will cancel the effective increase in power flow on line $1-2$ to maintain the line limit of 100 MW. This results in 50% of the incremental load being supplied by $G_1$ and the remaining 50% by $G_2$. Therefore, LMP at bus 2 can be calculated as $0.5X10 + 0.5X20 = 15$.

## Case 3: 250 MW line limit on line $1-3$

In Case 3, the binding line flow on line $1-3$ causes both generators to become marginal as in Case 2. The important point, however, is that the LMP at bus 3 is higher than the expensive bid price (i.e., bid price of $G_2$).

This is because the line flow constraint necessitates a reduction in the cheaper generation at bus 1 in order to increase the generation from the expensive generation

[2]According to the dc power flow equation, power flows between two nodes in different paths are inversely proportional to the reactance of the path.

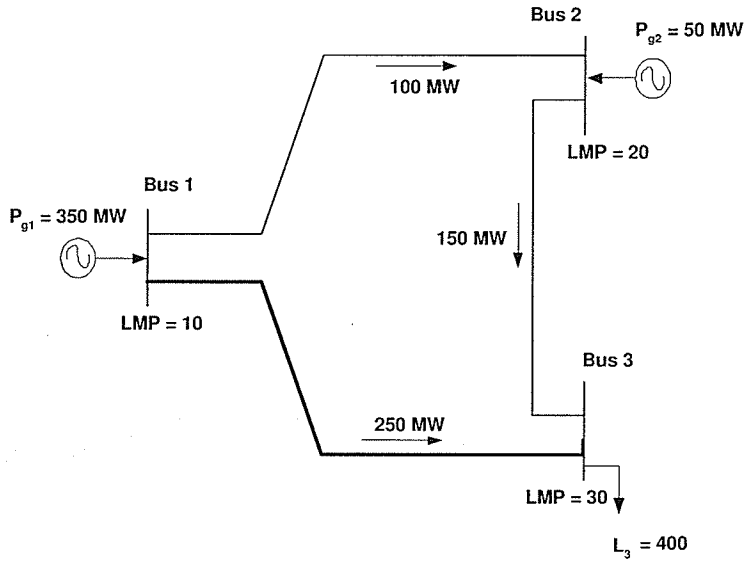


Figure 2.6: LMPs - with 250 MW limit on line $1-3$

at bus 2 in catering any increase in real power demand at bus 3. In other words, to keep the line flow of line $1-3$ at 250 MW (which is the thermal limit of the line), the generation from $G_1$ must be reduced to counteract on line $1-3$, so that the increase in line flow on line $1-3$ due to the increase in $G_2$ is exactly compensated by the decrease in line flow on line $1-3$ due to the decrease in $G_1$. Following a similar analysis to Case 2, the LMP value at bus 3 is calculated as 30.

### Case 4: 100 MW line limit on line $2-3$, while shifting the 400 MW load to bus 2

In Case 4, the LMP at bus 3 is zero, which is less than the cheapest bid (i.e., bid price of $G_1$). This case illustrates that the incremental load at bus 3 will improve the usage of the cheaper generator $G_1$ by relieving the binding line flow constraint on line $3-2$. The zero value for the LMP at bus 3 can be confirmed by performing the same analysis explained in Case 2.

In summary, it can be seen that the effects of binding line flow constraints are embedded in the LMP at each bus in the system.

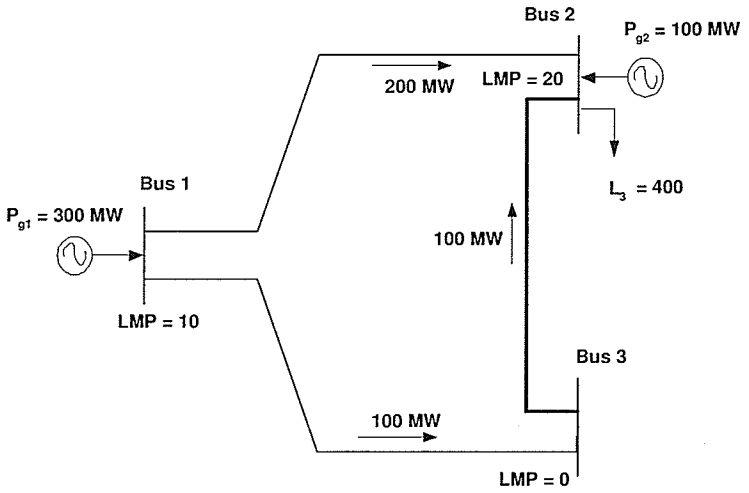


Figure 2.7: LMPs - with 100 MW limit on line $2-3$ and shifting the load to bus 2

## 2.4 Concluding Remarks

This chapter defined a common market framework to be used in the subsequent analysis presented in this thesis. After reviewing the operation of the current electricity markets and identifying the common features to most of the electricity markets, the pool-based market has been chosen as the market model for the work presented in this thesis.

The OPF, which is used to determine the optimal dispatch, and the concept of Locational Marginal Pricing, which is used to settle the transactions between market participants, have also been discussed. In that regard, the marginal pricing theory and the mathematical model of the OPF have been presented. It has been stated that LMPs provide important pricing signals for the participants. Examples using a simple 3 bus system have been presented to demonstrate how LMPs are determined and what they physically mean. This chapter also demonstrated how LMPs vary in the network due to binding line flow constraints. The effects of losses and other binding constraints on LMPs are studied further in the subsequent chapters.

# Chapter 3

# Incorporating Reactive Power in Market Dispatch

In restructured electricity markets, market participants compete with each other by bidding to buy and sell real power. Although, consumers bid only for real power, they also consume reactive power. In addition to this, reactive power is also required to support the voltage in the network which is directly related to the system security. Insufficient reactive power supply can lead to a voltage collapse, similar to the US−Canada blackout in 2003 [26]. Therefore, the ISO has the responsibility of acquiring the required amount of reactive power from suppliers at appropriate locations of the network [27]. Although, the cost of generating reactive power is almost negligible compared to the cost of generating real power, the unavailability of reactive power at certain strategic nodes may have a significant influence on the real power dispatch and prices [28], [29].

Generally, rules of the electricity market specify the amount of reactive power that each generator has to supply. If the reactive power available from the generators is insufficient, the ISO may have to acquire some additional reactive power from other sources. As discussed in Chapter 1, the problem addressed in this chapter is reactive power pricing using the nodal pricing approach. Nodal pricing of reactive power has been discussed in the context of restructured electricity industry in [30], [31].

With the present practice, real power is dispatched first and reactive power is dispatched or acquired subsequently as an ancillary service. This may result in adjustments to the real power dispatch. Therefore, the generator owners have to indicate their cost of adjusting real power as a separate piece of information [32], [33]. This sequential approach, however, does not guarantee the optimal simultaneous dispatch of real and reactive power.

In this chapter, a new reactive power model is proposed to be used in the OPF for a simultaneous dispatch of real and reactive power. In the proposed model, the opportunity cost of supplying reactive power is implicitly modeled using the rating of the machine as a constraint. Fairness of reactive power supply obligation is also ensured by splitting the reactive power supplied by the generator into two components with the first component being proportional to real power dispatch.

This chapter is organized as follows. A discussion of reactive power management in current electricity markets is given in Section 3.1. Different reactive power models that have been put forward together with the proposed reactive power model are given in Section 3.2. The OPF problem is presented in Section 3.3. Some important relationships derived for the optimality conditions are also presented in Section 3.3. Section 3.4 presents a case study and an analysis of different price components to prove the suitability of the proposed model.

## 3.1 Present Reactive Power Management

Reactive power management receives greater attention in restructured electricity markets. Although, the cost of production of reactive power is very small compared to that of real power, the assumption of zero cost is not acceptable in a competitive market. However, still there is no well-developed and widely accepted reactive power procurement method. Instead, each electricity market uses its own procurement strategies based on its market rules. The FERC has also made recommendations, that the reactive power providers should be financially compensated in an equatable fashion

according to an agreed way between market participants [34].

Presently, under the restructured environment, reactive power and other ancillary services are not treated integrally with the real power dispatch. Therefore, the ISO has the responsibility of acquiring the required amount of reactive power from suppliers. The common approach for the provision of reactive power services is based on long term contracts between the ISO and generator owners. These long term contracts are usually bilateral agreements based on market experience rather than based on a competitive framework. In the context of the US, New York ISO, PJM interconnection, and California ISO have such long term contracts that compensate generators for their reactive power services [35], [36], [37]. In addition to this, an opportunity cost payment is also made when real power generation is compromised in order to increase the reactive power availability. However, most of the time, generators are bound to produce free amount of reactive power within a specified range of operation of the generation.

The National Grid Company (NGC) in the UK and Wales also uses this type of long term contracts to procure the reactive power services [38]. In Australia, all the generators receive an availability payment for their preparedness in providing the reactive power when the ISO requires [39]. Furthermore, a compensation payment based on the opportunity cost is also paid for the generators, if the real power is compensated.

## 3.2 Modeling Reactive Power Supply in Market Dispatch

In a competitive environment, reactive power procurement should also be done in an optimal way similar to that for real power. For that purpose, there is a need for a reactive power pricing structure or a model which captures technical and economical issues associated with reactive power procurement and pricing. Over the years different ways of modeling reactive power in a market environment have been put forward. In [40] the cost of production of reactive power is modeled as a polynomial function

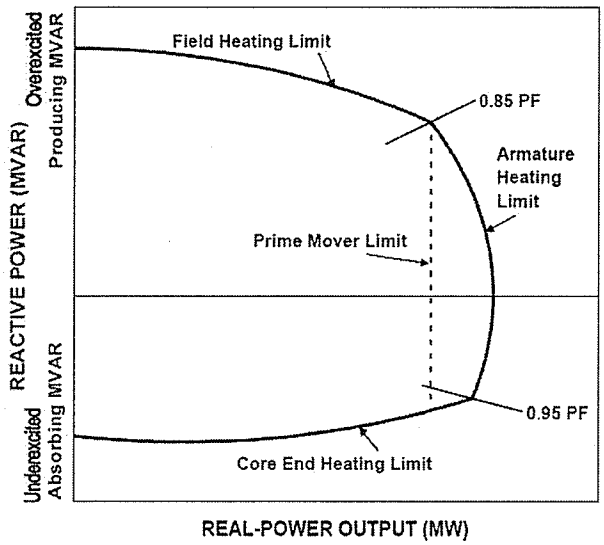


Figure 3.1: Capability region of the synchronous generator

of reactive power generation, and the maximum limit of reactive power generation is treated as a constant. However, as the limiting value of reactive power is determined by the stator current limit or the field current limit, it depends on the real power generation as shown in figure 3.1. Therefore, when a generator is generating the limiting value of reactive power, the amount of real power generation is compromised and thus, there is an opportunity cost. This opportunity cost has been modeled in [41] as a function supplied by the generator owner to the ISO. Furthermore, in this model, the generator owners are obliged to supply a fixed amount of reactive power free of charge. Any amount in excess of this up to a certain limit is priced as a linear function of reactive power generation, beyond which the cost is modeled as the opportunity cost. This model was proposed for a sequential dispatch where the real power is dispatched first, and the reactive power dispatch is done with the flexibility to adjust the real power dispatch.

The ideas presented in [41] are extended in this chapter with some modifications for a simultaneous real power and reactive power dispatch. The model proposed here, has two components for reactive power. The first component $Q_{g1}$ is the obligation of

the generator owner to supply reactive power. Unlike in [41], in the proposed model, the reactive power obligation of the generator is proportional to the amount of real power supplied by the generator, because reactive power is needed to transmit real power and to maintain correct voltages. This concept is rigorously analyzed in [42], where it is pointed out that the generators must supply a certain amount of reactive power free of charge as an obligation and this amount is related to the real power generation in a nonlinear manner.

In the analysis presented in this chapter, the obligation of reactive power supply is modeled as a linear relationship for simplicity (i.e., constant power factor). This linear relationship is given in (3.1) for the generator connected to bus $i$ with the proportionality constant $K_i^Q$. The term $Q_{g1i}^{max}$ is the maximum obligation of reactive power and $\sum P_{ik}$ is the dispatched real power for the generator at bus $i$ from its $k$ number of bids. The proportionality constant $K_i^Q$ is considered to be common to all generators and it is specified as a market rule. For example, in the California electricity market generators are obliged to supply reactive power free of charge within the range of 0.9 lagging to 0.95 leading [37].

$$Q_{g1i}^{max} = \left( \sum_{k \in B_i} P_{ik} \right) K_i^Q \tag{3.1}$$

The nonlinear model proposed in [42] is a more accurate representation and can be used in place of (3.1). The equation included will have additional terms to represent the nonlinearity, but the method of analysis remains the same.

The second component $Q_{g2}$ has a price that represents the cost of additional real power losses in the field winding due to reactive power generation. This cost, which is a nonlinear function of reactive power generation, is approximated to a linear function. This linear relationship for the $Q_{g2i}$ amount of reactive power from the generator connected to bus $i$ is given in (3.2), where $S_i^Q$ is the cost of reactive power.

$$\text{price of } Q_{g2i} = S_i^Q Q_{g2i} \tag{3.2}$$

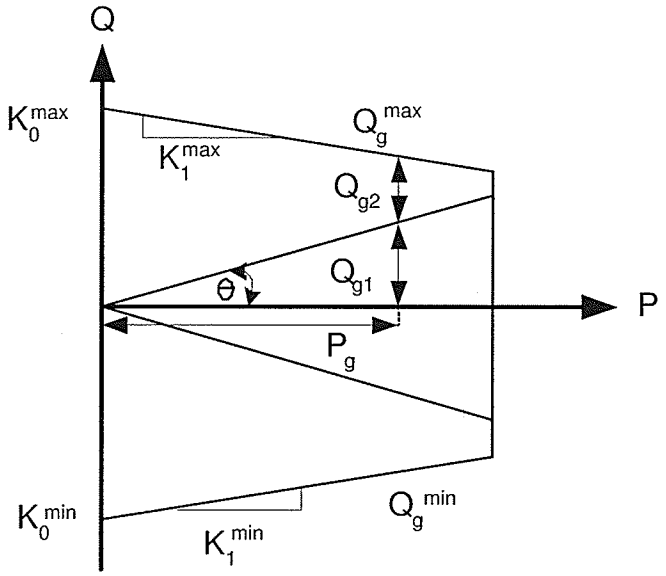


Figure 3.2: Proposed reactive power model for the generator

This model of reactive power can be viewed as having two bids of reactive power with the price of the first bid equal to zero and the quantity proportional to the dispatched real power. In this chapter, these two components of reactive power are referred to as Block 1 Reactive Power, and Block 2 Reactive Power respectively. This structure is also in agreement with [43], where it is proposed to pay the generator owner for extra reactive power made available beyond the level dictated by the performance standards. The value of $S^Q$ or the Block 2 Reactive Power price has to be submitted by the generator owner as a separate piece of information along with the real power bids.

The net amount of reactive power supplied by the generator at bus $i$ is the sum of $Q_{g1i}$ and $Q_{g2i}$. This is constrained by the operating capability of the generator. In here, the feasible operating region of the generator is modeled by a trapezoid as shown in figure 3.2, which is a straight line approximation of the typical operating capability curve of the synchronous generator shown in figure 3.1. Therefore, the maximum limit of reactive power is a function of real power generation and thus, the opportunity cost is implicit and need not be modeled explicitly.

The total amount of reactive power supplied by the generator at bus $i$, $Q_{gi}$ is the sum of $Q_{g1i}$ and $Q_{g2i}$.

$$Q_{gi} = Q_{g1i} + Q_{g2i} \tag{3.3}$$

According to the trapezoidal model of the capability curve, the maximum and minimum reactive power limits for a given amount of real power generation, $P_{ik}$ are given by the straight line approximations to the generator capability curve. This can be written as,

$$Q_{gi}^{max} = K_{i,0}^{max} + K_{i,1}^{max} \sum_{k \in B_i} P_{ik} \tag{3.4}$$

$$Q_{gi}^{min} = K_{i,0}^{min} + K_{i,1}^{min} \sum_{k \in B_i} P_{ik} \tag{3.5}$$

where $K_{i,0}^{max}$, $K_{i,0}^{min}$, $K_{i,1}^{max}$ and $K_{i,1}^{min}$ are the coefficients of the straight line approximation.

## 3.3 OPF Problem

As discussed in Appendix B, the OPF problem can be written as a problem of minimizing the total cost of real and reactive power production subject to real and reactive power balance at all nodes, real power generation is within the limits specified by the bid quantity, reactive power generation is within limits, and the voltages are within specified limits.

Minimize:

$$J = \sum_{i \in I} \sum_{k \in B_i} P_{ik} S_{ik}^{B} + \sum_{i \in I} S_i^{Q} Q_{g2i}$$

Subject to:

$$\sum_{k \in B_i} P_{ik} - P_{Di} = \sum_{ij \in T_i} V_i [g_{ij}(V_i - V_j \cos\theta_{ij}) - b_{ij} V_j \sin\theta_{ij}] \qquad \forall i$$

$$Q_{gi} - Q_{Di} = \sum_{ij \in T_i} V_i [-b_{ij}(V_i - V_j \cos\theta_{ij}) - g_{ij} V_j \sin\theta_{ij}] \qquad \forall i$$

$$
\begin{aligned}
0 \le P_{ik} \le P_{ik}^{B} \qquad & \forall i, \forall k \quad \text{(bid quantity limit)} \\
Q_{gi} = Q_{g1i} + Q_{g2i} \qquad & \forall i \quad \text{(total reactive power)} \\
Q_{gi}^{min} \le Q_{gi} \le Q_{gi}^{max} \qquad & \forall i \quad \text{(reactive power limits)} \\
Q_{g1i} \le \left( \sum_{k \in B_i} P_{ik} \right) K_i^{Q} \qquad & \forall i \quad \text{(Reactive Power Block 1)} \\
V_i^{min} \le V_i \le V_i^{max} \qquad & \forall i \quad \text{(voltage limits)}
\end{aligned}
\tag{3.6}
$$

Where $Q_{gi}^{max}$ and $Q_{gi}^{min}$ are given in (3.4) and (3.5) respectively. For simplicity of presentation, line flow limits have been ignored in the above formulation. However, line flow constraints, $-PF_{ij}^{max} \le PF_{ij} \le PF_{ij}^{max}$ can be directly incorporated into (3.6) in order to take line congestion into account.

The Lagrangian for the above OPF can be written as:

$$
\begin{aligned}
L = & \sum_{i \in I} \sum_{k \in B_i} P_{ik} S_{ik}^{B} + \sum_{i \in I} S_i^{Q} Q_{g2i} \\
& + \sum_{i \in I} \lambda_i \left[ - \sum_{k \in B_i} P_{ik} + P_{Di} + \sum_{ij \in T_i} V_i [g_{ij}(V_i - V_j \cos\theta_{ij}) - b_{ij} V_j \sin\theta_{ij}] \right] \\
& + \sum_{i \in I} \sigma_i \left[ -Q_{g1i} - Q_{g2i} + Q_{Di} + \sum_{ij \in T_i} V_i [-b_{ij}(V_i - V_j \cos\theta_{ij}) - g_{ij} V_j \sin\theta_{ij}] \right] \\
& + \sum_{i \in I} \sum_{k \in B_i} \beta_{ik}^{+}(P_{ik} - P_{ik}^{B}) + \sum_{i \in I} \sum_{k \in B_i} \beta_{ik}^{-}(-P_{ik}) \\
& + \sum_{i \in I} \eta_i^{+}(Q_{g1i} + Q_{g2i} - Q_{gi}^{max}) + \sum_{i \in I} \eta_i^{-}(Q_{gi}^{min} - Q_{g1i} + Q_{g2i}) \\
& + \sum_{i \in I} \gamma_i (Q_{g1i} - K_i^{Q} \sum_{k \in B_i} P_{ik}) \\
& + \sum_{i \in I} \phi_i^{+}(V_i - V_i^{max}) + \sum_{i \in I} \phi_i^{-}(V_i^{min} - V_i)
\end{aligned}
\tag{3.7}
$$

where $\lambda_i, \sigma_i, \beta_{ik}, \eta_i, \gamma_i$, and $\phi_i$ are the Lagrange multipliers associated with constraints of the OPF problem.

The optimal solution must satisfy the following KKT optimality conditions (see Appendix B for more detail).

$$\frac{\partial L}{\partial P_{ik}} = S_{ik}^{B} - \lambda_i + \beta_{ik}^{+} - \beta_{ik}^{-} - \eta_i^{+}(\frac{\partial Q_{gi}^{max}}{\partial P_{ik}}) + \eta_i^{-}(\frac{\partial Q_{gi}^{min}}{\partial P_{ik}}) - \gamma_i(K_i^{Q}) = 0 \tag{3.8}$$

$$\frac{\partial L}{\partial Q_{g1i}} = -\sigma_i + \eta_i^{+} - \eta_i^{-} + \gamma_i = 0 \tag{3.9}$$

$$\frac{\partial L}{\partial Q_{g2i}} = S_i^{Q} - \sigma_i + \eta_i^{+} - \eta_i^{-} = 0 \tag{3.10}$$

$$\begin{aligned}\frac{\partial L}{\partial V_i} &= \lambda_i \sum_{ij \in T_i} [g_{ij}(2V_i - V_j \cos\theta_{ij}) - b_{ij} V_j \sin\theta_{ij}] - \sum_{j \neq i} \lambda_j [(g_{ij} V_j \cos\theta_{ji} + b_{ij} V_j \sin\theta_{ji})] \\ &- \sigma_i \sum_{ij \in T_i} [b_{ij}(2V_i - V_j \cos\theta_{ij}) + g_{ij} V_j \sin\theta_{ij}] + \sum_{j \neq i} \sigma_j [(b_{ij} V_j \cos\theta_{ji} - g_{ij} V_j \sin\theta_{ji})] \\ &+ \phi_i^{+} - \phi_i^{-} = 0 \end{aligned} \tag{3.11}$$

$$\begin{aligned}\frac{\partial L}{\partial \theta_i} &= \lambda_i \sum_{ij \in T_i} [V_i(g_{ij} V_j \sin\theta_{ij} - b_{ij} V_j \cos\theta_{ij})] + \sum_{j \neq i} \lambda_j [(-g_{ij} V_i V_j \sin\theta_{ji} + b_{ij} V_i V_j \cos\theta_{ji})] \\ &+ \sigma_i \sum_{ij \in T_i} [V_i(-b_{ij} V_j \sin\theta_{ij} - g_{ij} V_j \cos\theta_{ij})] + \sum_{j \neq i} \sigma_j [(b_{ij} V_i V_j \cos\theta_{ji} + g_{ij} V_i V_j \sin\theta_{ji})] \\ &= 0 \end{aligned} \tag{3.12}$$

$$\frac{\partial L}{\partial \lambda_i} = \sum_{k \in B_i} P_{ik} - P_{Di} - \sum_{ij \in T_i} V_i [g_{ij}(V_i - V_j \cos\theta_{ij}) - b_{ij} V_j \sin\theta_{ij}] = 0 \tag{3.13}$$

$$\frac{\partial L}{\partial \sigma_i} = Q_{gi} - Q_{Di} - \sum_{ij \in T_i} V_i [-b_{ij}(V_i - V_j \cos\theta_{ij}) - g_{ij} V_j \sin\theta_{ij}] = 0 \tag{3.14}$$

The complementary slackness conditions are,

$$\beta_{ik}^{+}(P_{ik} - P_{ik}^{B}) = 0 \tag{3.15}$$

$$\beta_{ik}^{-}(-P_{ik}) = 0 \tag{3.16}$$

$$\eta_i^{+}(Q_{g1i} + Q_{g2i} - Q_{gi}^{max}) = 0 \tag{3.17}$$

$$\eta_i^{-}(Q_{gi}^{min} - Q_{g1i} + Q_{g2i}) = 0 \tag{3.18}$$

$$\gamma_i(Q_{g1i} - K_i^{Q} \sum_{k \in B_i} P_{ik}) = 0 \tag{3.19}$$

$$\phi_i^{+}(V_i - V_i^{max}) = 0 \tag{3.20}$$

$$\phi_i^{-}(V_i^{min} - V_i) = 0 \tag{3.21}$$

Further,

$$\beta_{ik}^{+}\beta_{ik}^{-} = 0 \Longrightarrow \beta_{ik} = \beta_{ik}^{+} - \beta_{ik}^{-}$$

$$\eta_{i}^{+}\eta_{i}^{-} = 0 \Longrightarrow \eta_{i} = \eta_{i}^{+} - \eta_{i}^{-}$$

$$\phi_{i}^{+}\phi_{i}^{-} = 0 \Longrightarrow \phi_{i} = \phi_{i}^{+} - \phi_{i}^{-}$$

From (3.4) and (3.5),

$$\frac{\partial Q_{gi}^{max}}{\partial P_{ik}} = K_{i,1}^{max} \tag{3.22}$$

$$\frac{\partial Q_{gi}^{min}}{\partial P_{ik}} = K_{i,1}^{min} \tag{3.23}$$

If Block 1 Reactive Power is not fully used (i.e., $Q_{g2} = 0$), then (3.10) is not relevant. As the generator has not reached the maximum amount of Block 1, the Lagrange multiplier associated with this constraint, $\gamma_i$ and the Lagrange multiplier associated with the reactive power capability limit $\eta_i^+$ are zero.

Therefore, for the operation within the Reactive Power Block 1 region, (3.8) and (3.9) become:

$$\lambda_i = S_{ik}^{B} + \beta_{ik} \tag{3.24}$$

$$\sigma_i = 0 \tag{3.25}$$

However, when $Q_{g2} > 0$, (3.10) is also valid and when combined with (3.9) yields,

$$\gamma_i = S_i^{Q} \tag{3.26}$$

Therefore, (3.8) and (3.9) can be written as,

$$\lambda_i = S_{ik}^{B} + \beta_{ik} - \eta_i K_{i,1}^{max/min} - \gamma_i K_i^{Q} \tag{3.27}$$

$$\sigma_i = \eta_i + \gamma_i \tag{3.28}$$

$\lambda_i$'s and $\sigma_i$'s are the multipliers associated with the real power balance and reactive power balance equations. Therefore, they indicate the LMP of real power and reactive power respectively at the corresponding bus. This shows that by combining real and reactive power dispatch, the marginal pricing can be applied for reactive power as well. Thus, the LMP of reactive power indicates the marginal cost of delivered reactive power to a given location in the system.

The first two terms in (3.27) represent the marginal price of the supply bid; the next term represents the component of price due to operating the generator at the capability limit; and the final term represents the component of price due to the constraint on Reactive Power Block 1, which depends on real power generation.

Similarly, in the reactive power price given in (3.28), the first term represents the component of price due to operating the generator at the capability limit; and the second term represents the price of Block 2 Reactive Power.

## 3.4 Results

This section presents a case study to analyze the different price components produced by the proposed simultaneous real and reactive power dispatch model. In the presentation of results, all the real and reactive power values are in MW or MVAr, prices are in \$/h and marginal prices are in either \$/MWh or \$/MVArh depending on the quantitiy considered.

The simultaneous dispatch model was applied to the IEEE 30 bus system shown in Appendix A using the generator bid data given in table 3.1 to represent the competitive electricity market. There are six generator buses and it is assumed that each generator offers two bids. This assumption, however, does not affect the validity of the analysis presented. The reactive power details for the six generators are given in table 3.2. The value of $S_i^Q$ is chosen to be approximately 10 % of the real power cost as in [40]. The maximum and minimum voltage limits of each bus are set to 1.05 pu and 0.95 pu respectively. The OPF was solved using the developed software tool

explained in Chapter 6 and the results were validated using GAMS MINOS5 solver [62] by modeling the OPF in the GAMS environment.[1]

Table 3.1: Generator bid data

| Bus | bid 1 | | bid 2 | |
|---|---|---|---|---|
| | $P_{ik}^{B}$ | $S_{ik}^{B}$ | $P_{ik}^{B}$ | $S_{ik}^{B}$ |
| 1 | 40 | 3.60 | 40 | 5.20 |
| 2 | 40 | 3.20 | 40 | 4.60 |
| 13 | 20 | 4.00 | 20 | 5.00 |
| 22 | 25 | 4.10 | 25 | 7.25 |
| 23 | 15 | 3.75 | 15 | 4.75 |
| 27 | 27.5 | 3.70 | 27.5 | 4.20 |

Table 3.2: Reactive power generation data

| Bus | $K_{i,0}^{max}$ | $K_{i,1}^{max}$ | $K_{i,0}^{min}$ | $K_{i,1}^{min}$ | $K_{i}^{Q}$ | $S_{i}^{Q}$ |
|---|---|---|---|---|---|---|
| 1 | 40 | -0.2 | -40 | 0.2 | 0.3 | 0.47 |
| 2 | 40 | -0.2 | -40 | 0.2 | 0.3 | 0.67 |
| 13 | 30 | -0.2 | -30 | 0.2 | 0.3 | 0.44 |
| 22 | 30 | -0.1 | -30 | 0.2 | 0.3 | 0.52 |
| 23 | 20 | -0.2 | -20 | 0.2 | 0.3 | 0.22 |
| 27 | 35 | -0.3 | -30 | 0.2 | 0.3 | 0.36 |

Tables 3.3 and 3.4 show the optimal dispatch and the values of the Lagrangian multipliers, in which the cheaper bid of each unit has been fully dispatched and the second bid from generators at bus 2 and 27 have been partially dispatched. Therefore, both generators 2 and 27 become marginal generators. This is because the reactive load is locally supported by the inexpensive generator at bus 27 and in order to make that provision the real power dispatch is compromised. The remaining real power is now coming from the next cheapest available bid which is at bus 2. The reactive power dispatch of generator 27 given in table 3.3 and the non-zero Lagrangian multiplier (i.e., $\eta_{27}^{+}$) given in table 3.4 also reveal that Block 1 Reactive Power and Block 2 Reactive Power are fully dispatched and the generator is operating at its capability limit.

[1] Generalized Algebraic Modeling Systems (GAMS) is a commercially available software platform for mathematical programming.

Table 3.3: Generation dispatch with the proposed simultaneous model

| Bus | bid 1 | bid 2 | $Q_{g1}$ | $Q_{g2}$ | $Q_g^{max}$ | $\lambda$ | $\sigma$ |
|---|---|---|---|---|---|---|---|
| 1 | 40.00 | 0.00 | 12.00 | 15.05 | 32.00 | 4.412 | 0.470 |
| 2 | 40.00 | 13.97 | 16.19 | 0.00 | 29.21 | 4.449 | 0.503 |
| 13 | 20.00 | 0.00 | 6.00 | 13.01 | 26.00 | 4.560 | 0.440 |
| 22 | 25.00 | 0.00 | 7.50 | 13.03 | 27.50 | 4.603 | 0.520 |
| 23 | 15.00 | 0.00 | 4.50 | 12.50 | 17.00 | 4.558 | 0.419 |
| 27 | 27.50 | 9.17 | 11.00 | 13.00 | 24.00 | 4.429 | 0.482 |

Table 3.4: Values of the multipliers given by the OPF

| Bus | bid 1 | | bid 2 | | $\eta_i^+$ | $\eta_i^-$ | $\gamma_i$ |
|---|---|---|---|---|---|---|---|
| | $\beta_{ik}^-$ | $\beta_{ik}^+$ | $\beta_{ik}^-$ | $\beta_{ik}^+$ | | | |
| 1 | 0 | 0.953 | 0.647 | 0 | 0 | 0 | 0.470 |
| 2 | 0 | 1.400 | 0 | 0 | 0 | 0 | 0.503 |
| 13 | 0 | 0.692 | 0.308 | 0 | 0 | 0 | 0.440 |
| 22 | 0 | 0.659 | 2.491 | 0 | 0 | 0 | 0.520 |
| 23 | 0 | 0.835 | 0.165 | 0 | 0.199 | 0 | 0.220 |
| 27 | 0 | 0.800 | 0 | 0 | 0.122 | 0 | 0.360 |

On the other hand, if the dispatch is done based on the sequential approach, bid 2 of the generator at bus 2 is not dispatched while bid 2 of the generator at bus 27 is dispatched to a higher generation level. As far as the real power dispatch is concerned, this sequential dispatch is preferred, as the cheaper bids are dispatched ahead of the expensive bids. However, when accruing the required reactive power subsequently, the cheaper reactive power of generator at bus 27 cannot be utilized due to the higher real power dispatch of that generator. Thus, the ISO has to procure the reactive power from the next available generators at a higher price or from the generator at bus 27 by curtailing the real power dispatch. However, in order to curtail the real power, the associated opportunity cost has to be paid by the ISO.

Therefore, if the dispatch is done without considering the reactive power and then adjusted to satisfy the reactive power requirement, some participants will be benefited at the expense of the others and the overall dispatch is also inferior to that of simultaneous dispatch. Theoretically, the best solution that the two step approach can achieve is the solution of simultaneous dispatch. As illustrated above, there is no guarantee that the two step approach gives the same result as the simultaneous

dispatch.

### 3.4.1 Analysis of Price Components

Using (3.27), (3.28), and the OPF results given in tables 3.3 and 3.4, different price components of real and reactive power can be analyzed as shown below. The buses 2, 1, and 27 have been chosen for the analysis due to their unique features.

Bus 2 has a partially dispatched real power bid. The Block 1 Reactive Power is fully dispatched and the Block 2 Reactive Power is not dispatched at all due to the high Block 2 Reactive Power price. Therefore,

$$\beta_{ik} = 0; \qquad \eta_i = 0$$

The real power LMP can be calculated from (3.27):

$$\lambda_i = S_{ik}^B - \gamma_i(K_i^Q)$$

$$\lambda_2 = 4.6 - 0.503 \times 0.3 = 4.449$$

The term $\gamma_i.K_i^Q$ represents the value of free reactive power available to the system due to the increase in real power generation. Therefore, the cost of real power at bus 2 is 4.449, even though the bid price for real power is 4.6.

For reactive power, (3.28) gives:

$$\sigma_i = \gamma_i \quad \Rightarrow \quad \sigma_2 = 0.503$$

This gives the reactive power LMP at bus 2 as 0.503, which is less than the price of Block 2 Reactive Power at bus 2 indicating that any increase in reactive power demand at bus 2 will be supplied by some other cheaper generator in the system.

The situation at bus 1 is slightly different, where only the first real power bid is fully dispatched and the second real power bid is not dispatched. Further, Block 1

Reactive Power is fully dispatched and Block 2 Reactive Power is partially dispatched (maximum reactive power limit has not been reached).

From (3.27), the real power LMP can be calculated as:

$$\lambda_i = S_{ik}^B + \beta_{ik} - \gamma_i(K_i^Q)$$

$$\lambda_1 = 3.6 + 0.953 - 0.47 \times 0.3 = 4.412$$

The second component of $\lambda_1$ (i.e., 0.953) is the shadow cost of supply offer. This factor represents the marginal value of the offer to the whole system.

$$\sigma_i = \gamma_i \quad \Rightarrow \quad \sigma_1 = 0.47$$

The reactive power LMP at bus 1 is equal to the price of Block 2 Reactive Power at bus 1 indicating that any increase in reactive power demand at bus 1 will be supplied by the generator connected to bus 1.

Similar to bus 2, bus 27 also has a marginal real power generator. However, both Block 1 Reactive Power and Block 2 Reactive Power at bus 27 are fully dispatched and generator 27 is operating at the capability limit. Therefore,

$$\beta_{ik} = 0.800; \qquad \eta_i = 0.122$$

$$\lambda_i = S_{ik}^B + \beta_{ik} - \eta_i K_{i,1}^{max/min} - \gamma_i(K_i^Q)$$

$$\lambda_{27} = 3.7 + 0.800 + 0.3 \times 0.122 - 0.30 \times 0.36 = 4.429$$

$$\sigma_i = \gamma_i + \eta_i \quad \Rightarrow \quad \sigma_2 = 0.36 + 0.122 = 0.482$$

Therefore, at bus 27, both real and reactive power LMPs have a positive component of price due to operating the generator at the capability limit, causing an increase in both real and reactive power price. This is because the reactive power

availability is decreased as the generation is increased, indicating that any increase in generation is discouraged when there is a reactive power shortage.

The lower limit of reactive power is important when generators are absorbing reactive power. Typically, generators supply reactive power and hence the lower limit becomes irrelevant. Therefore, in the above analysis, the typical situation is considered. However, the same analysis can be done, when generators are absorbing reactive power as well.

The real and reactive power LMPs for all the buses can be summarized as shown in table 3.5. These values can also be analytically obtained by solving (3.11) and (3.12).

Table 3.5: Real and reactive power LMPs

| Bus | LMP | | Bus | LMP | | Bus | LMP | |
|---|---|---|---|---|---|---|---|---|
| | Real | Reactive | | Real | Reactive | | Real | Reactive |
| 1 | 4.41 | 0.47 | 11 | 4.61 | 0.55 | 21 | 4.62 | 0.54 |
| 2 | 4.45 | 0.50 | 12 | 4.58 | 0.49 | 22 | 4.60 | 0.52 |
| 3 | 4.53 | 0.52 | 13 | 4.56 | 0.44 | 23 | 4.56 | 0.42 |
| 4 | 4.55 | 0.53 | 14 | 4.65 | 0.50 | 24 | 4.60 | 0.51 |
| 5 | 4.53 | 0.54 | 15 | 4.63 | 0.49 | 25 | 4.51 | 0.51 |
| 6 | 4.57 | 0.55 | 16 | 4.63 | 0.53 | 26 | 4.59 | 0.56 |
| 7 | 4.60 | 0.57 | 17 | 4.65 | 0.56 | 27 | 4.43 | 0.48 |
| 8 | 4.60 | 0.58 | 18 | 4.71 | 0.54 | 28 | 4.55 | 0.54 |
| 9 | 4.61 | 0.55 | 19 | 4.73 | 0.56 | 29 | 4.58 | 0.62 |
| 10 | 4.63 | 0.55 | 20 | 4.71 | 0.56 | 30 | 4.59 | 0.63 |

### 3.4.2 Market Signals Produced by the Proposed Model

If the Block 1 Reactive Power is sufficient to supply the total reactive power demand, then according to (3.27), $\lambda_i$ does not show any reactive power component. The reactive power LMP, $\sigma_i$, is also zero. Therefore, the price of electricity is only due to the dispatched real power. However, if at least one generator is providing Block 2 Reactive Power, then, there will be a component in the real power LMP. The reactive power LMP is also non-zero (note that reactive power LMP is $\gamma_i$ when the generator is supplying reactive power and -$\gamma_i$ when the generator is absorbing reactive power).

This shows that when the reactive power LMP is positive (i.e., generating), consumers at that location are encouraged to consume less reactive power to improve the power factor, and when the reactive power LMP is negative (i.e., absorbing), consumers are encouraged to consume more reactive power to improve the power factor.

If a particular generator is operating at its upper capability limit (i.e., $\eta_i^+ \neq 0$), then according to (3.27) the real power LMP does show an additional component (i.e., $-\eta_i^+ K_{i,1}^{max}$). Since $K_{i,1}^{max}$ is negative this component is positive and that increases the real power LMP. Since $\eta_i^+$ also appears in the reactive power LMP, the reactive power price is also high and therefore, the consumers are encouraged to consume less reactive power. This is because, when the generator is operating at its upper capability limit, the reactive power availability is decreased as the generation is increased indicating that any increase in generation is discouraged when there is a reactive power shortage.

On the other hand, if a generator is operating at its lower capability limit (i.e., $\eta_i^- \neq 0$), the real power LMP also has an additional component $\eta_i^- K_{i,1}^{min}$. Since $K_{i,1}^{min}$ is positive this component is positive and that increases the real power LMP. Since $\eta_i^-$ is also appearing in the reactive power LMP, the reactive power LMP is further negative and therefore, the consumers are encouraged to consume more reactive power.

As mentioned earlier, the value of $K_i^Q$ has an important role to play under the competitive market environment and should be specified as a market rule. According to (3.27), if the value of $K_i^Q$ is sufficiently large to make Block 1 Reactive Power alone enough for the dispatch, then the real power LMP will not show the reactive power component. In practice, this is not possible as this requires generators to operate at low power factors leading to low efficiency.

## 3.5 Concluding Remarks

A new reactive power model considering both the capability of the synchronous generator and the fairness of reactive power supply obligation in a competitive market environment has been introduced in this chapter. The model has been proposed for

simultaneous dispatch of real and reactive power. The main features of this model are, (a) generators are not required to supply reactive power free of charge when they are not supplying real power, (b) generators are required to make a minimum amount of reactive power available to the system and this amount is proportional to the real power, (c) the maximum limit of the reactive power is determined by the capability curve of the generator and is dependent on the real power generation.

In summary, the opportunity cost of supplying reactive power is implicitly modeled using the physical constraint related to the rating of the machine. The fairness of reactive power supplying obligation is ensured by the Block 1 Reactive power.

A case study has been presented using the proposed reactive power model . Based on the results, it has been shown that, (a) real power LMP has a reactive power component, (b) LMP for reactive power can also be defined, and (c) sequential dispatch may give rise to an unfair advantage for some participants, and the overall dispatch is also inferior to that of simultaneous dispatch.

# Chapter 4

# Incorporating Dynamic Security in Market Dispatch

The security of a power system is a measure of risk of interruption in an event of a contingency [44]. A secured power system operates without interrupting participant's requirements and survives during a disturbance by settling to a new operating condition in which none of the system physical constraints are violated. Unlike in a single owner electricity industry, maintaining the secure operation of the power system is a challenging task in the competitive electricity market. This is because, each market participant has its own individual interests in maximizing the profits, which could possibly override the system security requirements.

The ISO has the responsibility of ensuring the security of the system, so that sufficient safety margin is maintained in allocating market driven transactions. The security assessment in ensuring the security of the system can be broadly categorized as static security assessment and dynamic security assessment. Static security assessment determines whether the steady state post-disturbance conditions violate any device limits or voltage limits, and dynamic security assessment determines whether the power system reaches an acceptable operating condition after the transition [44].

The static security of the dispatch is easily assured by including the static security constraints in the OPF using sensitivity factors [45]. However, Dynamic Security

Constraints (DSCs) are not used in the traditional OPF, due to the unavailability of such a constraint in the functional form compatible with the OPF.

The current industry practice of determining a generation dispatch that is secure from a dynamic stability point of view is by performing a dynamic stability simulation after solving the OPF [46], [47], or by performing the generation dispatch by some other means. In the former approach, if the solution is unstable against a credible contingency, then the solution is modified, so that the new solution is stable. These modifications are based on engineering experience and judgments using a trial and error approach. This is a time consuming process and cannot guarantee the accuracy of the modified result. In the latter approach, 'nomograms' commonly used in industry are translated into constraints and are used in the dispatch algorithms. However, 'nomograms' are two variable linear approximations to the stability boundary and thus, do not accurately represent the nonlinear nature of such a boundary [48].

Recently, due to the restructuring of the power industry and the availability of fast computers, there has been a motivation towards the development of Dynamic Security Constrained Optimal Power Flow (DSCOPF) programs [49], [50]. In contrast to the traditional sequential OPF, where the solution is adjusted by some other way to ensure the dynamic security, the DSCOPF determines the same in a single step. This is achieved by incorporating the differential equations governing the dynamics of the system into the OPF in the form of difference equations. The disadvantages of this approach are (1) replacing the differential equations by difference equations in solving the problem sacrifices accuracy, (2) there are convergence difficulties due to the introduction of a large number of variables and equations to the original OPF problem [49], [50], and (3) the approach uses simplified models of power system devices to reduce the computational burden.

A novel technique to derive an accurate transient stability boundary for a given credible contingency is proposed in [51], which can be readily used as a constraint in the DSCOPF. In this way, for each credible contingency, a separate DSC can be

derived to incorporate in the OPF. The advantage is that dynamic security of the system for a given credible contingency is modeled in the OPF using a single function of power system variables, and consequently a secured generation dispatch can be obtained in a single step.

The rest of the chapter is organized as follows. A brief introduction to the DSC is given in Section 4.1. The DSCOPF is then presented in Section 4.2. Finally a case study using IEEE New-England 39 bus system is presented in Section 4.3 to demonstrate the effects of DSC in market dispatch.

## 4.1 Dynamic Security Constraint

This section briefly explains how to derive an accurate transient stability boundary for a given credible contingency. A detailed derivation of this method is given in [52], where the theoretical formulation of statistical learning is explained and the application of this theory to IEEE New-England 39 bus system and a 470 bus system is presented.

An operating point of a power system can be uniquely defined using $2 * nbus - 1$ number of variables, where $nbus$ is the number of buses in the system. For example, if the bus voltage magnitudes and bus voltage angles (with angles measured with respect to the reference bus) are known, an operating point can be uniquely defined and every other variable can be calculated. An operating point vector: $\boldsymbol{x}$ in the $2 * nbus - 1$ Euclidean space (where the co-ordinate axes represent the power system variables) can be identified either as stable or as unstable depending on whether the power system is transiently stable or not in an event of a specific contingency [44].

The boundary that separates the transiently stable region from the transiently unstable region is the DSC. The estimated function given in (4.1) is used to approximate the Critical Clearing Time (CCT) corresponding to a given contingency. This approximation is an $m^{th}$ order polynomial function and was estimated from a data sample of $n$ training points. Note that there is an optimum value for m, where the

estimated DSC is most accurate.

$$CCT \approx \sum_{t=1}^{n} \alpha_t (\langle \boldsymbol{x}, \boldsymbol{x}_t \rangle + 1)^m \tag{4.1}$$

where, $\alpha_t$ is a set of real scalers and $\boldsymbol{x}_t$ represents an operating point vector in the transient stability database. The Transient Stability Margin (TSM) is defined as the difference between the CCT and actual fault clearing time: $T_{ac}$ of the contingency. Therefore, the approximated TSM can be written as given below.

$$TSM \approx [\sum_{t=1}^{n} \alpha_t (\langle \boldsymbol{x}, \boldsymbol{x}_t \rangle + 1)^m] - T_{ac} \tag{4.2}$$

An operating point in the stable operating region has a positive TSM. Therefore, the DSC can be written as given in (4.3).

$$f(\boldsymbol{x}) \approx [\sum_{t=1}^{n} \alpha_t (\langle \boldsymbol{x}, \boldsymbol{x}_t \rangle + 1)^m] - T_{ac} \geq 0 \tag{4.3}$$

Similarly, for any other credible contingency, a separate DSC can be derived. The DSC given in (4.3) is differentiable with respect to the operating point variables, and thus suitable for optimization algorithms such as Successive Linear Programming (SLP) and Newton method type algorithms. The derivative of (4.3) with respect to a variable $x_p$ (essentially a voltage magnitude or a bus voltage angle) can be written as,

$$\frac{\partial f(\boldsymbol{x})}{\partial x_p} \approx [\sum_{t=1}^{n} \alpha_t m (\langle \boldsymbol{x}, \boldsymbol{x}_t \rangle + 1)^{m-1} x_{t,p}] \tag{4.4}$$

## 4.2 OPF Problem

After including the above DSC, the OPF problem can be written as given in (4.5)[1].

[1]Note that the reactive power model discussed in Chapter 3 is not considered in this OPF formulation.

Minimize:

$$J = \sum_{i \in I} \sum_{k \in B_i} P_{ik} S^B_{ik} + \sum_{i \in I} Q_{gi} S^Q_i$$

Subject to:

$$\begin{aligned}
&\sum_{k \in B_i} P_{ik} - P_{Di} = \sum_{ij \in T_i} V_i [g_{ij}(V_i - V_j \cos\theta_{ij}) - b_{ij} V_j \sin\theta_{ij}] && \forall i \\
&Q_{gi} - Q_{Di} = \sum_{ij \in T_i} V_i [-b_{ij}(V_i - V_j \cos\theta_{ij}) - g_{ij} V_j \sin\theta_{ij}] && \forall i \\
&0 \le P_{ik} \le P^B_{ik} && \forall i, \forall k \\
&-PF^{max}_{ij} \le PF_{ij} \le PF^{max}_{ij} && \forall (i,j) \subset T \\
&V^{min}_i \le V_i \le V^{max}_i && \forall i \\
&f(\boldsymbol{x}) = [\sum_{t=1}^{n} \alpha_t (\langle \boldsymbol{x}, \boldsymbol{x}_t \rangle + 1)^2] - T_{ac} \ge 0 \\
&PF_{ij} = g_{ij}(V_i^2 - V_i V_j \cos\theta_{ij}) - b_{ij} V_i V_j \sin\theta_{ij} && \forall (i,j) \subset T
\end{aligned} \tag{4.5}$$

In (4.5), only one DSC is included to clearly demonstrate the formulation of the OPF.

Typically, for a given power system, there can be several credible contingencies, which are identified based on historical information. Inclusion of DSCs corresponds to all the credible contingencies, however, increases the complexity of the OPF problem, and hence requires more execution time. On the other hand, neglecting the critical contingencies result in insecure operation of the power system. Each of these contingencies has a different risk associated with ignoring them, which depends on the probability of the contingency occurring and the cost of exposing the power system to that contingency. Thus, choosing the correct credible contingencies is also an important issue, which is not discussed in this thesis.

The Lagrangian for the above problem can be written as:

$$
\begin{aligned}
L = & \sum_{i\in I}\sum_{k\in B_i} P_{ik}S^B_{ik} + \sum_{i\in I} Q_{gi}S^Q_i \\
& + \sum_{i\in I}\lambda_i\left[-\sum_{k\in B_i} P_{ik} + P_{Di} + \sum_{ij\in T_i} V_i[g_{ij}(V_i - V_j\cos\theta_{ij}) - b_{ij}V_j\sin\theta_{ij}]\right] \\
& + \sum_{i\in I}\sigma_i\left[-Q_{gi} + Q_{Di} + \sum_{ij\in T_i} V_i[-b_{ij}(V_i - V_j\cos\theta_{ij}) - g_{ij}V_j\sin\theta_{ij}]\right] \\
& + \sum_{i\in I}\sum_{k\in B_i}\beta^+_{ik}(P_{ik} - P^B_{ik}) + \sum_{i\in I}\sum_{k\in B_i}\beta^-_{ik}(-P_{ik}) \\
& + \sum_{ij\in T}\mu^+_{ij}(PF_{ij} - PF^{max}_{ij}) + \sum_{ij\in T}\mu^-_{ij}(-PF^{max}_{ij} - PF_{ij}) \\
& + \sum_{i\in I}\phi^+_i(V_i - V^{max}_i) + \sum_{i\in I}\phi^-_i(V^{min}_i - V_i) \\
& + \gamma\left[[\sum_{t=1}^{n}\alpha_t(\langle \boldsymbol{x}, \boldsymbol{x}_t\rangle + 1)^2] - T_{ac}\right]
\end{aligned}
\tag{4.6}
$$

By solving the KKT conditions of (4.6), the secured generation dispatch against the considered contingency can be obtained.

## 4.3 Case Studies and Results

This section presents a case study to demonstrate the application of DSC in market dispatch. For the following analysis, a competitive electricity market is modeled for the New-England 39 bus system shown in Appendix A, using price-quantity bids for the generators as given in table 4.1. The reactive power is considered as free from the generators. In the presentation of results, all the real and reactive power values are in MW or MVAr, voltages are in pu, prices are in \$/h and marginal prices are in \$/MWh, \$/MVArh or \$/pu.h depending on the quantity considered. The DSC is incorporated in the OPF as explained in Section 4.2 to ensure the dynamic security of the power system. The maximum and minimum voltage limits of each bus are set to 1.10 pu and 0.90 pu respectively and a line limit of 1000 MW is imposed on each

line. A higher line limit of 1000 MW is purposely selected, so that the effects of the binding line flow constraints can be overridden, as the main objective is to study the effects of the DSC (note that in Section 3.3, the line flow limits were not included in the OPF formulation, to override the line flow constraints).

The contingency considered in this analysis is a three-phase-to-ground fault on the line connecting bus 16 to bus 24 near bus 16 and the fault is cleared by opening the faulted line after 10 cycles. Therefore, in the OPF formulation the lower limit of the DSC is taken as 10 cycles (which is $T_{ac}$) and the upper limit is set to infinity. This implies that if the estimated CCT for a given operating point is greater than or equal to the fault clearing time, then the system is transiently stable.

The OPF was solved using the developed software tool explained in Chapter 6 and the results were validated using GAMS MINOS5 solver [62] by modeling the OPF in the GAMS environment.

Table 4.1: Generator bid data

| Bus | bid 1 | | bid 2 | |
|---|---|---|---|---|
| | $P_{ik}^B$ | $S_{ik}^B$ | $P_{ik}^B$ | $S_{ik}^B$ |
| 30 | 250 | 3.6 | 750 | 5.2 |
| 31 | 500 | 3.2 | 500 | 4.2 |
| 32 | 600 | 4.0 | 400 | 5.4 |
| 33 | 550 | 3.8 | 450 | 7.25 |
| 34 | 500 | 3.75 | 500 | 4.9 |
| 35 | 650 | 3.7 | 350 | 5.05 |
| 36 | 500 | 3.8 | 500 | 7.4 |
| 37 | 550 | 2.9 | 450 | 5.0 |
| 38 | 900 | 3.8 | 100 | 8.2 |
| 39 | 500 | 3.9 | 500 | 4.1 |

The following 3 cases are considered.

1. Case 1: OPF without the DSC
2. Case 2: OPF with the DSC representing the Contingency
3. Case 3: OPF with the DSC representing the same Contingency, but the fault is cleared 1 cycle faster

Table 4.2: Generation dispatch

| Bus | Generation dispatch (MW) | | | | | |
|---|---|---|---|---|---|---|
| | Case 1 | | Case 2 | | Case 3 | |
| | bid 1 | bid 2 | bid 1 | bid 2 | bid 1 | bid 2 |
| 30 | 250.00 | 0.00 | 250.00 | 350.15 | 250.00 | 269.69 |
| 31 | 500.00 | 139.03 | 500.00 | 292.42 | 500.00 | 359.72 |
| 32 | 600.00 | 0.00 | 600.00 | 0.00 | 600.00 | 0.00 |
| 33 | 550.00 | 0.00 | 550.00 | 0.00 | 550.00 | 0.00 |
| 34 | 500.00 | 0.00 | 0.00 | 0.00 | 13.07 | 0.00 |
| 35 | 650.00 | 0.00 | 650.00 | 0.00 | 650.00 | 0.00 |
| 36 | 500.00 | 0.00 | 500.00 | 0.00 | 500.00 | 0.00 |
| 37 | 550.00 | 0.00 | 550.00 | 0.00 | 550.00 | 0.00 |
| 38 | 900.00 | 0.00 | 900.00 | 0.00 | 900.00 | 0.00 |
| 39 | 500.00 | 500.00 | 500.00 | 500.00 | 500.00 | 500.00 |
| **Total dispatch** | **6139.03** | | **6142.57** | | **6142.48** | |
| **Total cost** | **22768.94** | | **23358.93** | | **23272.25** | |

Table 4.2 shows the generation dispatch and the total generation cost for the three cases. In Case 1, there is only one marginal bid, which is at bus 31 (i.e., $2^{nd}$ bid). It can be seen from table 4.2 and the generator bids given in table 4.1, that the generation dispatch in Case 1 is according to the merit order where cheaper bids are dispatched before more expensive bids. This is expected, because in the OPF formulation the transmission line congestion has been overridden. In general, the losses in the system could result in out of merit order dispatch, but in this case the effect of losses has not been significant enough to cause an out of merit order dispatch. The total dispatch is 6139.03 MW and the total cost of generation is 22768.94.

In Case 2, where the OPF is solved with DSC, the generation dispatch deviates from the merit order significantly as seen in table 4.2. The cheaper generation at bus 34 (i.e., $1^{st}$ bid) is not dispatched at all, while the expensive generation at buses 30 (i.e., $2^{nd}$ bid) and 31 (i.e., $2^{nd}$ offer) are partly dispatched. This is expected because the power system operates on the DSC, as evident from the non-zero marginal cost of DSC ($\gamma = 94.51$). The marginal cost of 94.51 implies that the cost of operation can be reduced by that amount if the fault could be cleared 1 cycle faster. Table 4.2 also reveals that the total losses in Case 2 are slightly higher than in Case 1 (note that

the total dispatch in Case 2 is 6142.57 MW, whereas in Case 1 it is 6139.03 MW). Further, the total cost of generation is also increased to 23358.93.

In Case 3, when the breaker operates 1 cycle faster in clearing the fault, the DSC is still binding as seen from the out of merit order dispatch given in table 4.2. It can be seen that the cheaper bid at bus 34 (i.e., $1^{st}$ bid) is now partly dispatched, while there is reduction in expensive bids. The total cost of generation is also reduced by 86.68 (i.e., 23358.93 – 23272.25). This is the amount saved due to the fault being cleared 1 cycle faster, which is approximately equal to the $\gamma$ value in Case 2 (i.e., $\gamma$= 94.51). The slight difference in these two amounts is due to the linearization.

Table 4.3: LMPs for the three cases

| Bus | Case | | | Bus | Case | | | Bus | Case | | |
|---|---|---|---|---|---|---|---|---|---|---|---|
| | 1 | 2 | 3 | | 1 | 2 | 3 | | 1 | 2 | 3 |
| 1 | 4.22 | 5.68 | 5.62 | 14 | 4.20 | 4.97 | 4.98 | 27 | 4.17 | 4.84 | 4.89 |
| 2 | 4.19 | 5.19 | 5.19 | 15 | 4.21 | 4.91 | 4.95 | 28 | 4.05 | 4.75 | 4.81 |
| 3 | 4.22 | 5.11 | 5.11 | 16 | 4.19 | 4.81 | 4.87 | 29 | 4.01 | 4.73 | 4.79 |
| 4 | 4.22 | 5.04 | 5.03 | 17 | 4.19 | 4.88 | 4.92 | 30 | 4.19 | 5.20 | 5.20 |
| 5 | 4.21 | 4.95 | 4.93 | 18 | 4.21 | 4.96 | 4.99 | 31 | 4.20 | 4.20 | 4.20 |
| 6 | 4.20 | 4.89 | 4.88 | 19 | 4.13 | 4.85 | 4.93 | 32 | 4.17 | 4.77 | 4.79 |
| 7 | 4.22 | 5.02 | 5.00 | 20 | 4.14 | 5.02 | 5.11 | 33 | 4.11 | 4.33 | 4.47 |
| 8 | 4.23 | 5.09 | 5.07 | 21 | 4.16 | 4.66 | 4.74 | 34 | 4.11 | 3.46 | 3.75 |
| 9 | 4.23 | 5.63 | 5.57 | 22 | 4.13 | 4.47 | 4.57 | 35 | 4.13 | 4.36 | 4.47 |
| 10 | 4.17 | 4.87 | 4.88 | 23 | 4.13 | 4.47 | 4.57 | 36 | 4.11 | 4.21 | 4.34 |
| 11 | 4.18 | 4.89 | 4.88 | 24 | 4.19 | 4.76 | 4.83 | 37 | 4.04 | 4.97 | 4.96 |
| 12 | 4.18 | 4.94 | 4.93 | 25 | 4.07 | 5.04 | 5.04 | 38 | 3.96 | 4.35 | 4.47 |
| 13 | 4.18 | 4.91 | 4.91 | 26 | 4.11 | 4.87 | 4.91 | 39 | 4.23 | 5.84 | 5.77 |

The LMPs at each bus for the three cases are given in table 4.3. It reveals that except at bus 34, higher LMPs are resulted in Case 2 and Case 3 due to the binding DSC. However at bus 34, LMP in Case 2 and Case 3 are lower than that of Case 1. This is because in Case 2, due to the binding DSC, the cheaper generator at bus 34 is not dispatched, enabling it to cater any increase in load at bus 34. Alternatively, in Case 1, bid 1 at bus 34 is fully dispatched and any increase in load at bus 34 has to be supplied from the next available generator which is bid 2 at bus 31, having a higher bid price. Same explanation can be given for the Case 3 as well.

The difference in generation cost between Case 2 and Case 3 reflects the effects of fast operating circuit breaker, and thus can be used to perform a cost benefit analysis of the fast operating circuit breakers. As pointed out earlier, the results of Case 1 and Case 2 could be further used in determining the associated risk in ignoring the contingency in market dispatch. This could lead to a quantitative decision of whether or not to ignore the particular contingency in market dispatch from the economical and reliability point of view.

## 4.4 Concluding Remarks

The incorporation of the dynamic security constraint in the OPF has been demonstrated in this chapter in order to ensure the dynamic security in market dispatch. This approach has been enabled by the availability of the dynamic security constraint in a functional form. The key advantage is that the dynamic security of the system is modeled in the OPF using a function of power system variables, and consequently a secured generation dispatch can be obtained in one step. The function used is differentiable, and thus suitable for optimization algorithms such as Sequential Linear Programming (SLP) and Newton type algorithms.

The resulting DSCOPF ensures security of the system in the event of the contingency represented by the DSC. In this way, any number of DSCs, each representing a credible contingency, can be incorporated in the OPF. A case study has been presented to demonstrate the effects of DSC on dispatch as well as on LMPs. The results of the case study revealed that the binding DSC constraint has a significant effect on LMPs for the case considered. These results could also be used in performing (a) cost benefit analysis of fast operating circuit breakers, and (b) risk analysis of ignoring the dynamic security in market dispatch.

# Chapter 5

# Analyzing Market Signals

The inclusion of reactive power and Dynamic Security Constraint (DSC) in market dispatch is discussed in Chapters 3 and 4 respectively. Having incorporated these constraints, this chapter investigates different methods to analyze the associated market signals. In fact, market signals are the main driving forces for the market participants to make their operational and investment decisions, which ultimately drive the market toward further competition [2]. Thus, correctly determining these market signals is an important issue in the context of restructured electricity market.

Under the present market operation, LMPs are commonly and extensively used as market signals [12]. The SMD proposed by FERC also advocates the use of LMPs in settling the transactions [5]. This is further insisted upon in their recent documents, subsequent to SMD [6], [7]. LMP at a given node of a power system is the sensitivity of operational cost to the change in load at that node, or in simple terms, the least cost of getting the next increment at that node, while respecting the constraints imposed due to the operational and the capability limits of the power system. Thus, this design provides participants with a clear signal of the price of electricity at each location [8].

While these LMPs provide valuable information at each location of the system, they do not provide a detailed description in terms of contributions coming from transmission losses and different constraints in the power system. The LMP components

proposed in [54] can be used to overcome this problem, as they show the decomposition of LMP into its contributing components due to each binding constraint. This explicit decomposition serves as better market signals for the participants than LMP itself. However, the effects of the losses cannot be seen explicitly from these components. Thus, supplementary information showing the effects of losses on LMPs is necessary in providing full insight to the operation of the electricity market.

A new method of analyzing the network rental components is presented in this chapter by determining those individual components. The network rental is the surplus solely paid by the consumers, and thus, the components of network rental show the breakdown of the network rental to each consumer due to each binding constraint and transmission losses. The key advantage is that the network rental components show how each consumer has actually overpaid due to marginal losses and each binding constraint. Thus, unlike in LMP components, network rental components show the effects of losses explicitly as a separate component.

In order to proceed with this analysis, the components of network rental must be correctly determined. It is however, found that the available methods are not sufficient in determining these components, specially when the general NLP-OPF is considered, where different types of constraints contribute to the network rental. Thus, a new method to determine these network rental components is proposed in this chapter.

This chapter is organized as follows. The existing method of analyzing LMP components is explained in Section 5.1 together with some examples to show how these individual components are calculated. Section 5.2 presents the concept of network rental and then the calculation of components of network rental using a LP-OPF is investigated in Section 5.3. The novel technique to determine the components of network rental based on NLP-OPF is then proposed in Section 5.4. Some case studies are also presented in Section 5.4 for a clear understanding of the proposed method.

## 5.1 LMP Components

### 5.1.1 Traditional Approach

With the present practice, the loss factors and shift factors are used to determine the components of LMP due to losses and congestion[1] [10], [12]. Thus, the LMP at bus $i$ can be expressed as;

$$LMP_i = LMP^{energy} + LMP^{loss} + LMP^{congestion} \tag{5.1}$$

$$LMP_i = \lambda^{ref} - LF_i\lambda^{ref} + \sum_t \mu_t SF_{it} \tag{5.2}$$

where $LF_i$ is the loss factor at bus $i$ and $SF_{it}$ is the generator shift factor at bus $i$ on line $t$. The value of $\mu_t$ indicates the shadow cost of the congested line $t$ whereas $\lambda^{ref}$ denotes the real power price at the reference bus.[2] The summation of the first two components in (5.2) is commonly known as the energy component.

The $LF_i$ indicates the sensitivity of system losses to the change in the injection at bus $i$. In other words, it reflects how system losses will change due to the injection of an additional unit MW. Because the reference bus always makes up for this additional unit MW, loss factors depend on the selection of the reference bus. The $SF_{it}$ shows how the line flow of line $t$ is changed if the injection at bus $i$ is pertubated. Shift factors also depend on the choice of the reference bus. Therefore, by definition the loss factor and the shift factor at the reference bus are zero.

Due to this dependency, the components calculated using this method do not reflect the true contributions of LMP at a node. In other words, even though, the LMPs are independent of the selection of the reference bus, the individual components are not independent of the selection of the reference bus [53]. This dependency indicates that the importance should be kept on the value of each component. The difference between such components at two locations are also dependent on the reference

[1]The line flow limits are the only constraints considered in LP-OPF.

[2]The reference bus is sometimes called as the slack bus. In a power flow solution, the unknown losses in the system are assigned to the reference bus.

bus. For example, the difference between congestion cost components at two different locations does not give any valuable information at all.

The drawback in this approach is due to the fact that transmission losses are balanced at a designated reference bus whereas in reality losses are balanced according to the governing physical laws. This results in different power flows once the location of the reference bus is changed.

However, if losses are approximately balanced at bus level in a predefined way, the energy component and the congestion component can be made reference bus independent for a given loss distribution. The loss distribution factors proposed in [10] allow the explicit balance of losses at each bus, so that the dc power flow solution will be unique irrespective of the choice of the slack bus. The problem however, is that the whole process depends on the predefined loss distribution factors which do not represent how the actual losses are consumed.

The need for the reference bus can be eliminated, once the actual nonlinear power flows are considered (i.e., NLP-OPF). Further, with the NLP-OPF, the reactive power and security issues can be easily incorporated as discussed in Chapters 3 and 4. Unlike in LP-OPF where only line flow constraints are considered, with the NLP-OPF different other binding constraints also contribute to the LMP at a given location. Despite the associated difficulties in dealing with the NLP-OPF, the recent advancements in computing technology allow solving a NLP-OPF in an efficient manner.

A generalized method to unbundle LMP into its contributing components is presented in [54]. This approach is based on post processing the KKT optimality conditions of the NLP-OPF as explained below.

### 5.1.2 Unbundling LMP Based on KKT Conditions

The Lagrangian function for the OPF given in Appendix B (also given in Chapters 3 and 4) can be written in compact form by considering that there are $N$ equality

constraints, $R$ inequality constraints and $M$ decision variables, as,

$$L = f(x) + \sum_{n=1}^{N} \lambda_n^T g_n(x) + \sum_{r=1}^{R} \mu_r^T h_r(x) \tag{5.3}$$

If the optimal solution is known, then all the binding or the active inequality constraints are also known. As the remaining inequality constraints are non-active, the Lagrangian function can be rewritten by eliminating those constraints as given in (5.4).

$$L = f(x) + \sum_{n=1}^{N} \lambda_n^T g_n(x) + \sum_{r=1}^{\overline{R}} \overline{\mu_r}^T \overline{h_r}(x) \tag{5.4}$$

where $\overline{h_r}(x)$ and $\overline{\mu_r}$ are the binding inequality constraints among $h$ and their multipliers among $\mu$ respectively. The KKT optimality conditions of (5.4) can be written as,

$$\frac{\partial L}{\partial x_m} = \frac{\partial f(x)}{\partial x_m} + \sum_{n=1}^{N} \lambda_n^T \frac{\partial g_n(x)}{\partial x_m} + \sum_{r=1}^{\overline{R}} \overline{\mu_r}^T \frac{\partial \overline{h_r}(x)}{\partial x_r} = 0; \quad m = 1, \ldots, M \tag{5.5}$$

$$\frac{\partial L}{\partial \lambda_n} = g_n(x) = 0; \quad n = 1, \ldots, N \tag{5.6}$$

$$\frac{\partial L}{\partial \overline{\mu_r}} = \overline{h_r}(x) = 0; \quad r = 1, \ldots, \overline{R} \tag{5.7}$$

From the Lagrangian function given in (5.4), LMP at bus $i$ can be calculated by taking the partial derivative of L with respect to the load $P_{Di}$ as given by (5.8). This is because, the LMP at bus $i$ is the sensitivity of L to the change in load $P_{Di}$.

$$\begin{aligned}\frac{\partial L}{\partial P_{Di}} =& \sum_{m=1}^{M} \frac{\partial f(x)}{\partial x_m} \frac{\partial x_m}{\partial P_{Di}} + \frac{\partial f(x)}{\partial P_{Di}} \\ &+ \sum_{n=1}^{N} \lambda_n^T \sum_{m=1}^{M} \frac{\partial g_n(x)}{\partial x_m} \frac{\partial x_m}{\partial P_{Di}} + \sum_{n=1}^{N} \lambda_n^T \frac{\partial g_n(x)}{\partial P_{Di}} + \sum_{n=1}^{N} g_n(x) \frac{\partial \lambda_n}{\partial P_{Di}} \\ &+ \sum_{r=1}^{\overline{R}} \overline{\mu_r}^T \sum_{m=1}^{M} \frac{\partial \overline{h_r}(x)}{\partial x_m} \frac{\partial x_m}{\partial P_{Di}} + \sum_{r=1}^{\overline{R}} \overline{\mu_r}^T \frac{\partial \overline{h_r}(x)}{\partial P_{Di}} + \sum_{r=1}^{\overline{R}} \overline{h_r}(x) \frac{\partial \overline{\mu_r}}{\partial P_{Di}}\end{aligned} \tag{5.8}$$

$[\frac{\partial x_m}{\partial P_{Di}}, \frac{\partial \lambda_n}{\partial P_{Di}}, \frac{\partial \overline{\mu_r}}{\partial P_{Di}}]^T$ can be calculated by differentiating (5.5), (5.6), and (5.7) with respect to $P_{Di}$ as given in (5.9), (5.10), and (5.11) respectively.

$$\frac{\partial^2 f(x)}{\partial x_m^2}\frac{\partial x_m}{\partial P_{Di}} + \frac{\partial^2 f(x)}{\partial x_m \partial P_{Di}} + \sum_{n=1}^{N} \lambda_n^T \frac{\partial^2 g_n(x)}{\partial x_m^2}\frac{\partial x_m}{\partial P_{Di}} + \sum_{n=1}^{N} \frac{\partial g_n(x)}{\partial x_m}\frac{\partial \lambda_n}{\partial P_{Di}} + \sum_{n=1}^{N} \lambda_n^T \frac{\partial^2 g_n(x)}{\partial x_m \partial P_{Di}}$$
$$+ \sum_{r=1}^{\overline{R}} \overline{\mu_r}^T \frac{\partial^2 \overline{h_r}(x)}{\partial x_m^2}\frac{\partial x_m}{\partial P_{Di}} + \sum_{r=1}^{\overline{R}} \frac{\partial \overline{h_r}(x)}{\partial x_m}\frac{\partial \overline{\mu_r}^T}{\partial P_{Di}} + \sum_{r=1}^{\overline{R}} \overline{\mu_r}^T \frac{\partial^2 \overline{h_r}(x)}{\partial x_m \partial P_{Di}} = 0$$
$$m = 1, \ldots, M \tag{5.9}$$

$$\sum_{n=1}^{N} \frac{\partial g_n(x)}{\partial x_m}\frac{\partial x_m}{\partial P_{Di}} + \frac{\partial g_n(x)}{\partial P_{Di}} = 0 \quad n = 1, \ldots, N \tag{5.10}$$

$$\sum_{r=1}^{R} \frac{\partial \overline{h_r}(x)}{\partial x_m}\frac{\partial x_m}{\partial P_{Di}} + \frac{\partial \overline{h_r}(x)}{\partial P_{Di}} = 0 \quad r = 1, \ldots, \overline{R} \tag{5.11}$$

Equations (5.9), (5.10), and (5.11) can be written in matrix form as given in (5.12).

$$\begin{bmatrix} \frac{\partial^2 f(x)}{\partial x_m^2} + \sum_n \lambda_n^T \frac{\partial^2 g_n(x)}{\partial x_m^2} + \sum_r \overline{\mu_r}^T \frac{\partial^2 \overline{h_r}(x)}{\partial x_m^2} & \frac{\partial g_n(x)}{\partial x_m} & \frac{\partial \overline{h_r}(x)}{\partial x_m} \\ \frac{\partial g_n^T(x)}{\partial x_m} & 0 & 0 \\ \frac{\partial \overline{h_r}^T(x)}{\partial x_m} & 0 & 0 \end{bmatrix} \begin{bmatrix} \frac{\partial x_m}{\partial P_{Di}} \\ \frac{\partial \lambda_n}{\partial P_{Di}} \\ \frac{\partial \overline{\mu_r}}{\partial P_{Di}} \end{bmatrix}$$
$$= - \begin{bmatrix} \frac{\partial^2 f(x)}{\partial x_m \partial P_{Di}} + \sum_n \lambda_n^T \frac{\partial^2 g_n(x)}{\partial x_m \partial P_{Di}} + \sum_n \frac{\partial \lambda_n^T}{\partial P_{Di}}\frac{\partial g_n(x)}{\partial x_m} + \sum_r \overline{\mu_r}^T \frac{\partial^2 \overline{h_r}(x)}{\partial x_m \partial P_{Di}} + \sum_r \frac{\partial \overline{\mu_r}^T}{\partial P_{Di}}\frac{\partial \overline{h_r}(x)}{\partial x_m} \\ \frac{\partial g_n(x)}{\partial P_{Di}} \\ \frac{\partial \overline{h_r}}{\partial P_{Di}} \end{bmatrix} \tag{5.12}$$

Some terms in the left hand side matrix and the right hand side array of (5.12) are zero, and thus, (5.12) can be simplified as given in (5.13).

$$\begin{bmatrix} \frac{\partial^2 f(x)}{\partial x_m^2} + \sum_n \lambda_n^T \frac{\partial^2 g_n(x)}{\partial x_m^2} & \frac{\partial g_n(x)}{\partial x_m} & \frac{\partial \overline{h_r}(x)}{\partial x_m} \\ \frac{\partial g_n^T(x)}{\partial x_m} & 0 & 0 \\ \frac{\partial \overline{h_r}^T(x)}{\partial x_m} & 0 & 0 \end{bmatrix} \begin{bmatrix} \frac{\partial x_m}{\partial P_{Di}} \\ \frac{\partial \lambda_n}{\partial P_{Di}} \\ \frac{\partial \overline{\mu_r}}{\partial P_{Di}} \end{bmatrix} = - \begin{bmatrix} 0 \\ \frac{\partial g_n(x)}{\partial P_{Di}} \\ 0 \end{bmatrix} \tag{5.13}$$

The left hand side matrix in (5.13) is a Hessian matrix at the optimal solution

with additional rows and columns corresponding to binding inequality constraints, $\overline{h_r}(x)$. The three elements shown in the right hand side vector represent three column vectors. The 0 entries represent column vectors with all the elements equal to zero. $\frac{\partial g_n(x)}{\partial P_{Di}}$ is a column vector with one entry equal to unity and the rest equal to zero. This is because the term $P_{Di}$ appears only in the corresponding power balance equation where $n = i$.

**Remark** *It is important to note that the matrix in (5.13) is always non-singular irrespective of the number of binding constraints, which is explained as follows. If the number of buses and the number of generators in the system are nbus and ngen respectively and assuming there is only a single bid from each generator, then the sub matrix* $[\frac{\partial^2 f(x)}{\partial x_m^2} + \sum \lambda_n^T \frac{\partial^2 g_n(x)}{\partial x_m^2}]$ *in (5.13) has* $2 * ngen + 2 * nbus - 1$ *rows and columns (note that the size of the sub matrix is equal to the number of variables, which include generator bid quantities, reactive power generations, voltage magnitudes, and voltage angles excluding the reference bus), whereas sub matrix* $\frac{\partial g_n(x)}{\partial x_m}$ *has* $2*ngen+2*nbus-1$ *columns (same number of columns as above) and* $2 * nbus$ *rows. Therefore, for the whole matrix to be non-singular, the maximum number of rows of the sub matrix* $\frac{\partial \overline{h_r}(x)}{\partial x_m}$ *(i.e., the number of binding inequality constraints) should be* $2 * ngen - 1$*. If there are no binding line flows or voltage limits, then at least one real power bid is marginal resulting in less than* $2 * ngen - 1$ *rows, and if there are* $r$ *binding constraints, then there should be at least* $r+1$ *marginal generators, resulting in an even fewer number of rows in* $\frac{\partial \overline{h_r}(x)}{\partial x_m}$*. This shows that under any circumstances, the total number of binding constraints does not exceed* $2 * ngen - 1$.

Therefore, by inverting the left hand side matrix and taking the column corresponding to the non-zero element yields the array $[\frac{\partial x_m}{\partial P_{Di}}, \frac{\partial \lambda_n}{\partial P_{Di}}, \frac{\partial \overline{\mu_r}}{\partial P_{Di}}]^T$ as shown in (5.14).

This array shows the sensitivity of the variables in the OPF to the change in load. Thus, these sensitivities also provide some insight to the operation of the electricity

market [55].

$$\begin{bmatrix} \frac{\partial x_m}{\partial P_{Di}} \\ \frac{\partial \lambda_n}{\partial P_{Di}} \\ \frac{\partial \overline{\mu_r}}{\partial P_{Di}} \end{bmatrix} = (-1).\text{corresponding column of} \begin{bmatrix} \frac{\partial^2 f(x)}{\partial x_m^2} + \sum_n \lambda_n^T \frac{\partial^2 g_n(x)}{\partial x_m^2} & \frac{\partial g_n(x)}{\partial x_m} & \frac{\partial \overline{h_r}(x)}{\partial x_m} \\ \frac{\partial g_n^T(x)}{\partial x_m} & 0 & 0 \\ \frac{\partial \overline{h_r}^T(x)}{\partial x_m} & 0 & 0 \end{bmatrix}^{-1} \tag{5.14}$$

Equation (5.8) can be simplified using (5.10) and (5.11) as,

$$\frac{\partial L}{\partial P_{Di}} = \sum_{m=1}^{M} \frac{\partial f(x)}{\partial x_m} \frac{\partial x_m}{\partial P_{Di}} \tag{5.15}$$

This implies that LMP at bus $i$ can be expressed only in terms of contributions from the marginal generators (note that $f(x)$ is only a function of generation and $\frac{\partial x_m}{\partial P_{Di}}$ equals zero for non-marginal generators). The effects of binding constraints are embedded in the contributions of marginal generators.

By removing (5.11) in determining $[\frac{\partial x_m}{\partial P_{Di}}, \frac{\partial \lambda_n}{\partial P_{Di}}, \frac{\partial \overline{\mu_r}}{\partial P_{Di}}]^T$, the contributions of binding constraints can be made explicit as seen from (5.8). Thus, the LMP at bus $i$ can be written as,

$$\frac{\partial L}{\partial P_{Di}} = \sum_{m=1}^{M} \frac{\partial f(x)}{\partial x_m} \frac{\partial x_m}{\partial P_{Di}} + \sum_r \overline{\mu_r}^T \sum_{m=1}^{M} \frac{\partial \overline{h_r}(x)}{\partial x_m} \frac{\partial x_m}{\partial P_{Di}} \tag{5.16}$$

The first term represents the contributions coming from marginal generators whereas the remaining terms under the summation represent the contributions coming from binding inequality constraints.

However, it is important to note that even though the expressions $\sum_m \frac{\partial f(x)}{\partial x_m} \frac{\partial x_m}{\partial P_{Di}}$ and $\sum_r \overline{\mu_r}^T \sum_m \frac{\partial \overline{h_r}(x)}{\partial x_m} \frac{\partial x_m}{\partial P_{Di}}$ have a large number of terms (equal to the number of variables in the OPF problem), most of these terms become zero by application of the chain rule as explained below:

- $f(x)$ is only a function of generation. Therefore, the partial derivative of $f(x)$ with respect to any other variable is zero.

- $\overline{h_r}(x)$ always represents the limit of a variable. Therefore, it has a value only when the partial derivative with respect to the corresponding variable is considered. Further, the value of $\frac{\partial \overline{h_r}(x)}{\partial x_m}$ is either $+1$ or $-1$ depending on whether the constraint is at the maximum limit or the minimum limit.

### 5.1.3 Numerical Example to Evaluate the LMP Components

This section presents some case studies using a 3 bus system to analyze the components of LMP. The single line diagram of the 3 bus system with line parameters are shown in figure 5.1.

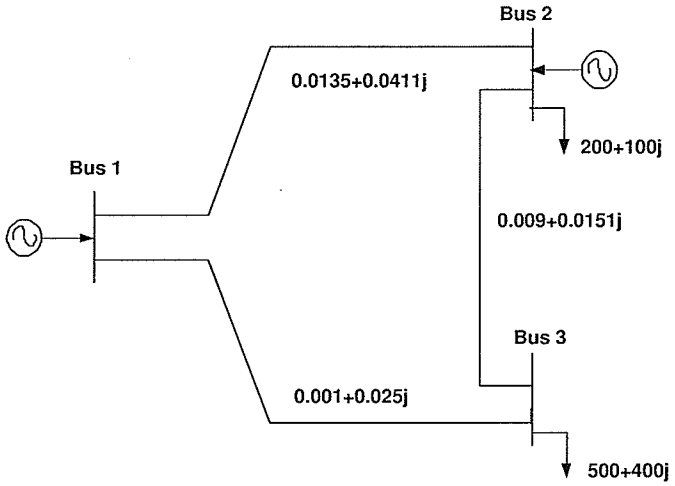


Figure 5.1: 3 bus system

In the presentation of results, all the real and reactive power values are in MW and MVAr, line flows are in MW, voltages are in pu, and marginal prices are in either \$/MWh or \$/MVArh depending on the quantity considered.

There are two generators connected to buses 1 and 2, having bid data given in table 5.1. Buses 2 and 3 have real and reactive loads as shown in figure 5.1. For simplicity, a fixed reactive power cost is considered and the reactive power limits are set to $\pm 1000$ MVAr. The minimum and the maximum voltages at each bus are 0.95 pu and 1.05 pu respectively. The following two cases are considered; in Case 1, line

flow limits are ignored and in Case 2, a line limit of 300 MW is applied to all lines.

Table 5.1: Generator bid data

| Bus | bid 1 | | bid 2 | | $S_i^Q$ |
|---|---|---|---|---|---|
| | $P_{ik}^B$ | $S_{ik}^B$ | $P_{ik}^B$ | $S_{ik}^B$ | |
| 1 | 250 | 3.6 | 750 | 5.2 | 0.1 |
| 2 | 600 | 3.2 | 400 | 4.2 | 0.2 |

The dispatch for the two cases together with shadow costs are shown in table 5.2.

Table 5.2: Dispatch for the Case 1 and Case 2

| | Case 1 | | Case 2 | |
|---|---|---|---|---|
| | Dispatch | $\mu$ | Dispatch | $\mu$ |
| $P_{11}$ | 117.51 | 0.00 | 250.00 | 1.60 |
| $P_{12}$ | 0.00 | -1.60 | 19.89 | 0.00 |
| $P_{21}$ | 600.00 | 0.26 | 442.49 | 0.00 |
| $P_{22}$ | 0.00 | -0.74 | 0.00 | 1.00 |
| $Q_{g1}$ | 535.87 | 0.00 | 487.55 | 0.00 |
| $Q_{g2}$ | 33.84 | 0.00 | 75.06 | 0.00 |
| $V_1$ | 1.05 | 160.49 | 1.05 | 191.11 |
| $V_2$ | 1.00 | 0.00 | 1.00 | 0.00 |
| $V_3$ | 0.96 | 0.00 | 0.96 | 0.00 |
| $PF_{12}$ | -16.78 | 0.00 | 59.49 | 0.00 |
| $PF_{13}$ | 134.30 | 0.00 | 210.40 | 0.00 |
| $PF_{23}$ | 380.79 | 0.00 | 300.00 | 3.72 |

## Case 1

The dispatch and $\mu$ shown in table 5.2 reveal that the voltage at bus 1 is at the maximum limit of 1.05 pu. Bid 1 of generator 2 (i.e., $P_{21}$) is fully dispatched and bid 1 of generator 1 (i.e., $P_{11}$) is partly dispatched. This is expected, as the bids are dispatched according to the merit order in the absence of line flow limits. The reactive power at both generators are partly dispatched.

According to Section 5.1.2, if all the binding constraints are used in formulating (5.12), only the components associated with marginal generators are explicitly shown as given in table 5.3, where $\lambda$ and $\sigma$ denote the LMPs of active and reactive power

respectively. The effect of the binding voltage at bus 1 is embedded in the cost components of marginal generators. These results were validated using a sensitivity analysis, by perturbing the active and reactive load at each bus and measuring the changes in generations.

Table 5.3: Components of LMP for Case 1

| | LMP | $P_{11}$ | $Q_{g1}$ | $Q_{g2}$ |
|---|---|---|---|---|
| $\lambda_1$ | 3.600 | 3.600 | 0.000 | 0.000 |
| $\lambda_2$ | 3.464 | 3.478 | 0.010 | -0.024 |
| $\lambda_3$ | 3.684 | 3.666 | 0.002 | 0.015 |
| $\sigma_1$ | 0.100 | 0.000 | 0.100 | 0.000 |
| $\sigma_2$ | 0.200 | 0.000 | 0.000 | 0.200 |
| $\sigma_3$ | 0.229 | 0.081 | 0.083 | 0.065 |

In order to understand the meaning of quantities shown in Table 5.3, consider the LMP of bus 3. The LMP indicates that the cost of getting an increment unit of real power at bus 3 is 3.684. This cost is made up of the cost of increasing the real power generation at bus 1 (3.666), the cost of increasing reactive power generation at bus 1 (0.002), and the cost of increasing reactive power generation at bus 2 (0.015). Since the generator bid prices are known, the changes in generation can also be determined as: an increase of 1.018 MW (=3.666/3.6) real power generation at bus 1, an increase of 0.02 MVAr (=0.002/0.1) reactive power generation at bus 1, and an increase of 0.075 MVAr(=0.015/0.2) reactive power generation at bus 2.

Table 5.3 also reveals that $\lambda_1$ has only one component, which is due to $P_{11}$. This is as expected, because an additional unit of real power at bus 1 is supplied by the marginal bid which is also at bus 1. The same is true for $\sigma_1$ and $\sigma_2$, due to the fact that reactive power generation is marginal at those two buses. On the other hand, $\lambda_2$, $\lambda_3$, and $\sigma_3$ have contributions from real and reactive power marginal generators due to losses in the network. Note that cost of reactive power is modeled as a fixed cost in this study. If the reactive power is assumed to be free, reactive power components will not appear in LMPs.

Effects of the binding voltage constraint on LMPs can be explicitly obtained by

removing the corresponding constraint from (5.12) as explained in Section 5.1.2. This is shown in table 5.4.

Table 5.4: Components of LMP for Case 1

| | LMP | $P_{11}$ | $Q_{g1}$ | $Q_{g2}$ | $V_1$ |
|---|---|---|---|---|---|
| $\lambda_1$ | 3.600 | 3.600 | 0.000 | 0.000 | 0.000 |
| $\lambda_2$ | 3.464 | 3.535 | -0.016 | 0.037 | -0.092 |
| $\lambda_3$ | 3.684 | 3.623 | 0.022 | -0.035 | 0.073 |
| $\sigma_1$ | 0.100 | 0.000 | 0.100 | 0.000 | 0.000 |
| $\sigma_2$ | 0.200 | 0.000 | 0.000 | 0.200 | 0.000 |
| $\sigma_3$ | 0.229 | 0.019 | 0.110 | 0.000 | 0.100 |

Table 5.4 reveals that the contributions from binding voltage constraint at bus 1 on $\lambda_1$, $\sigma_1$, and $\sigma_2$ are zero. This is as expected, because the binding constraint has no effect if the generator is delivering to a load connected to the same bus.

## Case 2

The difference between this case and Case 1 is that a 300 MW line limit is imposed on all lines. This resulted in $PF_{23}$ reaching the 300 MW limit. The dispatch and $\mu$ shown in table 5.2 indicate that bid 2 at bus 1 (i.e, $P_{12}$) and bid 1 at bus 2 (i.e, $P_{21}$) are partly dispatched (i.e., marginal bids). The reactive power at both generators are also partly dispatched. The binding constraints are the $PF_{23}$ limit and the voltage limit at bus 1. As before, if all the binding constraints are used in formulating (5.12), only the components associated with marginal generators are explicitly shown as given in table 5.5.

Table 5.5: Components of LMP for Case 2

| | LMP | $P_{21}$ | $P_{12}$ | $Q_{g1}$ | $Q_{g2}$ |
|---|---|---|---|---|---|
| $\lambda_1$ | 5.200 | 5.200 | 0.000 | 0.000 | 0.000 |
| $\lambda_2$ | 3.200 | 0.000 | 3.200 | 0.000 | 0.000 |
| $\lambda_3$ | 6.450 | 8.335 | -1.876 | 0.047 | -0.056 |
| $\sigma_1$ | 0.100 | 0.000 | 0.000 | 0.100 | 0.000 |
| $\sigma_2$ | 0.200 | 0.000 | 0.000 | 0.000 | 0.200 |
| $\sigma_3$ | 0.535 | 0.861 | -0.460 | 0.100 | 0.034 |

The value of $\lambda_3$ is greater than the highest bid dispatched, (i.e., 5.2). This is due to the binding line flow $PF_{23}$, which necessitates a reduction in the cheaper bid $P_{21}$, in order to increase the generation from the expensive bid $P_{12}$ in catering the additional unit of real power at bus 3. The negative contribution of $P_{12}$ in $\lambda_3$ (i.e., $-1.876$) shown in table 5.5 also reveals this. Same explanation can be given for the remaining terms as well.

Effects of the binding constraints (i.e., $PF_{23}$ and $V_1$) can be explicitly determined by removing these constraint from (5.12). The resulting components are shown in table 5.6.

Table 5.6: Components of LMP for Case 2

| | LMP | $P_{12}$ | $P_{21}$ | $Q_{g1}$ | $Q_{g2}$ | $V_1$ | $PF_{23}$ |
|---|---|---|---|---|---|---|---|
| $\lambda_1$ | 5.200 | 5.200 | 0.000 | 0.000 | 0.000 | 0.000 | 0.000 |
| $\lambda_2$ | 3.200 | 0.000 | 3.200 | 0.000 | 0.000 | 0.000 | 0.000 |
| $\lambda_3$ | 6.450 | 2.802 | 1.512 | 0.021 | -0.036 | 0.156 | 1.995 |
| $\sigma_1$ | 0.100 | 0.000 | 0.000 | 0.100 | 0.000 | 0.000 | 0.000 |
| $\sigma_2$ | 0.200 | 0.000 | 0.000 | 0.000 | 0.200 | 0.000 | 0.000 |
| $\sigma_3$ | 0.535 | 0.043 | -0.001 | 0.096 | 0.025 | 0.117 | 0.256 |

It can be seen from both cases, that the effects of losses are implicit to the explicitly considered components. Therefore, the effects of losses cannot be seen explicitly as a separate component.

## 5.2 Network Rental

When LMPs are used in settling the transactions, there exists a difference between what consumers pay to the ISO and what generators get paid by the ISO [17]. This difference, which is accumulated with the ISO, is referred to as Network Rental.

Network rental is made up of two components known as the loss rental and the constraint rental. Loss rental is due to the difference between average losses and marginal losses. The marginal cost of real power losses can be twice as high as the average cost of real power losses [56], [57]. This is illustrated in Fig. 5.2. For a given power flow $PF_{ij}$, the average loss is equal to the gradient of line joining the origin and

the corresponding point, which is equal to $\tan\theta$, whereas the marginal loss is equal to the gradient of the tangent line passing through the corresponding point, which is equal to $\tan\alpha$.

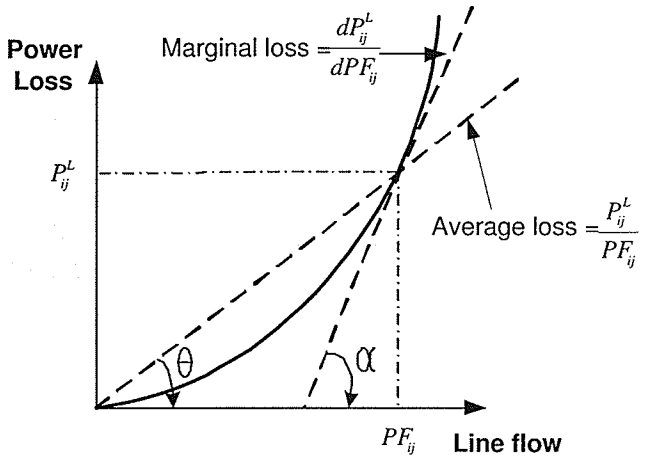


Figure 5.2: Average loss and marginal loss

The other component of the network rental is the constraint rental which is due to operating the power system at the binding constraints imposed by the OPF. The remaining constraints neither influence the outcome of the OPF nor accumulate any constraint rental.

With the present practice of market dispatch based on solving an LP-OPF, the line flows are the only constraints (other than the real power balance equations) considered in the dispatch. Therefore, the constraint rental is only due to the binding line flows. Some markets do not consider transmission losses in market dispatch, and therefore, in those markets no loss rental is accumulated. In some markets, losses are incorporated into the LP-OPF with piece-wise linear approximation for losses [11], while some other markets use loss factors to represent the effects of system losses [12]. However, irrespective of the method of loss modeling, a loss rental will be accumulated with the ISO.

On the other hand, with the NLP-OPF, the inclusion of additional constraints such as voltage limits and DSCs lead to further accumulation of rental with the

ISO in the form of constraint rental. Furthermore, due to reactive power dispatch, additional rental will also be accumulated. This is true even when the reactive power is free from the reactive power sources, because reactive power LMPs at load buses are non-zero due to real power losses associated with transmitting reactive power.

### 5.2.1 Components of Network Rental

As the network rental is an overpayment made by consumers due to the transmission losses and the binding constraints imposed by the OPF, these rental components do provide the detailed description of each consumer's overpayment. However, to get the advantage of this method, the components of network rental must be correctly determined.

From the available methods, the components of network rental due to the dispatch based on the LP-OPF can be easily determined. The constraint rental is only due to the binding line flow constraints, which makes it easier to decompose the network rental. If the losses are modeled approximately as discussed in Section 5.1.1, the resulting loss rental component can also be determined. However, later in this chapter, it is shown that these individual components only show the total rental accumulated with the ISO due to losses or a given binding constraint.

On the other hand, if the dispatch is based on the NLP-OPF, reactive power dispatch and various other binding constraints also contribute to the network rental. Therefore, new approach will be required in determining each consumer's portion of network rental due to each binding constraint and losses.

## 5.3 Calculating the Components of Network Rental Based on LP-OPF

In determining the network rental components, the LP-OPF is first considered by formulating the corresponding OPF and analyzing the price relationships based on

the KKT optimality conditions. To make the analysis clear, cases with and without transmission losses modeled are discussed separately.

### 5.3.1 Neglecting Transmission Losses

When transmission losses are neglected, the power flows can be approximately written either based on dc power flow equations or based on shift factors.

#### a) using dc power flow equations

The nonlinear power flow equations given in (5.17) can be simplified using dc power flow approximations, which state that line resistance is very small compared to line reactance; voltage across the network is around 1.0 pu; and voltage angle differences are small. This leads to the dc power flow equations as given in (5.18).

$$PF_{ij} = g_{ij}(V_i^2 - V_i V_j \cos\theta_{ij}) - b_{ij} V_i V_j \sin\theta_{ij} \qquad \forall (i,j) \subset T \tag{5.17}$$

$$PF_{ij} \simeq -b_{ij}\theta_{ij} \qquad \forall (i,j) \subset T \tag{5.18}$$

Using the above dc power flow equations, the LP-OPF is formulated as given in (5.19).

Minimize:

$$J = \sum_{i \in I} \sum_{k \in B_i} P_{ik} S_{ik}^B$$

Subject to:

$$\sum_{k \in B_i} P_{ik} - P_{Di} - \sum_{ij \in T_i} PF_{ij} = 0 \qquad \forall i \tag{5.19}$$

$$0 \le P_{ik} \le P_{ik}^B \qquad \forall i, \forall k$$

$$-PF_{ij}^{max} \le PF_{ij} \le PF_{ij}^{max} \qquad \forall (i,j) \subset T$$

$$PF_{ij} = -b_{ij}(\theta_i - \theta_j) \qquad \forall (i,j) \subset T$$

The Lagrangian for the above problem can be written as:

$$\begin{aligned} L = & \sum_{i\in I}\sum_{k\in B_i} P_{ik}S^B_{ik} + \lambda_i\left[[\sum_{k\in B_i} P_{ik} - P_{Di}] - \sum_{ij\in T_i} PF_{ij}\right] \\ & + \sum_{i\in I}\sum_{k\in B_i} \beta^+_{ik}(P_{ik} - P^B_{ik}) + \sum_{i\in I}\sum_{k\in B_i} \beta^-_{ik}(-P_{ik}) \\ & + \sum_{ij\in T} \mu^+_{ij}(PF_{ij} - PF^{max}_{ij}) + \sum_{ij\in T} \mu^-_{ij}(-PF^{max}_{ij} - PF_{ij}) \\ & + \sum_{ij\in T} \gamma_{ij}[PF_{ij} + b_{ij}(\theta_i - \theta_j)] \end{aligned} \tag{5.20}$$

The price relationships can be obtained by considering the following KKT conditions of (5.20).

$$\frac{\partial L}{\partial P_{ik}} = S^B_{ik} - \lambda_i + \beta_{ik} = 0 \qquad \forall i, \forall k \tag{5.21}$$

$$\frac{\partial L}{\partial PF_{ij}} = \lambda_i + \mu_{ij} - \gamma_{ij} = 0 \qquad \forall (i,j) \subset T \tag{5.22}$$

$$\frac{\partial L}{\partial \theta_i} = \sum_{ij\in T_i} b_{ij}\gamma_{ij} - \sum_{ij\in T_i} b_{ji}\gamma_{ji} = 0 \qquad \forall i \tag{5.23}$$

Thus, the Network Rental (NR) can be calculated as,

$$\begin{aligned} NR &= -\sum_{i\in I} \lambda_i[P_{Di} - \sum_{k\in B_i} P_{ik}] = -\sum_{i\in I}[\lambda_i \sum_{ij\in T_i} PF_{ij}] \\ &= \sum_{i\in I}\sum_{ij\in T_i} [\mu_{ij} - \gamma_{ij}]PF_{ij} = \sum_{ij\in T} \mu_{ij}PF_{ij} - \sum_{i\in I}\sum_{ij\in T_i} \gamma_{ij}PF_{ij} \\ &= \sum_{ij\in T} \mu_{ij}PF_{ij} + \sum_{i\in I}\sum_{ij\in T_i} \gamma_{ij}b_{ij}(\theta_i - \theta_j) \\ &= \sum_{ij\in T} \mu_{ij}PF_{ij} + \sum_{i\in I} \theta_i \sum_{ij\in T_i} \gamma_{ij}b_{ij} - \sum_{i\in I}\sum_{ij\in T_i} \gamma_{ij}b_{ij}\theta_j \\ &= \sum_{ij\in T} \mu_{ij}PF_{ij} + \sum_{i\in I} \theta_i\{\sum_{ij\in T_i} [\gamma_{ij}b_{ij} - \gamma_{ji}b_{ji}]\} \\ &= \sum_{ij\in T} \mu_{ij}PF_{ij} + \sum_{i\in I} \theta_i[0] \\ &= \sum_{ij\in T} \mu_{ij}PF_{ij} \end{aligned} \tag{5.24}$$

This reveals that the rental is due to all the binding line flow constraints. Since the transmission losses are not considered, no loss rental is accumulated. Further, for each binding line flow constraint, the rental component is equal to the Lagrange multiplier associated with that constraint (i.e., shadow cost), times the limit of the line flow (i.e., $\mu_{ij}.PF_{ij}^{max/min}$). This asserts that the higher the shadow cost of a given binding constraint, the greater will be the network rental collected due to that constraint.

## b) using shift factors

Instead of using dc power flow equations, the line flows can also be approximately written using shift factors [10] as shown in (5.25). To eliminate the confusion in notation, *subscript* $t$ is used to denote the transmission line, instead of $ij$. Thus, $SF_{it}$ shows how the line flow of line $t$ is changed, if the injection at bus $i$ is pertubated.

$$PF_t = \sum_{i \in I} SF_{it}[\sum_{k \in B_i} P_{ik} - P_{Di}] \qquad \forall t \subset T \tag{5.25}$$

Thereby, the LP-OPF can be reformulated in the following way.

Minimize:

$$J = \sum_{i \in I} \sum_{k \in B_i} P_{ik} S_{ik}^B$$

Subject to:

$$\sum_{i \in I} [\sum_{k \in B_i} P_{ik} - P_{Di}] = 0 \tag{5.26}$$

$$0 \leq P_{ik} \leq P_{ik}^B \qquad \forall i, \forall k$$

$$-PF_t^{max} \leq PF_t \leq PF_t^{max} \qquad \forall t \subset T$$

$$PF_t = \sum_{i \in I} SF_{it}[\sum_{k \in B_i} P_{ik} - P_{Di}] \qquad \forall t \subset T$$

The Lagrangian for the above problem becomes:

$$\begin{aligned} L = & \sum_{i\in I}\sum_{k\in B_i} P_{ik}S^B_{ik} + \lambda\left[\sum_{i\in I}[\sum_{k\in B_i} P_{ik} - P_{Di}]\right] \\ & + \sum_{i\in I}\sum_{k\in B_i}\beta^+_{ik}(P_{ik} - P^B_{ik}) + \sum_{i\in I}\sum_{k\in B_i}\beta^-_{ik}(-P_{ik}) \\ & + \sum_{t\in T}\mu^+_t(PF_t - PF^{max}_t) + \sum_{t\in T}\mu^-_t(-PF^{max}_t - PF_t) \\ & + \sum_{t\in T}\gamma_t\left[PF_t - \sum_{i\in I} SF_{it}[\sum_{k\in B_i} P_{ik} - P_{Di}]\right] \end{aligned} \tag{5.27}$$

The price relationships can be obtained by considering the following KKT conditions of (5.27).

$$\frac{\partial L}{\partial P_{ik}} = S^B_{ik} - \lambda + \beta_{ik} - \sum_{t\in T}\gamma_t SF_{it} = 0 \qquad \forall i, \forall k \tag{5.28}$$

$$\frac{\partial L}{\partial PF_t} = \mu_t + \gamma_t = 0 \qquad \forall t \subset T \tag{5.29}$$

The Lagrange multiplier $\beta_{ik}$ is the shadow cost of the supply bid $P^B_{ik}$. Therefore, $S^B_{ik}+\beta_{ik}$ indicates the price at bus $i$ for all $k$, and hence, the LMP at bus $i$, $\lambda_i$ becomes,

$$S^B_{ik} + \beta_{ik} = \lambda_i = \lambda - \sum_{t\in T}\mu_t SF_{it} \tag{5.30}$$

Thus, the Network Rental (NR) can be calculated as,

$$\begin{aligned} NR &= -\sum_{i\in I}\lambda_i[P_{Di} - \sum_{k\in B_i} P_{ik}] = -\sum_{i\in I}[\lambda - \sum_{t\in T}\mu_t SF_{it}][P_{Di} - \sum_{k\in B_i} P_{ik}] \\ &= -\lambda\sum_{i\in I}[P_{Di} - \sum_{k\in B_i} P_{ik}] + \sum_{i\in I}\sum_{t\in T}\mu_t SF_{it}[P_{Di} - \sum_{k\in B_i} P_{ik}] \\ &= 0 + \sum_{t\in T}\sum_{i\in I}\mu_t SF_{it}[P_{Di} - \sum_{k\in B_i} P_{ik}] \\ &= \sum_{t\in T}\mu_t PF_t \end{aligned} \tag{5.31}$$

Once again, (5.31) reveals that the calculated network rental is entirely due to binding line flow constraints. However, since the two OPF formulations given in (5.19) and (5.26) are different, the calculated rental will be numerically different for the two cases. Furthermore, the calculated rental in this case is reference bus dependent, which is a serious drawback of this method [10].

### 5.3.2 Including Transmission Losses

Due to the vast geographical span of the power system, transmission losses can cause significant impact on optimal generation dispatch depending on the topology of the power system network. Therefore, in some electricity markets losses are incorporated into the LP-OPF by piece-wise linear approximation for losses [11]. Some other markets use loss factors to represent the effects of the system losses [12]. Therefore, in these markets, rental due to losses is also accumulated in addition to rental due to binding line flow constraints, as shown below.

#### a) using dc power flow equations and piece-wise linear loss equation

The transmission loss in line $ij$, $PF_{ij}^{L}$ can be calculated as,

$$\begin{aligned} PF_{ij}^{L} &= PF_{ij} + PF_{ji} \\ PF_{ij}^{L} &= g_{ij}(2V_i^2 + 2V_j^2 - 2V_iV_j\cos\theta_{ij}) \end{aligned} \tag{5.32}$$

For small angle differences and voltages close to 1.0 pu, (5.32) can be simplified as,

$$\begin{aligned} PF_{ij}^{L} &\simeq 2g_{ij}(1-\cos\theta_{ij}) \\ &\simeq g_{ij}\theta_{ij}^2 \end{aligned} \tag{5.33}$$

This indicates that in the most simple form, the transmission losses are quadratic in nature and hence, the nonlinear loss term $PF_{ij}^{L}$ can not be linearized for the whole range of line flow.

Thus, the losses can be incorporated in the line flow $PF_{ij}$ as,

$$\begin{aligned} PF_{ij} &= g_{ij}(V_i^2 - V_iV_j\cos\theta_{ij}) - b_{ij}V_iV_j\sin\theta_{ij} \\ &= g_{ij}(1-\cos\theta_{ij}) - b_{ij}\sin\theta_{ij} \\ &= -b_{ij}(\theta_i - \theta_j) + \frac{1}{2}PF_{ij}^{L} \end{aligned} \tag{5.34}$$

As pointed out earlier, (5.34) is no longer a linear equation, and cannot be used in the LP-OPF. However, piecewise linear approximation of $PF_{ij}^{L}$ as shown in figure 5.3 can be used to make it suitable for a LP-OPF. In this way, the nonlinear loss function is approximated by a set of linear segments. Different mathematical techniques can be used to obtain these line segments from the nonlinear loss curve [13].

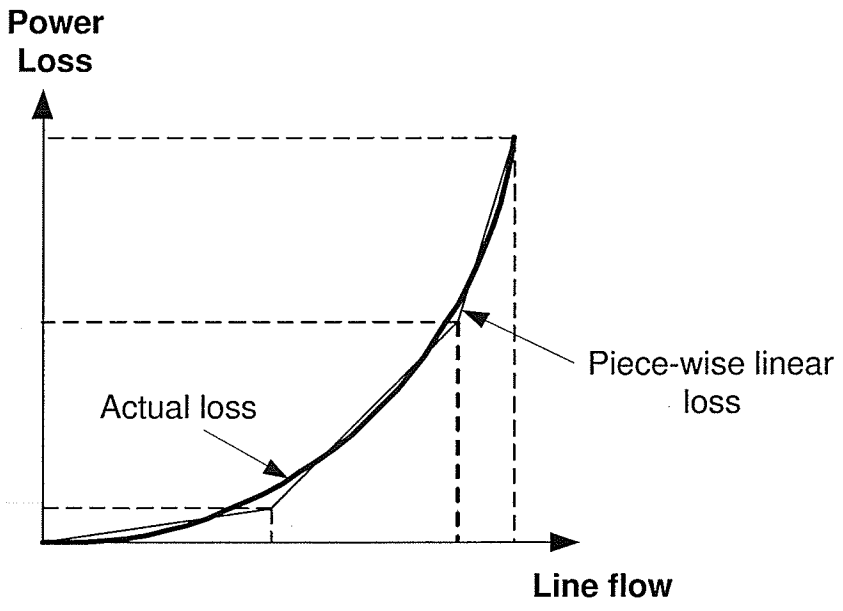


Figure 5.3: Piece-wise linear approximation for losses

Thereby, the OPF can be formulated as:

Minimize:

$$J = \sum_{i \in I} \sum_{k \in B_i} P_{ik} S^B_{ik}$$

Subject to:

$$\sum_{k \in B_i} P_{ik} - P_{Di} - \sum_{ij \in K_i} PF_{ij} = 0 \qquad \forall i \tag{5.35}$$

$$0 \leq P_{ik} \leq P^B_{ik} \qquad \forall i, \forall k$$

$$-PF^{max}_{ij} \leq P_{ij} \leq PF^{max}_{ij} \qquad \forall (i,j) \subset T$$

$$PF_{ij} = -b_{ij}(\theta_i - \theta_j) + \frac{1}{2} PF^L_{ij} \qquad \forall (i,j) \subset T$$

The Lagrangian for the above problem can be written as:

$$\begin{aligned} L = & \sum_{i \in I} \sum_{k \in B_i} P_{ik} S^B_{ik} + \lambda_i \left[ [\sum_{k \in B_i} P_{ik} - P_{Di}] - \sum_{ij \in T_i} PF_{ij} \right] \\ & + \sum_{i \in I} \sum_{k \in B_i} \beta^+_{ik} (P_{ik} - P^B_{ik}) + \sum_{i \in I} \sum_{k \in B_i} \beta^-_{ik} (-P_{ik}) \\ & + \sum_{ij \in T} \mu^+_{ij} (PF_{ij} - PF^{max}_{ij}) + \sum_{ij \in T} \mu^-_{ij} (-PF^{max}_{ij} - PF_{ij}) \\ & + \sum_{ij \in T} \gamma_{ij} [PF_{ij} + b_{ij}(\theta_i - \theta_j) - \frac{1}{2} PF^L_{ij}] \end{aligned} \tag{5.36}$$

The price relationships can be obtained by considering the following KKT conditions of (5.36).

$$\frac{\partial L}{\partial P_{ik}} = S^B_{ik} - \lambda_i + \beta_{ik} = 0 \qquad \forall i, \forall k \tag{5.37}$$

$$\frac{\partial L}{\partial PF_{ij}} = \lambda_i + \mu_{ij} - \gamma_{ij} = 0 \qquad \forall (i,j) \subset T \tag{5.38}$$

$$\frac{\partial L}{\partial \theta_i} = \sum_{ij \in T_i} \gamma_{ij} [b_{ij} - \frac{1}{2} \frac{\partial PF^L_{ij}}{\partial \theta_i}] - \sum_{ij \in T_i} \gamma_{ji} [b_{ji} - \frac{1}{2} \frac{\partial PF^L_{ji}}{\partial \theta_i}] = 0 \qquad \forall i \tag{5.39}$$

Equation (5.39) can be further simplified as,

$$\sum_{ij\in T_i} \gamma_{ij}[b_{ij} - \frac{1}{2}\frac{\partial PF_{ij}^L}{\partial \theta_i}] - \sum_{ij\in T_i} \gamma_{ji}[b_{ji} - \frac{1}{2}\frac{\partial PF_{ji}^L}{\partial \theta_i}] = 0$$

$$\sum_{ij\in T_i} [\gamma_{ij} b_{ij} - \gamma_{ji} b_{ji}] = \frac{1}{2}\sum_{ij\in T_i} [\gamma_{ij}\frac{\partial PF_{ij}^L}{\partial \theta_i} - \gamma_{ji}\frac{\partial PF_{ji}^L}{\partial \theta_i}] \tag{5.40}$$

Thus, the Network Rental (NR) can be calculated as,

$$\begin{aligned} NR &= -\sum_{i\in I} \lambda_i [P_{Di} - \sum_{k\in B_i} P_{ik}] = -\sum_{i\in I} [\lambda_i \sum_{ij\in T_i} PF_{ij}] \\ &= \sum_{i\in I}\sum_{ij\in T_i} [\mu_{ij} - \gamma_{ij}] PF_{ij} = \sum_{ij\in T} \mu_{ij} PF_{ij} - \sum_{i\in I}\sum_{ij\in T_i} \gamma_{ij} PF_{ij} \\ &= \sum_{ij\in T} \mu_{ij} PF_{ij} - \sum_{i\in I}\sum_{ij\in T_i} \gamma_{ij}[-b_{ij}(\theta_i - \theta_j) + \frac{1}{2} PF_{ij}^L] \\ &= \sum_{ij\in T} \mu_{ij} PF_{ij} + A \end{aligned} \tag{5.41}$$

Equation (5.41) indicates that there are two components of network rental. Close examination reveals that the first term shows the constraint rental due to all binding line flow constraints and the second term denoted by $A$ shows the accumulated loss rental. This can be further clarified by simplifying the expression of $A$ in (5.41) using the relationship obtained in (5.40). This simplified expression of A also conforms that loss rental is proportional to the difference between marginal loss and average loss.

$$\begin{aligned} A &= -\sum_{i\in I}\sum_{ij\in T_i} \gamma_{ij}[-b_{ij}(\theta_i - \theta_j) + \frac{1}{2} PF_{ij}^L] \\ &= \sum_{i\in I}\left[\sum_{ij\in T_i} \gamma_{ij} b_{ij}\theta_i - \sum_{ij\in T_i} \gamma_{ij} b_{ij}\theta_j\right] - \frac{1}{2}\sum_{ij\in T} [\gamma_{ij} PF_{ij}^L + \gamma_{ji} PF_{ji}^L] \\ &= \sum_{i\in I} \theta_i [\sum_{ij\in T_i} \gamma_{ij} b_{ij} - \sum_{ij\in T_i} \gamma_{ji} b_{ji}] - \frac{1}{2}\sum_{ij\in T} [\gamma_{ij} PF_{ij}^L + \gamma_{ji} PF_{ji}^L] \\ &= \sum_{i\in I} \theta_i \left[\frac{1}{2}\sum_{ij\in T_i} [\gamma_{ij}\frac{\partial PF_{ij}^L}{\partial \theta_i} - \gamma_{ji}\frac{\partial PF_{ji}^L}{\partial \theta_i}]\right] - \frac{1}{2}\sum_{ij\in T} [\gamma_{ij} PF_{ij}^L + \gamma_{ji} PF_{ji}^L] \end{aligned}$$

## b) using shift factors and loss factors

Instead of using the piecewise linear loss approximation as explained above, the losses can alternatively be incorporated using loss factors as shown below.

$$\sum_{i\in I}[\sum_{k\in B_i} P_{ik} - P_{Di}] - P^L = 0$$

$$P^L - \sum_{i\in I} LF_i[\sum_{k\in B_i} P_{ik} - P_{Di}] + \mathit{offset} = 0$$

A base case power flow is used to determine the actual power loss, $P^L$. Then, based on the loss factors, the linearized offset of loss is determined (this step is required to offset the difference between the actual loss and the linearized loss based on loss factors).

Thereby, the OPF can be formulated as:

Minimize:

$$J = \sum_{i\in I}\sum_{k\in B_i} P_{ik} S^B_{ik}$$

Subject to:

$$\begin{aligned}
&\sum_{i\in I}[\sum_{k\in B_i} P_{ik} - P_{Di}] - P^L = 0 && \\
&P^L - \sum_{i\in I} LF_i[\sum_{k\in B_i} P_{ik} - P_{Di}] + \mathit{offset} = 0 && \\
&0 \le P_{ik} \le P^B_{ik} && \forall i, \forall k \\
&-PF^{max}_t \le PF_t \le PF^{max}_t && \forall t \subset T \\
&PF_t = \sum_{i\in I} SF_{it}[\sum_{k\in B_i} P_{ik} - P_{Di}] && \forall t \subset T
\end{aligned} \tag{5.42}$$

The Lagrangian for the above problem can be written as:

$$
\begin{aligned}
L = & \sum_{i\in I}\sum_{k\in B_i} P_{ik}S^B_{ik} + \lambda\left[\sum_{i\in I}[\sum_{k\in B_i} P_{ik} - P_{Di}] - P^L\right] \\
& + \psi\left[P^L + \sum_{i\in I} LF_i[\sum_{k\in B_i} P_{ik} + P_{Di}] + offset\right] \\
& + \sum_{i\in I}\sum_{k\in B_i}\beta^+_{ik}(P_{ik} - P^B_{ik}) + \sum_{i\in I}\sum_{k\in B_i}\beta^-_{ik}(-P_{ik}) \\
& + \sum_{t\in T}\mu^+_t(PF_t - PF^{max}_t) + \sum_{t\in T}\mu^-_t(-PF^{max}_t - PF_t) \\
& + \sum_{t\in T}\gamma_t\left[PF_t - \sum_{i\in I} SF_{it}[\sum_{k\in B_i} P_{ik} - P_{Di}]\right]
\end{aligned} \tag{5.43}
$$

The price relationships can be obtained by considering the following KKT conditions of (5.43).

$$\frac{\partial L}{\partial P_{ik}} = S^B_{ik} - \lambda - \psi LF_i + \beta^+_{ik} - \beta^-_{ik} - \sum_{t\in T}\gamma_t SF_{it} = 0 \qquad \forall i, \forall k \tag{5.44}$$

$$\frac{\partial L}{\partial PF_t} = \mu^+_t - \mu^-_t + \gamma_t = 0 \qquad \forall t \subset T \tag{5.45}$$

$$\frac{\partial L}{\partial P^L} = \lambda - \psi = 0 \tag{5.46}$$

Therefore,

$$S^B_{ik} + \beta_{ik} = \lambda - \lambda LF_i - \sum_{t\in T_i}\mu_t SF_{it} = \lambda_i \tag{5.47}$$

Thus, the Network Rental (NR) can be calculated as,

$$
\begin{aligned}
NR &= -\sum_{i\in I}\lambda_i[P_{Di} - \sum_{k\in B_i} P_{ik}] \\
&= -\sum_{i\in I}[\lambda - \lambda LF_i - \sum_{t\in T_i}\mu_t SF_{it}][P_{Di} - \sum_{k\in B_i} P_{ik}] \\
&= -\lambda\sum_{i\in I}[P_{Di} - \sum_{k\in B_i} P_{ik}] + \lambda\sum_{i\in I} LF_i[P_{Di} - \sum_{k\in B_i} P_{ik}] + \sum_{i\in I}\sum_{t\in T_i}\mu_t SF_{it}[P_{Di} - \sum_{k\in B_i} P_{ik}] \\
&= -\lambda P^L + \lambda P^{L\_mag} + \sum_{t\in T_i}\sum_{i\in I}\mu_t SF_{it}[P_{Di} - \sum_{k\in B_i} P_{ik}] \\
&= \lambda[P^{L\_mag} - P^L] + \sum_{t\in T_i}\mu_t PF_t
\end{aligned} \tag{5.48}
$$

Once again, the first term in (5.48) shows the accumulated loss rental and the second term shows the accumulated constraint rental due to binding line flows. The important point is that the calculated rental is reference bus dependent. This is because, as discussed in Section 5.1.1, the losses are balanced at a designated slack bus. Thus, once the slack bus is changed, the calculated rental components appearing in (5.48) are also changed. This can be eliminated by introducing the loss distribution factors as explained in the next formulation.

### c) using shift factors, loss factors and loss distribution factors

If the losses are balanced at the bus level using loss distribution factors [10] (which indicate the fraction of losses to be balanced at each bus), the calculated rental components appearing in (5.48) can be made reference bus independent, as shown below.

$$PF_t = \sum_{i \in I} SF_{it}[\sum_{k \in B_i} P_{ik} - P_{Di} - LDF_i P^L] \qquad \forall t \subset T$$

where, $LDF_i$ is the loss distribution factor at bus $i$, which shows the assigned portion of losses to bus $i$. Further, $\sum_i LDF_i = 1$. Thus, the OPF can be formulated as:

Minimize:

$$J = \sum_{i \in I} \sum_{k \in B_i} P_{ik} S^B_{ik}$$

Subject to:

$$\begin{aligned}
&\sum_{i \in I}[\sum_{k \in B_i} P_{ik} - P_{Di}] - P^L = 0 \\
&P^L - \sum_{i \in I} LF_i[\sum_{k \in B_i} P_{ik} - P_{Di}] + offset = 0 \\
&0 \le P_{ik} \le P^B_{ik} && \forall i, \forall k \\
&-PF^{max}_t \le PF_t \le PF^{max}_t && \forall t \subset T \\
&PF_t = \sum_{i \in I} SF_{it}[\sum_{k \in B_i} P_{ik} - P_{Di} - LDF_i P^L] && \forall t \subset T
\end{aligned} \tag{5.49}$$

The Lagrangian for the above problem can be written as:

$$\begin{aligned} L = & \sum_{i\in I}\sum_{k\in B_i} P_{ik}S^B_{ik} \\ & + \lambda\left[\sum_{i\in I}[\sum_{k\in B_i} P_{ik} - P_{Di}] - P^L\right] \\ & + \psi\left[P^L + \sum_{i\in I} LF_i[\sum_{k\in B_i} P_{ik} + P_{Di}] + offset\right] \\ & + \sum_{i\in I}\sum_{k\in B_i}\beta^+_{ik}(P_{ik} - P^B_{ik}) + \sum_{i\in I}\sum_{k\in B_i}\beta^-_{ik}(-P_{ik}) \\ & + \sum_{t\in T}\mu^+_t(PF_t - PF^{max}_t) + \sum_{t\in T}\mu^-_t(-PF^{max}_t - PF_t) \\ & + \sum_{t\in T}\gamma_t\left[PF_t - \sum_{i\in I} SF_{it}[\sum_{k\in B_i} P_{ik} - P_{Di} - LDF_iP^L]\right] \end{aligned} \tag{5.50}$$

The price relationships can be obtained by considering the following KKT conditions of (5.50).

$$\frac{\partial L}{\partial P_{ik}} = S^B_{ik} - \lambda - \psi LF_i + \beta^+_{ik} - \beta^-_{ik} - \sum_{t\in T}\gamma_t SF_{it} = 0 \qquad \forall i, \forall k \tag{5.51}$$

$$\frac{\partial L}{\partial PF_t} = \mu^+_t - \mu^-_t + \gamma_t = 0 \qquad \forall t \subset T \tag{5.52}$$

$$\frac{\partial L}{\partial P^L} = \lambda - \psi - \sum_{t\in T}\gamma_t\sum_{i\in I} SF_{it}LDF_i = 0 \tag{5.53}$$

Therefore,

$$S^B_{ik} + \beta_{ik} = \lambda - \psi LF_i - \sum_{t\in T}\mu_t SF_{it} = \lambda_i \tag{5.54}$$

The above expression for $\lambda_i$ can be simplified as,

$$\lambda_i = \psi - \psi LF_i - \sum_{t\in T}\mu_t SF_{it} + \sum_{t\in T}\mu_t SF_{it}LDF_i \tag{5.55}$$

$$\lambda_i = \psi - \psi LF_i - [1 - LDF_i]\sum_{t\in T}\mu_t SF_{it} \tag{5.56}$$

Thus, the Network Rental (NR) can be calculated as,

$$
\begin{aligned}
NR &= -\sum_{i\in I}\lambda_i[P_{Di} - \sum_{k\in B_i} P_{ik}] \\
&= -\sum_{i\in I}\left[\psi - \psi LF_i - [1-LDF_i]\sum_{t\in T}\mu_t SF_{it}\right][P_{Di} - \sum_{k\in B_i} P_{ik}] \\
&= -\psi\sum_{i\in I}[P_{Di} - \sum_{k\in B_i} P_{ik}] + \psi\sum_{i\in I} LF_i[P_{Di} - \sum_{k\in B_i} P_{ik}] \\
&\qquad + \sum_{i\in I}\sum_{t\in T}[1-LDF_i]\mu_t SF_{it}[P_{Di} - \sum_{k\in B_i} P_{ik}] \\
&= -\psi P^L + \psi P^{L\_mag} + \sum_{t\in T}\sum_{i\in I}[1-LDF_i]\mu_t SF_{it}[P_{Di} - \sum_{k\in B_i} P_{ik}] \\
&= \psi[P^{L\_mag} - P^L] + \sum_{t\in T}\mu_t PF_t
\end{aligned}
\tag{5.57}
$$

Expression (5.57) is very much similar to (5.48), except it can be shown that the calculated rental components appearing in (5.57) are reference bus independent [10]. The problem, however, is that the whole process depends on these predefined loss distribution factors, which do not represent how the actual losses are consumed.

### 5.3.3 Discussion

Based on the above LP based formulations, it can be seen that the calculated components of network rental do not show each consumer's contribution due to each binding constraint explicitly. In other words, these components only show the total rental paid by all the consumers due to losses and each binding constraint. Since the LP-OPF is considered, the rental components due to reactive power dispatch and other system constraints cannot be determined.

As pointed out earlier, to be considered as better market signals, the portion of network rental to each consumer due to each binding constraint and losses must be correctly determined. Thus, a new method is required to determine these network rental components, especially when the general NLP-OPF is considered in representing the actual operation of the system. The next section presents the proposed method of determining the rental components paid by each consumer due to losses

and each binding constraint, by considering the general NLP-OPF.

## 5.4 Proposed Method of Calculating the Components of Network Rental

The proposed method of computing the components of network rental is developed in two stages. In the first stage, necessary equations for LMP difference between two buses is developed for a network with only one load. This LMP difference is expressed in terms of the contributing components, which include the effects of losses and binding constraints as separate terms, and can be written for any two buses. Then, these LMP differences are used to determine the components of the network rental paid by the single consumer by expressing the network rental in terms of LMP differences between generator buses and the load bus. In the second stage, the single load bus approach is extended to a general case of multiple load buses by tracing the power flow to identify how each load and the associated losses are supplied by the generators in the system.

### 5.4.1 Determining the LMP Difference Between Two Buses in Terms of Contributing Components

In this section, the first stage of the proposed method is explained, in which the KKT optimality conditions obtained from the NLP-OPF are used to determine the LMP difference between two buses in terms of contributing components.

As before, the OPF is first formulated and the KKT optimality conditions are analyzed to determine the LMP relationships. This NLP-OPF formulation is given in (5.58)[3].

[3]Note that in order to clearly explain the proposed method, the reactive power model and the DSC discussed in Chapters 3 and 4 are not considered in this OPF formulation. However, these constraints are considered in the case study presented in Chapter 7.

Minimize:

$$J = \sum_{i \in I} \sum_{k \in B_i} P_{ik} S^B_{ik} + \sum_{i \in I} Q_{gi} S^Q_i$$

Subject to:

$$\begin{aligned}
&\sum_{i \in I} [\sum_{k \in B_i} P_{ik} - P_{Di}] - P^L = 0 \\
&\sum_{i \in I} [Q_{gi} - Q_{Di}] - Q^L = 0 \\
&0 \leq P_{ik} \leq P^B_{ik} && \forall i, \forall k \\
&Q^{min}_{gi} \leq Q_{gi} \leq Q^{max}_{gi} && \forall i \\
&-PF^{max}_{ij} \leq PF_{ij} \leq PF^{max}_{ij} && \forall (i,j) \subset T \\
&V^{min}_i \leq V_i \leq V^{max}_i && \forall i
\end{aligned} \tag{5.58}$$

The Lagrangian for the above problem can be written as:

$$\begin{aligned}
L = &\sum_{i \in I} \sum_{k \in B_i} P_{ik} S^B_{ik} + \sum_{i \in I} Q_{gi} S^Q_i \\
&+ \lambda [\sum_{i \in I} [\sum_{k \in B_i} P_{ik} - P_{Di}] - P^L] + \sigma [\sum_{i \in I} [Q_{gi} - Q_{Di}] - Q^L] \\
&+ \sum_{i \in I} \sum_{k \in B_i} \beta^+_{ik} (P_{ik} - P^B_{ik}) + \sum_{i \in I} \sum_{k \in B_i} \beta^-_{ik} (-P_{ik}) \\
&+ \sum_{ij \in T} \mu^+_{ij} (PF_{ij} - PF^{max}_{ij}) + \sum_{ij \in T} \mu^-_{ij} (-PF^{max}_{ij} - PF_{ij}) \\
&+ \sum_{i \in I} \phi^+_i (V_i - V^{max}_i) + \sum_{i \in I} \phi^-_i (V^{min}_i - V_i) \\
&+ \sum_{i \in I} \eta^+_i (Q_{gi} - Q^{max}_{gi}) + \sum_{i \in I} \eta^-_i (Q^{min}_{gi} - Q_{gi})
\end{aligned} \tag{5.59}$$

Further,

$$\beta_{ik}^{+}\beta_{ik}^{-} = 0 \Longrightarrow \beta_{ik} = \beta_{ik}^{+} - \beta_{ik}^{-}$$

$$\mu_{ij}^{+}\mu_{ij}^{-} = 0 \Longrightarrow \mu_{ij} = \mu_{ij}^{+} - \mu_{ij}^{-}$$

$$\phi_{i}^{+}\phi_{i}^{-} = 0 \Longrightarrow \phi_{i} = \phi_{i}^{+} - \phi_{i}^{-}$$

$$\eta_{i}^{+}\eta_{i}^{-} = 0 \Longrightarrow \eta_{i} = \eta_{i}^{+} - \eta_{i}^{-}$$

$$\beta_{ik}^{+}, \beta_{ik}^{-}, \mu_{ij}^{+}, \mu_{ij}^{-}, \phi_{i}^{+}, \phi_{i}^{-}, \eta_{i}^{+}, \eta_{i}^{-} \geq 0$$

Price relationships can be obtained by considering the following KKT optimality conditions of (5.59).

$$\frac{\partial L}{\partial P_{ik}} = S_{ik}^{B} - \lambda\left[\frac{\partial P^{L}}{\partial P_{ik}} - 1\right] - \sigma\left[\frac{\partial Q^{L}}{\partial P_{ik}}\right] + \sum_{ij\in T}\mu_{ij}\left(\frac{\partial PF_{ij}}{\partial P_{ik}}\right)$$
$$+\beta_{ik} + \sum_{i\in I}\phi_{i}\left(\frac{\partial V_{i}}{\partial P_{ik}}\right) - \eta_{i}\left[\frac{\partial Q_{gi}^{max/min}}{\partial P_{ik}}\right] = 0 \qquad \forall i, \forall k \tag{5.60}$$

$$\frac{\partial L}{\partial Q_{gi}} = S_{i}^{Q} - \lambda\left[\frac{\partial P^{L}}{\partial Q_{gi}}\right] - \sigma\left[\frac{\partial Q^{L}}{\partial Q_{gi}} - 1\right] + \sum_{ij\in T}\mu_{ij}\left(\frac{\partial PF_{ij}}{\partial Q_{gi}}\right)$$
$$+\sum_{i\in I}\phi_{i}\left(\frac{\partial V_{i}}{\partial Q_{gi}}\right) + \eta_{i} = 0 \qquad \forall i \tag{5.61}$$

Note that to avoid complexities in explaining the analysis, the reactive power model proposed in Chapter 3 and the DSC discussed in Chapter 4 are not included in the above OPF formulation. However, these constraints can be easily incorporated as discussed in Chapters 3 and 4, and are considered in the case study presented in Chapter 7. However, only the dependency of the maximum and minimum limits of reactive power on the real power dispatch is considered in obtaining (5.60).

The same optimization problem given in (5.58) can be rewritten in a different form by considering real and reactive power balance equations at each node separately as given in (5.62), where $PF_{ij} = g_{ij}(V_{i}^{2} - V_{i}V_{j}\cos\theta_{ij}) - b_{ij}V_{i}V_{j}\sin\theta_{ij}$.

In this way, the total active and reactive power loss $P^{L}$ and $Q^{L}$ are made implicit in the formulation as shown in (5.62). In this formulation of OPF, each power balance

equation has distinct multipliers (i.e., $\lambda_i$ and $\sigma_i$), which represent the real and reactive power LMPs at the respective bus.

Minimize:

$$J = \sum_{i \in I} \sum_{k \in B_i} P_{ik} S^B_{ik} + \sum_{i \in I} Q_{gi} S^Q_i$$

Subject to:

$$\begin{aligned}
&\sum_{k \in B_i} P_{ik} - P_{Di} = \sum_{ij \in T_i} V_i[g_{ij}(V_i - V_j \cos\theta_{ij}) - b_{ij} V_j \sin\theta_{ij}] && \forall i \\
&Q_{gi} - Q_{Di} = \sum_{ij \in T_i} V_i[-b_{ij}(V_i - V_j \cos\theta_{ij}) - g_{ij} V_j \sin\theta_{ij}] && \forall i \qquad (5.62) \\
&0 \le P_{ik} \le P^B_{ik} && \forall i, \forall k \\
&Q^{min}_{gi} \le Q_{gi} \le Q^{max}_{gi} && \forall i \\
&-PF^{max}_{ij} \le PF_{ij} \le PF^{max}_{ij} && \forall (i,j) \subset T \\
&V^{min}_i \le V_i \le V^{max}_i && \forall i
\end{aligned}$$

The Lagrangian for the above problem can be written as:

$$\begin{aligned}
L = &\sum_{i \in I} \sum_{k \in B_i} P_{ik} S^B_{ik} + \sum_{i \in I} Q_{gi} S^Q_i \\
&+ \sum_{i \in I} \lambda_i \left[ - \sum_{k \in B_i} P_{ik} + P_{Di} + \sum_{ij \in T_i} V_i[g_{ij}(V_i - V_j \cos\theta_{ij}) - b_{ij} V_j \sin\theta_{ij}] \right] \\
&+ \sum_{i \in I} \sigma_i \left[ -Q_{gi} + Q_{Di} + \sum_{ij \in T_i} V_i[-b_{ij}(V_i - V_j \cos\theta_{ij}) - g_{ij} V_j \sin\theta_{ij}] \right] \\
&+ \sum_{i \in I} \sum_{k \in B_i} \beta^+_{ik}(P_{ik} - P^B_{ik}) + \sum_{i \in I} \sum_{k \in B_i} \beta^-_{ik}(-P_{ik}) \qquad (5.63) \\
&+ \sum_{ij \in T} \mu^+_{ij}(PF_{ij} - PF^{max}_{ij}) + \sum_{ij \in T} \mu^-_{ij}(-PF^{max}_{ij} - PF_{ij}) \\
&+ \sum_{i \in I} \phi^+_i(V_i - V^{max}_i) + \sum_{i \in I} \phi^-_i(V^{min}_i - V_i) \\
&+ \sum_{i \in I} \eta^+_i(Q_{gi} - Q^{max}_{gi}) + \sum_{i \in I} \eta^-_i(Q^{min}_{gi} - Q_{gi})
\end{aligned}$$

The price relationships can be obtained by considering the following KKT optimality conditions.

$$\frac{\partial L}{\partial P_{ik}} = S^B_{ik} - \lambda_i + \beta_{ik} - \eta_i \left[\frac{\partial Q^{max/min}_{gi}}{\partial P_{ik}}\right] = 0 \qquad \forall i, \forall k \tag{5.64}$$

$$\frac{\partial L}{\partial Q_{gi}} = S^Q_i - \sigma_i + \eta_i = 0 \qquad \forall i \tag{5.65}$$

Hence, the real and reactive power LMPs at bus $i$ are,

$$\lambda_i = S^B_{ik} + \beta_{ik} + \eta_i \left[\frac{\partial Q^{max/min}_{gi}}{\partial P_{ik}}\right] \qquad \forall i, \forall k \tag{5.66}$$

$$\sigma_i = S^Q_i + \eta_i \qquad \forall i \tag{5.67}$$

The term $\frac{\partial P^L}{\partial P_{ik}}$ in (5.60) is the loss sensitivity, which represents the contribution from the supply offer $P_{ik}$ to the total system losses. However, this is only a function of location of the generator as any other offer at the same bus makes the same change in system losses. Therefore, offers from the same bus have the same loss sensitivity, which is the sensitivity of losses to the net injection into that node. Hence, $\frac{\partial P^L}{\partial P_{ik}}$ can be replaced with $\frac{\partial P^L}{\partial P_i}$ by removing suffix $k$. Similar explanation applies to the remaining terms in (5.60) and (5.61).

Equations (5.60) and (5.66) can be combined to obtain the real power LMP at bus $i$ as,

$$\lambda_i = \lambda \left[1 - \frac{\partial P^L}{\partial P_i}\right] + \sigma \left[-\frac{\partial Q^L}{\partial P_i}\right] - \sum_{ij \in T} \mu_{ij} \left(\frac{\partial PF_{ij}}{\partial P_i}\right) - \sum_{i \in I} \phi_i \left(\frac{\partial V_i}{\partial P_i}\right) \qquad \forall i \tag{5.68}$$

Similarly, by combining (5.61) and (5.67), the reactive power LMP at bus $i$ can be obtained as,

$$\sigma_i = \lambda \left[-\frac{\partial P^L}{\partial Q_i}\right] + \sigma \left[1 - \frac{\partial Q^L}{\partial Q_i}\right] - \sum_{ij \in T} \mu_{ij} \left(\frac{\partial PF_{ij}}{\partial Q_i}\right) - \sum_{i \in I} \phi_i \left(\frac{\partial V_i}{\partial Q_i}\right) \qquad \forall i \tag{5.69}$$

The first term in (5.68) represents the cost of delivered real power to bus $i$ from the reference bus in the event of delivering a unit of MW of real power to bus $i$. The second term represents the cost of associated reactive power loss in delivering the real power. The final two terms indicate the costs due to binding line flow and voltage constrains respectively. It is important to note that if a constraint is not binding, the corresponding Lagrangian multiplier (i.e., shadow cost) is zero, resulting in a zero contribution to the LMP. The same explanation can be given for the terms in (5.69) as well.

However, explicit evaluation of each partial derivative appearing in (5.68) and (5.69) for each LMP difference required, leads to a high computational burden as a large number of terms needs to be evaluated. To overcome this difficulty, these derivatives are implicitly calculated by post processing the following KKT optimality conditions of the Lagrangian equation in (5.63) as shown below.

$$\begin{aligned}\frac{\partial L}{\partial V_i} =&\lambda_i \sum_{ij\in T_i}[g_{ij}(2V_i - V_j\cos\theta_{ij}) - b_{ij}V_j\sin\theta_{ij}] + \sum_{j\neq i}\lambda_j[-g_{ij}V_j\cos\theta_{ji} - b_{ij}V_j\sin\theta_{ji}]\\ &+\sigma_i \sum_{ij\in T_i}[-b_{ij}(2V_i - V_j\cos\theta_{ij}) - g_{ij}V_j\sin\theta_{ij}] + \sum_{j\neq i}\sigma_j[b_{ij}V_j\cos\theta_{ji} - g_{ij}V_j\sin\theta_{ji}]\\ &+\phi_i^+ - \phi_i^- + \sum_{ij\in T}\mu_{ij}\frac{\partial PF_{ij}}{\partial V_i} = 0 \qquad \forall i \end{aligned} \tag{5.70}$$

$$\begin{aligned}\frac{\partial L}{\partial \theta_i} =&\lambda_i \sum_{ij\in T_i}[V_i(g_{ij}V_j\sin\theta_{ij} - b_{ij}V_j\cos\theta_{ij})] + \sum_{j\neq i}\lambda_j[-g_{ij}V_iV_j\sin\theta_{ji} + b_{ij}V_iV_j\cos\theta_{ji}]\\ &+\sigma_i \sum_{ij\in T_i}[V_i(-b_{ij}V_j\sin\theta_{ij} - g_{ij}V_j\cos\theta_{ij})] + \sum_{j\neq i}\sigma_j[b_{ij}V_iV_j\sin\theta_{ji} + g_{ij}V_iV_j\cos\theta_{ji}]\\ &+\sum_{ij\in T}\mu_{ij}\frac{\partial PF_{ij}}{\partial \theta_i} = 0 \qquad \forall i \end{aligned} \tag{5.71}$$

Equations (5.70) and (5.71) represent $2n$ number of equations (where n is the number of buses in the system), and these equations can be written in the compact

matrix form as,

$$\begin{bmatrix} \frac{\partial G}{\partial V} & \frac{\partial \overline{G}}{\partial V} \\ \frac{\partial G}{\partial \theta} & \frac{\partial \overline{G}}{\partial \theta} \end{bmatrix} \begin{bmatrix} \lambda \\ \sigma \end{bmatrix} = \begin{bmatrix} c \\ d \end{bmatrix} \tag{5.72}$$

where $G_i$ and $\overline{G}_i$ represent the expressions for real and reactive power injections at bus $i$, and, c and d are arrays of order $n$ with $i^{th}$ element given by,

$$c_i = -\phi_i^+ + \phi_i^- - \sum_{ij \in T} \mu_{ij} \frac{\partial PF_{ij}}{\partial V_i}$$

$$d_i = -\sum_{ij \in T} \mu_{ij} \frac{\partial PF_{ij}}{\partial \theta_i}$$

The Jacobian matrix appearing in (5.72) is a singular matrix having its first $n$ rows linearly independent and its last $n$ rows linearly dependent with rank $n-1$. Hence, by removing at least one equation from the last $n$ equations, the matrix can be inverted. Therefore, if the real and reactive power LMPs at any bus are known, the remaining real and reactive power LMPs can be determined. This results in an expression for LMPs in the form given in (5.68) and (5.69). This procedure is demonstrated for a 3 bus system in Appendix C.

After determining the partial derivatives, equations (5.68) and (5.69) can be re-arranged to obtain a relationship for the LMP difference between any two real power LMPs and any two reactive power LMPs respectively in the detailed form. For instance, if bus $j$ is the reference bus, the difference in LMPs between bus $j$ and any other bus $i$ can be written as given below. However, the associated partial derivatives are only meaningful, when one bus is a load bus and the other bus is a generator bus. In fact, later in Section 5.4.2, it is shown that only the LMP difference between a load bus and a generator bus is considered in the presented analysis.

$$\lambda_j - \lambda_i = \lambda_j \left[\frac{\partial P^L}{\partial P_i}\right] + \sigma_j \left[\frac{\partial Q^L}{\partial P_i}\right] + \sum_{ij \in T} \mu_{ij} \left(\frac{\partial PF_{ij}}{\partial P_i}\right) + \sum_{i \in I} \phi_i \left(\frac{\partial V_i}{\partial P_i}\right) \quad \forall i$$

$$\sigma_j - \sigma_i = \lambda_j \left[\frac{\partial P^L}{\partial Q_i}\right] + \sigma_j \left[\frac{\partial Q^L}{\partial Q_i}\right] + \sum_{ij \in T} \mu_{ij} \left(\frac{\partial PF_{ij}}{\partial Q_i}\right) + \sum_{i \in I} \phi_i \left(\frac{\partial V_i}{\partial Q_i}\right) \quad \forall i$$

### 5.4.2 Calculation of Components of Network Rental For a System Having a Single Load Bus

Network Rental (NR) is the difference between what consumers pay and what generators get paid. This can be mathematically stated as,

$$\begin{aligned} NR &= NR_P + NR_Q \\ &= \sum_{i \in I} \lambda_i \left[ P_{Di} - \sum_{k \in B_i} P_{ik} \right] + \sum_{i \in I} \sigma_i [Q_{Di} - Q_{gi}] \end{aligned} \tag{5.73}$$

where $NR_P$ and $NR_Q$ are the rentals due to real and reactive power dispatch respectively.

With the known dispatch and hence with the known LMPs, the network rental due to real and reactive power dispatch can be separately calculated from (5.73), despite, how each consumer contributes to the total network rental is still unknown. However, if the system has only one load, then it is obvious that the total network rental is paid by that consumer. Therefore, the total generation is to cater that single load and the associated losses. Hence, (5.73) can be expressed in terms of LMP differences between each generator bus and the load bus, corresponding power injections, and losses, in order to calculate the loss rental and the constraint rental paid by the single consumer.

This is explained using a simple 3 bus system, where the single line diagram is shown in figure 5.4. In the presentation of results, all the real and reactive power values are in MW or MVAr, voltages are in pu, prices are in \$/h, and marginal prices are in \$/MWh, \$/MVArh or \$/pu.h depending on the quantity considered. There are two generators connected to buses 1 and 2. Bus 3 has a real and reactive power load of 1000 and 300 respectively. Line data for the 3 bus system are shown in figure 5.4, and the generator bid data for the two generators are given in table 5.7. Further, it is assumed that the reactive power from generators is free and only constrained by maximum and minimum limits of $\pm$1000 MVAr. Each line has a limit of 700 MW and

the maximum and minimum voltage limits of each bus is set to 1.1 pu and 0.90 pu respectively. The real and reactive power dispatch obtained by solving a NLP-OPF

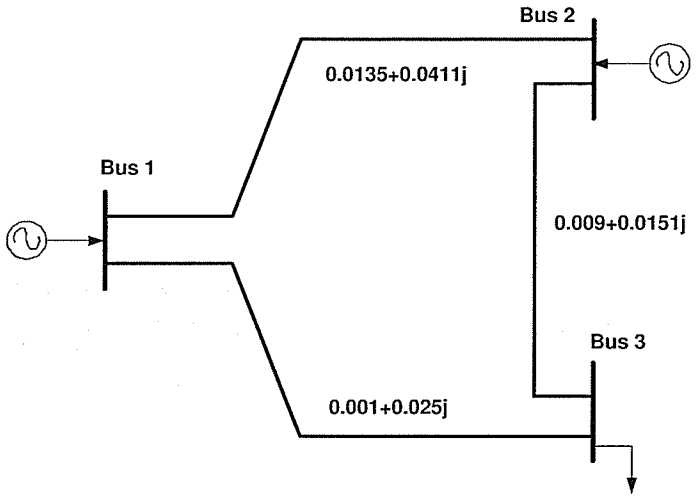


Figure 5.4: 3 bus system

Table 5.7: Generator bid data

| Bus | bid 1 | | bid 2 | | $S_i^Q$ |
|---|---|---|---|---|---|
| | $P_{ik}^B$ | $S_{ik}^B$ | $P_{ik}^B$ | $S_{ik}^B$ | |
| 1 | 250 | 3.60 | 750 | 5.20 | 0.0 |
| 2 | 600 | 3.20 | 400 | 4.20 | 0.0 |

are given in table 5.8. It can be seen that the expensive generation at bus 1 (i.e., bid 2) is partly dispatched, without fully dispatching the cheaper generation at bus 2 (i.e., bid 2). This is expected because the power system operates on the binding line flow constraints as evident from the non-zero marginal cost for $PF_{23}$ given in table 5.9.

Table 5.8: Generation dispatch

| Bus | $P_{ik}$ | | $Q_{gi}$ |
|---|---|---|---|
| | bid 1 | bid 2 | |
| 1 | 250.00 | 55.33 | 309.51 |
| 2 | 600.00 | 133.79 | 95.59 |

Apart from the binding line flow $PF_{23}$, voltages at buses 1 and 2 are also binding, resulting in three binding constraints altogether, as shown in table 5.9. The associated

Table 5.9: Binding constraints

| constraint | quantity | shadow cost |
|---|---|---|
| $PF_{23}$ | 700 MW | 1.37 |
| $V_1$ | 1.10 pu | 194.36 |
| $V_2$ | 1.10 pu | 253.21 |

Lagrangian multipliers or the shadow costs are also shown in table 5.9, which implies that the cost of operation can be reduced by that amount if the corresponding binding constraint could be relieved by a unit, or more precisely the sensitivity of operation cost to the limiting value of that constraint.

From (5.73), the total network rental can be calculated by analyzing the payments made/received by each generator and the consumer separately as tabulated in table 5.10. This shows that the rental paid by the consumer due to real and reactive power dispatch are 1148.39 and 57.90 respectively for the case considered.

Table 5.10: Network rental for the 3 bus system

| Bus | LMP | | Generator Receipt | | Consumer Payment | |
|---|---|---|---|---|---|---|
| | P | Q | P | Q | P | Q |
| 1 | 5.20 | 0.00 | 1587.69 | 0.00 | 0.00 | 0.00 |
| 2 | 4.20 | 0.00 | 3081.91 | 0.00 | 0.00 | 0.00 |
| 3 | 5.82 | 0.19 | 0.00 | 0.00 | 5818.00 | 57.90 |
| | Total | | 4669.60 | 0.00 | 5818.00 | 57.90 |
| | **Network Rental** | | | | **1148.39** | **57.90** |

By expanding the first term in (5.73), the rental paid by the consumer due to real power dispatch $NR_P$ can be written as,

$$NR_P = 1000\lambda_3 - [(250 + 55.33)\lambda_1 + (600 + 133.79)\lambda_2]$$

After rearranging the terms this can be rewritten as,

$$NR_P = 305.33[\lambda_3 - \lambda_1] + 733.79[\lambda_3 - \lambda_2] - 39.02\lambda_3 \tag{5.74}$$

As pointed out earlier, (5.74) indicates that the real power rental paid by the consumer can be expressed in terms of LMP differences between each generator bus and the

load bus, corresponding power injections, and losses (i.e., $P_1$=305.33, $P_2$=733.79 and $P^L$=39.02).

For known $\lambda_3$ and $\sigma_3$, (5.68) can be used to decompose $\lambda_1$ and $\lambda_2$ in the detailed form as given below. It is important to note that the required partial derivatives are with respect to an injection at a generator bus (i.e., $P_1$ or $P_2$), while withdrawing from the load bus. Thus, the load bus needs to be taken as the reference bus.

$$\lambda_1 = \lambda_3[1 - \frac{\partial P^L}{\partial P_1}] + \sigma_3[-\frac{\partial Q^L}{\partial P_1}] - \mu_{23}\left[\frac{\partial PF_{23}}{\partial P_1}\right] - \phi_1\left[\frac{\partial V_1}{\partial P_1}\right] - \phi_2\left[\frac{\partial V_2}{\partial P_1}\right]$$
$$\lambda_2 = \lambda_3[1 - \frac{\partial P^L}{\partial P_2}] + \sigma_3[-\frac{\partial Q^L}{\partial P_2}] - \mu_{23}\left[\frac{\partial PF_{23}}{\partial P_2}\right] - \phi_1\left[\frac{\partial V_1}{\partial P_2}\right] - \phi_2\left[\frac{\partial V_2}{\partial P_2}\right]$$

Thereby, the required LMP differences can be calculated as,

$$\lambda_3 - \lambda_1 = \lambda_3\left[\frac{\partial P^L}{\partial P_1}\right] + \sigma_3\left[\frac{\partial Q^L}{\partial P_1}\right] + \mu_{23}\left[\frac{\partial PF_{23}}{\partial P_1}\right] + \phi_1\left[\frac{\partial V_1}{\partial P_1}\right] + \phi_2\left[\frac{\partial V_2}{\partial P_1}\right]$$
$$\lambda_3 - \lambda_2 = \lambda_3\left[\frac{\partial P^L}{\partial P_2}\right] + \sigma_3\left[\frac{\partial Q^L}{\partial P_2}\right] + \mu_{23}\left[\frac{\partial PF_{23}}{\partial P_2}\right] + \phi_1\left[\frac{\partial V_1}{\partial P_2}\right] + \phi_2\left[\frac{\partial V_2}{\partial P_2}\right]$$

The above LMP differences are then substituted in the expression of $NR_P$ in (5.74) to yield,

$$\begin{aligned} NR_P = &\lambda_3\left[\frac{\partial P^L}{\partial P_1}P_1 + \frac{\partial P^L}{\partial P_2}P_2 - P^L\right] + \sigma_3\left[\frac{\partial Q^L}{\partial P_1}P_1 + \frac{\partial Q^L}{\partial P_2}P_2\right] \\ &+ \mu_{23}\left[\left(\frac{\partial PF_{23}}{\partial P_1}\right)P_1 + \left(\frac{\partial PF_{23}}{\partial P_2}\right)P_2\right] \\ &+ \phi_1\left[\left(\frac{\partial V_1}{\partial P_1}\right)P_1 + \left(\frac{\partial V_1}{\partial P_2}\right)P_2\right] + \phi_2\left[\left(\frac{\partial V_2}{\partial P_1}\right)P_1 + \left(\frac{\partial V_2}{\partial P_2}\right)P_2\right] \end{aligned}$$

This reveals that the first term of the above expression is the real power loss rental paid by the consumer, as it is the difference between the marginal loss and the average loss. Similarly the second term indicates the reactive power loss rental. The final three terms are the constraint rental paid by the consumer due to the three binding constraints $PF_{23}$, $V_1$, and $V_2$ respectively.

The same analysis can be done to determine the rental paid by the consumer due

to reactive power dispatch, $NR_Q$. Thereby, all the components of network rental paid by the consumer can be summarized as shown in table 5.11, where real power loss rental and reactive power loss rental are given in columns 3 and 4 respectively, and constraint rental due to $PF_{23}$, $V_1$, and $V_2$ are given in the final three columns respectively. Note that partial derivatives appearing in the above LMP differences have been numerically verified using a sensitivity analysis [57].

Table 5.11: Components of network rental

| | Network Rental | | | | | |
|---|---|---|---|---|---|---|
| | total | loss rental | | constraint rental | | |
| $NR_P$ | 1148.39 | 177.12 | 32.82 | 927.39 | 1.82 | 9.41 |
| $NR_Q$ | 57.90 | 24.84 | -14.84 | 31.70 | 10.13 | 6.03 |

This reveals that the bulk of the network rental collected by the ISO is due to the binding line flow constraint $PF_{23}$ for the case considered. This is because the binding line flow constraint caused significant out of merit order dispatch of generator bids, as evident from the generation dispatch given in table 5.8. This results in charging the consumer at a higher LMP (greater than the highest bid dispatched) for the total load, while the partly dispatched cheaper generator, which supplies part of the load, only receives at a low LMP (equal to its bid price) for the amount dispatched.

Further, a significant network rental is accumulated in the form of real power loss rental with the ISO. Likewise, all the components of network rental paid by the consumer can be quantitatively analyzed to get a better picture of what leads to the accumulation of network rental.

In practice, however, there exist more than one load in the system. If each load can be traced to all the dispatched generators (i.e., how each load is supplied by the dispatched generators in the system), then the single load bus approach presented in this section can still be applied to obtain the rental components for a general case of multiple load buses. Due to the nonlinear nature of the power flow, it is impossible to accurately determine the generator contributions to each load [61]. However, power flow tracing methods [58], [59], and the recently proposed Equivalent

Bilateral Exchanges (EBE) technique [60] can be used to approximately determine the generator contribution to each load. Each method gives rise to a different generator allocation, and thus, the chosen method should be agreeable to all the participants of the market.

### 5.4.3 Separation of Network Rental Among Consumers Using Power Flow Tracing

Tracing methods were originally proposed in transmission pricing [61] to cover the fixed transmission cost based on actual usage of the network by each participant. There are different tracing methods proposed in the literature such as Bialek tracing method [58] and Kirschen tracing method [59]. Tracing methods are topological in nature and can be used to trace both real and reactive power. This makes possible finding the contribution of each generating unit into each load separately. The other advantage is that power flow tracing allows the determination of the transmission losses apportioned to each load [58], which is also required for the proposed analysis.

Both of these methods are based on the proportional sharing principle, which states that each outflow leaving a node contains the same proportion of the inflows. Note that in these methods, the real and reactive power flows obtained by solving a nonlinear power flow is used to calculate the generator contributions and losses into each load.

Even though, both tracing methods are equally suited for the proposed approach, due to the slight advantage offered in combining with the OPF, Bialek tracing method is selected. This is because, in the Bialek method, tracing is performed based on actual buses in the system whereas in the Kirschen method tracing is done by grouping the buses supplied by the same generator which has to be determined beforehand based on the direction of the power flows in the system. The concept behind the Bialek tracing method is summarized for real power tracing in Appendix D.

A 4 bus system having two generators and two loads, shown in figure 5.5 is used

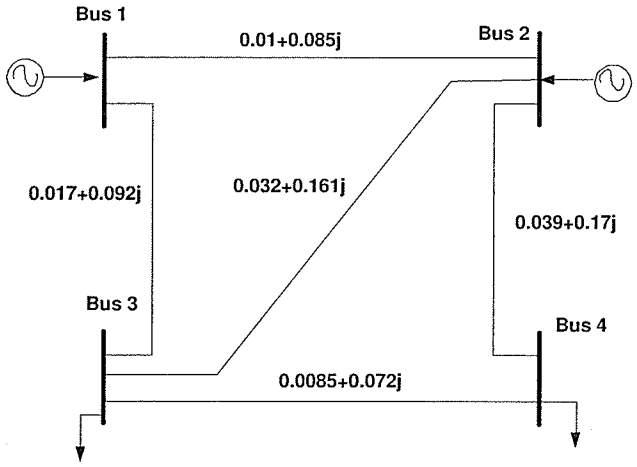


Figure 5.5: 4 bus system

to explain how each rental component is separated for a general case of multiple load bus system. The generator bids, reactive power limits, and voltage limits for this case are the same as for the previous 3 bus case. Buses 3 and 4 have a real and reactive power load of 220, 70 and 120, 10 respectively. Each line has a limit of 120 MW.

The generation dispatch obtained by solving a NLP-OPF for this case is given in table 5.12. It reveals that the generation dispatch is out of merit order due to the binding line flow constraint, $PF_{23}$, as evident from the non-zero shadow cost given in table 5.13.

Table 5.12: Generation dispatch

| Bus | $P_{ik}$ | | $Q_{gi}$ |
|---|---|---|---|
| | bid 1 | bid 2 | |
| 1 | 3.45 | 0.00 | 88.47 |
| 2 | 348.97 | 0.00 | 55.46 |

Table 5.13: Binding constraints

| constraint | quantity | shadow cost |
|---|---|---|
| $PF_{23}$ | 120 MW | 1.74 |
| $V_2$ | 1.10 pu | 93.77 |

The real power flows along the lines are shown in figure 5.6. Based on line flows, the matrices $A_u$, $PF_{ij}^{gross}$, and vectors $P^{gross}$, $P_D^{gross}$, $P^{L\_app}$ are calculated as explained

in Appendix D.

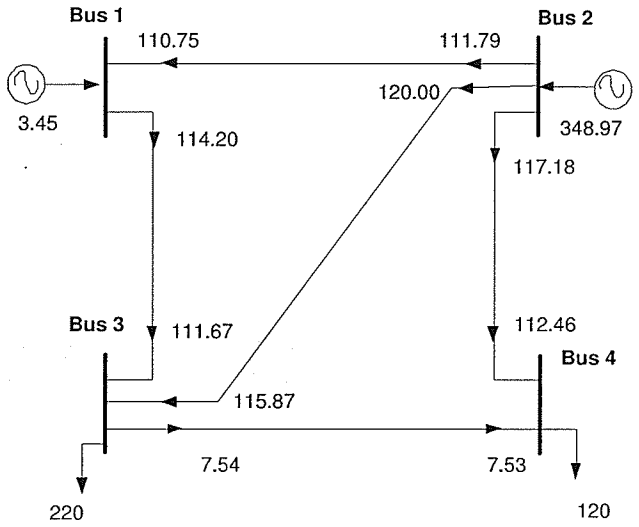


Figure 5.6: Real power flows for the 4 bus system

$$A_u = \begin{pmatrix} 1 & -\frac{111.79}{348.97} & 0 & 0 \\ 0 & 1 & 0 & 0 \\ -\frac{114.20}{114.20} & -\frac{120.00}{348.97} & 1 & 0 \\ 0 & -\frac{117.18}{348.97} & -\frac{7.54}{227.54} & 1 \end{pmatrix} \Rightarrow A_u^{-1} = \begin{pmatrix} 1.000 & 0.317 & 0.000 & 0.000 \\ 0.000 & 1.000 & 0.000 & 0.000 \\ 1.000 & 0.661 & 1.000 & 0.000 \\ 0.033 & 0.358 & 0.033 & 1.000 \end{pmatrix}$$

$$P^{gross} = \begin{pmatrix} 115.24 \\ 348.97 \\ 235.24 \\ 124.98 \end{pmatrix} \quad P_D^{gross} = \begin{pmatrix} 0.00 \\ 0.00 \\ 227.45 \\ 124.98 \end{pmatrix} \quad P^{L\_app} = \begin{pmatrix} 0.00 \\ 0.00 \\ 7.45 \\ 4.98 \end{pmatrix}$$

$$PF_{ij}^{gross} = \begin{pmatrix} 0.00 & 111.79 & 0.00 & 0.00 \\ 3.45 & 111.79 & 0.00 & 0.00 \\ 0.00 & 120.00 & 0.00 & 0.00 \\ 0.00 & 117.18 & 0.00 & 0.00 \\ 0.11 & 7.68 & 0.00 & 0.00 \end{pmatrix}$$

Thereby how each load and the apportioned losses supplied by each generator is determined and are shown in figure 5.7. For example, there is 7.45 MW of associated losses in catering 220 MW at bus 3 and generators at bus 1 and 2 supply this load and the losses in part by 3.34 MW and 224.10 MW respectively. Similarly, there is 4.98 MW of associated losses in catering 120 MW at bus 4 and generators at bus 1 and 2 supply this in part by 0.11 MW and 124.87 MW respectively (the underlined values shown in figure 5.7).

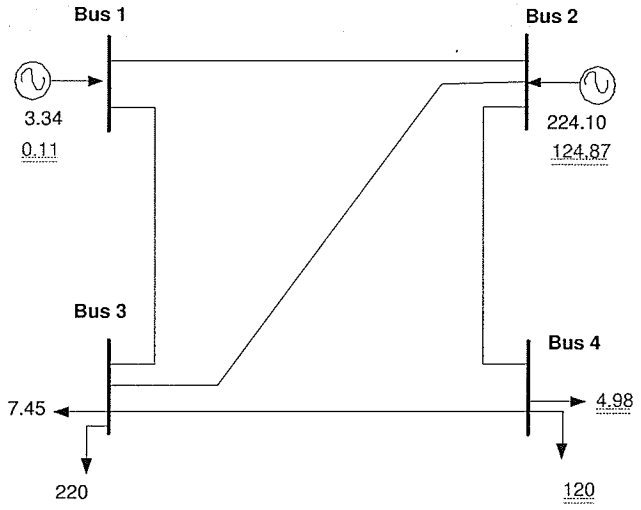


Figure 5.7: Generator contributions and apportioned losses for each load

As before, the total network rental paid by the two consumers is calculated and presented in table 5.14. This shows that the rental paid by both consumers due to real and reactive power dispatch are 254.36 and 5.41 respectively for the case considered.

Table 5.14: Network rental for the 4 bus system

| Bus | LMP | | Generator Receipt | | Consumer Payment | |
|---|---|---|---|---|---|---|
| | P | Q | P | Q | P | Q |
| 1 | 3.60 | 0.00 | 12.42 | 0.00 | 0.00 | 0.00 |
| 2 | 3.20 | 0.00 | 1116.70 | 0.00 | 0.00 | 0.00 |
| 3 | 4.13 | 0.07 | 0.00 | 0.00 | 909.48 | 4.62 |
| 4 | 3.95 | 0.08 | 0.00 | 0.00 | 474.00 | 0.79 |
| | Total | | 1129.12 | 0.00 | 1383.48 | 5.41 |
| | **Network Rental** | | | | **254.36** | **5.41** |

Once the tracing is done, the power system can be viewed as several independent networks each having a single load. Therefore, the method developed in Section 5.4.2 for a single load network can be repeatedly applied for each network to determine the network rental paid by each consumer. In this way $NR_P$ can be written as,

$$\begin{aligned} NR_P =& 220\lambda_3 - [3.34\lambda_1 + 223.10\lambda_2] + 120\lambda_4 - [0.11\lambda_1 + 124.83\lambda_2] \\ =& 3.34[\lambda_3 - \lambda_1] + 223.10[\lambda_3 - \lambda_2] - 6.44\lambda_3 + 0.11[\lambda_4 - \lambda_1] + 124.83[\lambda_4 - \lambda_2] - 4.94\lambda_4 \\ =& NR_{P3} + NR_{P4} \end{aligned}$$

Taking bus 3 as the reference bus,

$$\begin{aligned} \lambda_1 &= \lambda_3[1 - \frac{\partial P^L}{\partial P_1}] + \sigma_3[-\frac{\partial Q^L}{\partial P_1}] - \mu_{23}\left[\frac{\partial P_{23}}{\partial P_1}\right] - \phi_2\left[\frac{\partial V_2}{\partial P_1}\right] \\ \lambda_2 &= \lambda_3[1 - \frac{\partial P^L}{\partial P_2}] + \sigma_3[-\frac{\partial Q^L}{\partial P_2}] - \mu_{23}\left[\frac{\partial P_{23}}{\partial P_2}\right] - \phi_2\left[\frac{\partial V_2}{\partial P_2}\right] \end{aligned}$$

Thereby, the required LMP differences to calculate $NR_{P3}$ are,

$$\begin{aligned} \lambda_3 - \lambda_1 =& \lambda_3\left[\frac{\partial P^L}{\partial P_1}\right] + \sigma_3\left[\frac{\partial Q^L}{\partial P_1}\right] + \mu_{23}\left[\frac{\partial PF_{23}}{\partial P_1}\right] + \phi_2\left[\frac{\partial V_2}{\partial P_1}\right] \\ \lambda_3 - \lambda_2 =& \lambda_3\left[\frac{\partial P^L}{\partial P_2}\right] + \sigma_3\left[\frac{\partial Q^L}{\partial P_2}\right] + \mu_{23}\left[\frac{\partial PF_{23}}{\partial P_2}\right] + \phi_2\left[\frac{\partial V_2}{\partial P_2}\right] \end{aligned}$$

Similarly, taking bus 4 as the reference bus, the required LMP differences to calculate $NR_{P4}$ are,

$$\begin{aligned} \lambda_4 - \lambda_1 =& \lambda_4\left[\frac{\partial P^L}{\partial P_1}\right] + \sigma_4\left[\frac{\partial Q^L}{\partial P_1}\right] + \mu_{23}\left[\frac{\partial PF_{23}}{\partial P_1}\right] + \phi_2\left[\frac{\partial V_2}{\partial P_1}\right] \\ \lambda_4 - \lambda_2 =& \lambda_4\left[\frac{\partial P^L}{\partial P_2}\right] + \sigma_4\left[\frac{\partial Q^L}{\partial P_2}\right] + \mu_{23}\left[\frac{\partial PF_{23}}{\partial P_2}\right] + \phi_2\left[\frac{\partial V_2}{\partial P_2}\right] \end{aligned}$$

Substituting for LMP differences in the above expression for $NR_P$, the rental paid by consumers at buses 3 and 4 due to real power dispatch (i.e., $NR_{P3}$ and $NR_{P4}$) can be determined separately in terms of loss rental and constraint rental.

$$
\begin{aligned}
NR_P =& \lambda_3[\frac{\partial P^L}{\partial P_1}P_1 + \frac{\partial P^L}{\partial P_2}P_2 - P^L] + \sigma_3[\frac{\partial Q^L}{\partial P_1}P_1 + \frac{\partial Q^L}{\partial P_2}P_2] \\
&+ \mu_{23}[\left(\frac{\partial P_{23}}{\partial P_1}\right)P_1 + \left(\frac{\partial P_{23}}{\partial P_2}\right)P_2] + \phi_2[\left(\frac{\partial V_2}{\partial P_1}\right)P_1 + \left(\frac{\partial V_2}{\partial P_2}\right)P_2] \\
&+ \lambda_4[\frac{\partial P^L}{\partial P_1}P_1 + \frac{\partial P^L}{\partial P_2}P_2 - P^L] + \sigma_4[\frac{\partial Q^L}{\partial P_1}P_1 + \frac{\partial Q^L}{\partial P_2}P_2] \\
&+ \mu_{23}[\left(\frac{\partial P_{23}}{\partial P_1}\right)P_1 + \left(\frac{\partial P_{23}}{\partial P_2}\right)P_2] + \phi_2[\left(\frac{\partial V_2}{\partial P_1}\right)P_1 + \left(\frac{\partial V_2}{\partial P_2}\right)P_2]
\end{aligned}
$$

A similar analysis can be done to determine the rental paid by consumers due to the reactive power dispatch as well (i.e., $NR_{Q3}$ and $NR_{Q4}$). The results can be summarized as given in table 5.15, where real power loss rental and reactive power loss rental are given in columns 3 and 4 respectively, and constraint rental due to $PF_{23}$ and $V_2$ are given in the final two columns respectively. A closer look confirms that the summation of $NR_{P3}$ and $NR_{P4}$; and $NR_{Q3}$ and $NR_{Q4}$ equal to the previously calculated values given in table 5.14.

Table 5.15: Components of network rental

| | Network Rental | | | | |
|---|---|---|---|---|---|
| | total | loss rental | | constraint rental | |
| $NR_{P3}$ | 179.78 | 23.87 | 4.73 | 151.43 | -0.25 |
| $NR_{P4}$ | 74.72 | 11.62 | 3.26 | 60.33 | -0.50 |
| $NR_{Q3}$ | 4.65 | 4.82 | -2.17 | -2.80 | 4.79 |
| $NR_{Q4}$ | 0.79 | 0.58 | -1.93 | 0.07 | 2.07 |

As before, the individual rental components can be analyzed to determine the market signals. This is further discussed in Chapter 7 in more detail.

### 5.4.4 Discussion

The proposed method is evaluated using small 3 and 4 bus systems for convenience in understanding. However, the formulation of equations are general and therefore applicable for any large system.

When a particular bus consists of both dispatched generators and loads, and if the dispatched generation is greater than the load, then the particular consumer

does not pay any rental to the ISO. This is because neither associated losses nor binding constraints are associated with the delivery to that particular load. On the other hand, if the dispatched generation is less than the load, then the particular consumer pays the network rental only for the portion of the load supplied by other dispatched generators in the system. Even though, this situation did not arise in the two examples considered in this chapter, the proposed method does consider this automatically, as the net injection is only taken into account in power flow tracing.

Using this method, the components of network rental due to any binding constraint can be calculated separately. The Dynamic Security Constraint (DSC), discussed in Chapter 4 to obtain a secure dispatch, will also generate a constraint rental component, when the DSC is binding at the solution [51]. Therefore, the portion of the rental paid by each consumer due to the DSC can also be calculated from the proposed method, which is discussed in detail in Chapter 7.

## 5.5 Concluding Remarks

This chapter discussed different ways of analyzing market signals. Correct market signals are always sought, as they provide necessary incentives for the market participants.

As far as the present market operation is concerned, LMPs provide crucial market signals for the participants. On the other hand, the components of LMP can be considered as better market signals as they show the explicit decomposition of LMP due to marginal generators and binding constraints. However, LMP components do not provide the effects of the transmission losses explicitly. This has been demonstrated using a simple 3 bus system. The physical meaning of these individual LMP components has also been explained using the results of this 3 bus system.

A new method to analyze the market signals has been proposed in this chapter by means of analyzing the components of network rental. In this regard, a method to decompose the network rental among the consumers into loss rental, and constraint

rental due to each binding constraint, has been proposed by combining the power flow tracing and KKT optimality conditions of the NLP-OPF. The proposed method first determines the rental components for a single load bus by mathematically expressing the network rental in terms of LMP differences. The implicitly calculated sensitivity values, based on post processed KKT optimality conditions, are then substituted for the above LMP differences. This has then been extended to a general case of multiple load buses by tracing the power flow to identify how each load and the associated transmission losses are supplied by the generators in the system.

The novelty of the proposed method is that it yields the breakdown of network rental paid by each individual consumer into its components due to losses and binding constraints. The proposed method also utilizes an efficient way to calculate the LMP difference between two buses by implicitly calculating the individual components using the post processed KKT optimality conditions of the NLP-OPF.

As the network rental is an overpayment made by the consumers due to the losses and the binding constraints imposed by the OPF, it has been argued that these components do provide better market signals than LMP or LMP components. Several case studies have been presented using simple 3 and 4 bus systems by calculating these individual components using the proposed approach. Another case study is presented in Chapter 7, using the reactive power model and the DSC discussed in Chapters 3 and 4.

# Chapter 6

# Software Implementation

This chapter deals with the implemented software package that incorporates the market signal analysis methods discussed in Chapter 5. Since all these methods rely on the availability of the optimal dispatch, an OPF solver is required to solve the OPF. Recent developments in optimization techniques and the enhancement in computational capability have allowed commercial software packages to be put forward [62], [63], [64], [65] in solving either the general optimization problem or specifically the OPF problem. However, the detailed description of the algorithms used in the different software packages haven't been published and remain trade secrets.

Even though, the mathematics related to optimization is not new, due to the complexity associated with the OPF, solving an OPF is still a challenging task. The OPF was first introduced in early 1960's [1] and since then, different solving techniques have been proposed. These techniques can be broadly classified as;

- Sequential Linear Programming (SLP) [1]
- Newton Based Method [66], [67]
- Sequential Quadrature Programming (SQP) [68]
- Generalized Reduced Gradient Method (GRG) [69]
- Penalty, Barrier, and Augmented Lagrangian Method [70]

It is observed that the matrices associated with the above solution algorithms can be directly used when implementing the market signal analyzing methods. For example, the Hessian matrix associated with the Newton method can be directly used in determining the components of LMPs, while the Jacobian matrix found in the Newton method and the SLP method can be directly utilized in determining the components of the network rental. Further, the solution process of the Newton method implicity determines the LMPs, while the shadow costs can be easily extracted from the matrices. On the other hand, with the SLP algorithm, LMPs are the dual variables, which can also be easily determined.

However, if a commercial or any other software package is used to obtain the optimal dispatch, the above mentioned matrices are not explicitly available for such a post-process analysis. Thus, implementing the OPF in the software tool is required, so that both optimal dispatch and the associated market signals can be determined without using a separate software package. This allows re-using the already created matrices in incorporating the market signal analysis methods, once the OPF is solved.

This chapter gives an in depth analysis and implementation of two such popular methods to solve the NLP-OPF, the Newton method and the SLP method. Based on the analysis on capabilities of different OPF solving techniques conducted during the literature survey, the above two methods were selected in implementing the OPF. Sections 6.1 and 6.2 explain the corresponding algorithm and implementation issues of the Newton method and the SLP method respectively. Extending the above algorithms to incorporate market signal analyzing methods are also discussed in the respective sections. Finally, in Section 6.3, the performance of the developed software is presented together with the comparison of results against that of the OPF modeled in GAMS optimization software.

## 6.1 Implementing the Newton Based Approach

The Newton method is well-known in the area of power systems [45]. It has been a standard solution algorithm for the power flow problem for decades. Application of the Newton method in solving an OPF was first found in the literature in 1984 [66]. Rapid convergence near the solution makes the Newton method a very powerful solution algorithm [20]. This property is especially useful for power system applications, because an initial guess near the solution is easily obtained by solving a dc power flow. This method computes the optimal solution by applying Newton-Raphson algorithm to a set of nonlinear equations obtained from the optimality conditions based on the Lagrangian function of the OPF.

### 6.1.1 The Newton Approach

As discussed in Section 5.1.2, the Lagrangian function of the OPF L is,

$$L(x, \lambda, \mu) = f(x) + \lambda g(x) + \mu h(x) \tag{6.1}$$

The KKT conditions for the Lagrangian equation given in (6.1) can be written as,

$$\frac{\partial L}{\partial x} = \frac{\partial f(x)}{\partial x} + \lambda \frac{\partial g(x)}{\partial x} + \mu \frac{\partial h(x)}{\partial x} = 0 \tag{6.2}$$

$$\frac{\partial L}{\partial \lambda} = g(x) = 0 \tag{6.3}$$

$$\mu h(x) = 0 \tag{6.4}$$

$$\mu \geq 0 \tag{6.5}$$

$$h(x) \leq 0 \tag{6.6}$$

In the Newton approach, the above nonlinear KKT conditions are iteratively solved [66], [67]. The key problem however, is that the binding or the active inequality constraints at the optimal solution are not known beforehand, which makes it difficult to solve. This problem is overcome by removing all the inequality con-

straints from the OPF problem and modeling them through quadratic penalty terms augmented to the Lagrangian function.

By omitting the inequality constraints and adding the penalty terms, the Lagrangian equation can be reformulated as given in (6.7).

$$L(x, \lambda) = f(x) + \lambda g(x) + \text{penalty terms} \tag{6.7}$$

If all the inequality constraints are non-binding at the solution, then all the $\mu$ terms in (6.1) and all the penalty terms in (6.7) are zero. On the other hand, if an inequality constraint is binding at the solution, then it becomes an equality constraint in (6.1) and the penalty terms in (6.7) do not allow that variable to be moved from the limit. This indicates that the solution of (6.1) is the same as the solution of (6.7), and thus, the Newton method proceeds from (6.7).

The KKT conditions of (6.7) are,

$$\frac{\partial L}{\partial x} = \frac{\partial f(x)}{\partial x} + \lambda \frac{\partial g(x)}{\partial x} + \frac{\partial(\text{penalty terms})}{\partial x} = 0 \tag{6.8}$$

$$\frac{\partial L}{\partial \lambda} = g(x) = 0 \tag{6.9}$$

Equations (6.8) and (6.9) can be written in a compact form as,

$$\frac{\partial L}{\partial x} = A(x, \lambda) = 0 \tag{6.10}$$

$$\frac{\partial L}{\partial \lambda} = B(x, \lambda) = 0 \tag{6.11}$$

Equations (6.10) and (6.11) lead to a set of nonlinear equations, with the number of equations equal to the number of variables to be solved. By considering the Taylor series expansion around a starting point $z_0$=$(x_0, \lambda_0)$ and then, ignoring the second

and higher order terms, the following equations can be obtained.

$$A(x_0 + \Delta x_0, \lambda_0 + \Delta\lambda_0) \simeq A(x_0, \lambda_0) + \left.\frac{\partial A}{\partial x}\right|_{x_0,\lambda_0} \Delta x + \left.\frac{\partial A}{\partial \lambda}\right|_{x_0,\lambda_0} \Delta\lambda \simeq 0 \tag{6.12}$$

$$B(x_0 + \Delta x_0, \lambda_0 + \Delta\lambda_0) \simeq B(x_0, \lambda_0) + \left.\frac{\partial B}{\partial x}\right|_{x_0,\lambda_0} \Delta x + \left.\frac{\partial B}{\partial \lambda}\right|_{x_0,\lambda_0} \Delta\lambda \simeq 0 \tag{6.13}$$

Equations (6.12) and (6.13) can be written as a set of linear equations and can be represented in a compact form as,

$$\begin{bmatrix} -A(x_0, \lambda_0) \\ -B(x_0, \lambda_0) \end{bmatrix} = \begin{bmatrix} \left.\frac{\partial A}{\partial x}\right|_{x_0,\lambda_0} & \left.\frac{\partial A}{\partial \lambda}\right|_{x_0,\lambda_0} \\ \left.\frac{\partial B}{\partial x}\right|_{x_0,\lambda_0} & \left.\frac{\partial B}{\partial \lambda}\right|_{x_0,\lambda_0} \end{bmatrix} \begin{bmatrix} \Delta x \\ \Delta\lambda \end{bmatrix} \tag{6.14}$$

By substituting the values for A and B in (6.14),

$$\begin{bmatrix} -\left.\frac{\partial L}{\partial x}\right|_{x_0,\lambda_0} \\ -\left.\frac{\partial L}{\partial \lambda}\right|_{x_0,\lambda_0} \end{bmatrix} = \begin{bmatrix} \left.\frac{\partial^2 L}{\partial x^2}\right|_{x_0,\lambda_0} & \left.\frac{\partial^2 L}{\partial x \partial \lambda}\right|_{x_0,\lambda_0} \\ \left.\frac{\partial^2 L}{\partial \lambda \partial x}\right|_{x_0,\lambda_0} & \left.\frac{\partial^2 L}{\partial \lambda^2}\right|_{x_0,\lambda_0} \end{bmatrix} \begin{bmatrix} \Delta x \\ \Delta\lambda \end{bmatrix} \tag{6.15}$$

$$\begin{bmatrix} -\left.\frac{\partial L}{\partial x}\right|_{x_0,\lambda_0} \\ -\left.\frac{\partial L}{\partial \lambda}\right|_{x_0,\lambda_0} \end{bmatrix} = \begin{bmatrix} \left.\frac{\partial^2 L}{\partial x^2}\right|_{x_0,\lambda_0} & \left.\frac{\partial g(x)}{\partial x}\right|_{x_0,\lambda_0} \\ \left.\frac{\partial g(x)}{\partial x}^T\right|_{x_0,\lambda_0} & 0 \end{bmatrix} \begin{bmatrix} \Delta x \\ \Delta\lambda \end{bmatrix} \tag{6.16}$$

$$\begin{bmatrix} \Delta x \\ \Delta\lambda \end{bmatrix} = - \begin{bmatrix} \left.\frac{\partial^2 L}{\partial x^2}\right|_{x_0,\lambda_0} & \left.\frac{\partial g(x)}{\partial x}\right|_{x_0,\lambda_0} \\ \left.\frac{\partial g(x)}{\partial x}^T\right|_{x_0,\lambda_0} & 0 \end{bmatrix}^{-1} \begin{bmatrix} \left.\frac{\partial L}{\partial x}\right|_{x_0,\lambda_0} \\ \left.g(x)\right|_{x_0,\lambda_0} \end{bmatrix} \tag{6.17}$$

$$\Delta z = -H^{-1} D \tag{6.18}$$

The above matrix H is called the Hessian matrix evaluated at $z_0 = (x_0, \lambda_0)$ and

captures the gradient and the curvature information of the objective function and the constraints. Hessian is a symmetrical and heavily sparse matrix and thus, these features can be exploited in the solution algorithm [20]. The right hand side vector denoted by **D** contains the partial derivatives of L with respect to the variables. The calculated value for $\Delta z$ from (6.18) is then used to determine the next point $z_1$ (i.e., $z_1$=$z_0$+$\Delta z$). This iterative process is continued until the stopping criterion is met.

### 6.1.2 Handling the Inequality Constraints

Since the binding inequality constraints are not known beforehand, inequality constraints are enforced through quadratic penalty terms augmented to the Lagrangian function as shown in (6.7). The penalty term for a variable $x_m$ which has maximum and minimum limits of $x_m^{max}$ and $x_m^{min}$, is:

$$\begin{aligned} penalty &= 0 && : if\ x_m^{min} \leq x_m \leq x_m^{max} \\ penalty &= P(x_m^{min} - x_m)^2 && : if\ x_m^{min} > x_m \\ penalty &= P(x_m^{max} - x_m)^2 && : if\ x_m > x_m^{max} \end{aligned}$$

Where the positive quantity P is referred to as the penalty factor. In general, each constraint can have a separate penalty factor and the behavior of the penalty term is shown in figure 6.1.

If the inequality constraint is not violated, the penalty is zero. When the violation increases, the penalty term is increased in a quadratic manner. Since for a given violation the penalty term depends on the penalty factor, it is possible to control the nature of the constraint by changing the penalty factor. Based on this, all the constraints associated with the OPF can be divided in to two categories.

1. Soft constraints

2. Hard constraints

For soft constraints, a small penalty factor is used and that allows extra freedom to the solution process. As the OPF problem has a large number of constraints,

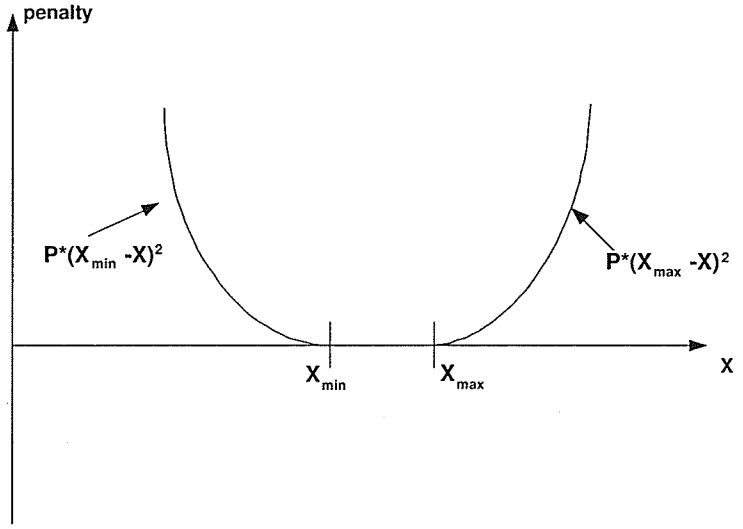


Figure 6.1: Penalty function for the variable X

applying soft constraints is preferred, in order to reduce the infeasibility of the OPF. The word "soft" signifies that the constraint is not absolutely enforced, instead it has the flexibility to violate within a tolerable range. On the other hand, a large penalty factor is used for the hard constraints so that strict enforcement can be obtained.

Typically, the voltage limits and the line flow limits are considered as soft constraints, whereas generator active and reactive power limits are considered as hard constraints.

It can be shown that if the inequality constraints are the limits of the variables specified in the OPF, adding the penalties will only affect the diagonal terms of the Hessian matrix. Let the Lagrangian of the original problem be $L^{old}$, and the augmented Lagrangian be $L^{new}$ (after including $x_m \leq x_m^{max}$). Then,

$$
\begin{aligned}
L^{new} &= L^{old} + P(x_m - x_m^{max})^2 \\
\frac{\partial L^{new}}{\partial x_m} &= \frac{\partial L^{old}}{\partial x_m} + 2P(x_m - x_m^{max}) \\
\frac{\partial^2 L^{new}}{\partial x_m^2} &= \frac{\partial^2 L^{old}}{\partial x_m^2} + 2P \\
\frac{\partial^2 L^{new}}{\partial x_m x_{m1}} &= \frac{\partial^2 L^{old}}{\partial x_m x_{m1}}
\end{aligned}
$$

Which proves that only the diagonal terms are modified, and hence the sparsity of the Hessian is preserved. In contrast, if a constraint is defined for a quantity expressed in terms of many variables, the sparsity of the Hessian is reduced. This can be avoided by explicitly defining that quantity as an equality constraint, at the expense of an additional row and a column in H. For example, the following equality constraint can be included to explicitly define $PF_{ij}$.

$$PF_{ij} = g_{ij}(V_i^2 - V_i V_j \cos\theta_{ij}) - b_{ij} V_i V_j \sin\theta_{ij} \tag{6.19}$$

This explicit definition allows the calculation of the shadow costs in a simple way as explained in Section 6.1.3.

### 6.1.3 Calculation of Marginal Prices, Components of LMP, Components of Network Rental

#### Marginal Prices

Marginal prices include both LMPs and shadow costs. The calculation of LMPs is implicit to the solution process of the Newton method as seen from (6.18). This means that once (6.18) is solved, the LMPs are also known. On the other hand, the shadow costs, which are the marginal prices of the binding constraints, are not directly available from the solution process. However, the shadow costs can be readily extracted from the elements of array **D** at the optimal solution as explained below.

The Lagrangian equation with upper and lower bounds on variable $x_m$ can be written as,

$$L = f(x) + \sum_n \lambda_n g_n(x) + \mu_m^+(x_m - x_m^{max}) + \mu_m^-(x_m^{min} - x_m)$$

$\mu_m^+$ and $\mu_m^-$ are the Lagrangian multipliers associated with the two inequality

constraints. Taking the partial derivative of L with respect to $x_m$,

$$\frac{\partial L}{\partial x_m} = \frac{\partial f(x)}{\partial x_m} + \sum_n \lambda_n \frac{\partial g_n(x)}{\partial x_m} + \mu_m^+ - \mu_m^- = 0 \tag{6.20}$$

Further,

$$\mu_m^+ \mu_m^- = 0 \tag{6.21}$$

$$\mu_m = \mu_m^+ - \mu_m^- \tag{6.22}$$

and,

*if*

$$\mu_m > 0 \quad : x_m = x_m^{max}$$
$$\mu_m < 0 \quad : x_m = x_m^{min}$$
$$\mu_m = 0 \quad : x_m^{min} < x_m < x_m^{max}$$

Now (6.20) becomes,

$$\frac{\partial f(x)}{\partial x_m} + \sum_n \lambda_n \frac{\partial g_n(x)}{\partial x_m} = -\mu_m \tag{6.23}$$

According to (6.8), the **D** vector contains all the partial derivatives of augmented L. Therefore the **D** vector calculated at the solution without adding the penalty terms is equal to the left hand side of (6.23) which is the negative value of the shadow cost $\mu_m$.

The shadow costs of the binding constraints associated with the additionally defined variables in the OPF (such as $PF_{ij}$) can be directly obtained from the solution vector as discussed below.

The Lagrangian with upper and lower bounds on variable $PF_{ij}$ can be written as given in (6.24), where the equality constraint defining the variable $PF_{ij}$ (given in (6.19)) is explicitly included.

$$L = f(x) + \lambda g(x) + \lambda_{ij}[PF_{ij} - g_{ij}(V_i^2 - V_iV_j\cos\theta_{ij}) - b_{ij}V_iV_j\sin\theta_{ij}] + \mu_{ij}^{+}(PF_{ij} - PF_{ij}^{max}) + \mu_{ij}^{-}(PF_{ij}^{min} - PF_{ij}) \quad (6.24)$$

$\mu_{ij}^{+}$ and $\mu_{ij}^{-}$ are the Lagrangian multipliers associated with the two inequality constraints and $\lambda_{ij}$ is the Lagrangian multiplier associated with the equality constraint that defines $PF_{ij}$. Taking the partial derivative of L with respect to $x_j$,

$$\frac{\partial L}{\partial PF_{ij}} = \lambda_{ij} + \mu_{ij}^{+} - \mu_{ij}^{-} = 0 \quad (6.25)$$

According the above remark, (6.25) can be written as,

$$\mu_{ij} = -\lambda_{ij} \quad (6.26)$$

This reveals that the shadow cost is equal to the negative value of the Lagrangian multiplier associated with the equality constraint used to explicitly define that variable.

## Components of LMP

The left hand side matrix appearing in (5.13) (in determining the components of LMP) is the Hessian matrix at the optimal solution with additional rows and columns corresponding to binding constraints. Thus, by augmenting the Hessian matrix in (6.18) at the optimal solution, components of LMP can be easily determined as explained in Chapter 5.

## Components of Network Rental

The Jacobian matrix required for determining the components of network rental in (5.72) is available within the Hessian matrix appearing in (6.18). Thus, the required

rows and columns from the Hessian matrix are extracted and input to the power flow tracing algorithm in determining the components of network rental (note that the optimal dispatch is also passed to this algorithm). This tracing algorithm includes the power flow tracing to determine the generator contributions to each load, and the post processing of KKT conditions in obtaining LMP relationships between two buses, as explained in Chapter 5.

### 6.1.4 Algorithm and Implementation Issues of the Newton Method

The algorithm of the Newton method is summarized in the flow chart shown in figure 6.2. By reading the raw data file, the required data is taken to individual arrays. The cost data file is also read to get the generator bid information. The added feature of reading conventional generator cost curve is also incorporated in this algorithm. This allows the user to experiment the single owner model as well. Initially an economic dispatch without losses is performed in order to find the starting values for the generator active power for the given load condition. The starting values for bus voltages are set to 1 pu and remaining variables are set to zero. Alternatively, a good starting value for bus voltages and angles can be obtained by performing a power flow analysis (either DC power flow or full AC power flow). Because the Newton method has the quadratic convergence only near the optimal point, a good initial guess is always favored [20].

If the initial guess is zero for all variables, it can be seen that matrix H is singular at the beginning. Further, since the initial guess and the optimal solution are quite apart and as the Newton method will have quadratic convergence only near the optimal, it may not provide a decent direction initially [20]. To overcome this difficulty a diagonal matrix, $\gamma.I$ (where $I$ is the identity matrix and $0 < \gamma < 1$), is added to the Hessian to guarantee decent direction initially (see Remark 2). This makes the method more robust. The diagonal matrix is successively reduced by a factor. In the

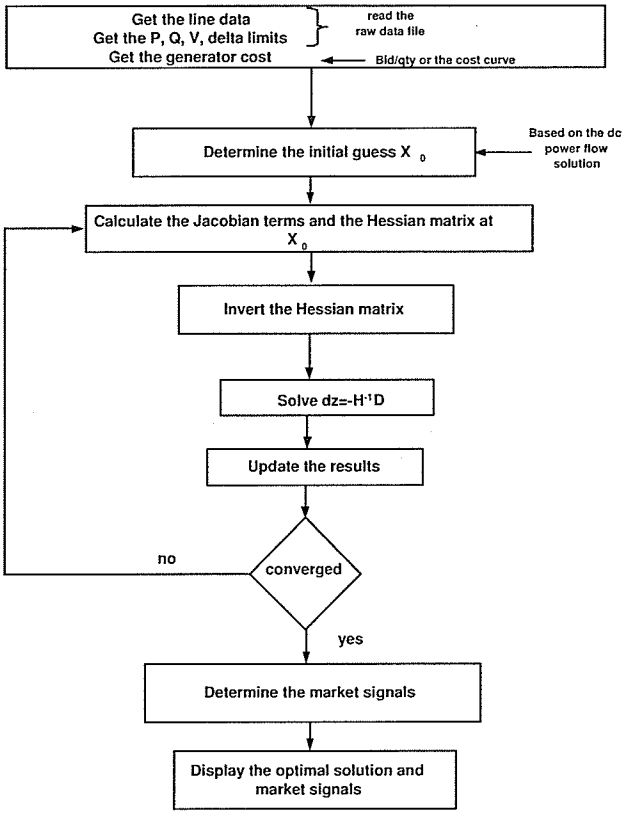


Figure 6.2: Algorithm of the Newton method

implementation, this factor is set as a function of the number of iterations. Hence, when the iterations go on, in the vicinity of the optimal solution, quadratic model of Lagrangian function is used and the effect of this alteration is almost negligible.

**Remark** *For a quadratic function, the Hessian matrix only contains constant elements. Therefore, irrespective of the starting point, the optimal point is reached in one iteration, which is referred to as the quadratic convergence property of the Newton method. However, the quadratic approximation of the Lagrangian equation is not a purely quadratic function and therefore, the elements of the Hessian matrix contain expressions involving variables which necessitate more than one iteration to converge to the optimal point. In the Newton method, (6.27) (same as (6.18) above) is solved*

*and (6.28) is updated iteratively.*

$$\Delta z_k = -H(z_k)^{-1}\nabla L(z_k) \tag{6.27}$$

$$z_{k+1} = z_k + \Delta z_k \tag{6.28}$$

*if H is positive definite, then $-H(z_k)^{-1}$ is the descent direction or the Newton's direction. Therefore, for the execution of this algorithm, Hessian at each iteration must be positive definite. In practice this condition is difficult to be satisfied all the time, specially during the first few iterations. To overcome this difficulty, the positive definite approximation given in (6.29) is used.*

$$\Delta z_k = -[H(z_k) + \gamma.I]^{-1}\nabla L(z_k) \tag{6.29}$$

*The starting value of this factor, $\gamma$ also plays an important role. If the factor is very large (close to 1), then the diagonal terms are significantly altered. Therefore, the initial iterations are approximated to the steepest decent direction (with unit step length) and the second order details embedded to the Hessian are overridden as given in (6.30). The rate of convergence is also reduced, resulting in a large number of iterations and hence more execution time required for the solution process. Thus, a compromised value is chosen for $\gamma$ using a trial and error approach*

$$\Delta z_k = -[\gamma_k.I]^{-1}\nabla L(z_k) \approx -\nabla L(z_k) \tag{6.30}$$

The stopping criteria is met, if the power balance equations are satisfied within a pre-specified tolerance. Therefore, once this condition is met, the control is exit from the iterative loop. This stopping criteria can be enhanced by checking the gradient of the Lagrangian as well. All these values can be easily calculated using the D vector.

Then, the resulting LMPs, LMP components and network rental components are determined as explained in Section 6.1.3. Finally, the results of the OPF including the

marginal prices are written to a text file, which has a similar format to that of GAMS output file [62]. The calculated LMP components and network rental components are also written to a text file for easy reviewing of the results.

## 6.2 Implementing the SLP Based Approach

As the name implies, the Sequential Linear Programming (SLP) method uses Linear Programming (LP) as the search technique. With this approach, the nonlinear objective function and constraints are linearized around an operating point by considering their Taylor series expansions. The resulting LP problem can be solved using the Simplex method or its variants. The solution of the Simplex method is used as the new point around which the nonlinear problem is linearized for the next iteration. This procedure is continued until a stopping criterion is met. The motivation of the SLP method is that successive LP problems can easily be solved using the Simplex method or its variants. However, the linearized model gives satisfactory results only in a small range in the neighborhood of the point used for linearization. The details of the Simplex method and its variants can be found in [9].

### 6.2.1 Linearized Problem

After omitting second and higher order terms, the linearized OPF problem around $x_0$ can be written as,

$$\begin{aligned} \text{optimize} \quad & f(x_0) + \left.\frac{\partial f}{\partial x}\right|_{x_0} \Delta x \\ \text{subject to} \quad & g(x_0) + \left.\frac{\partial g}{\partial x}\right|_{x_0} \Delta x = 0 \\ & h(x_0) + \left.\frac{\partial h}{\partial x}\right|_{x_0} \Delta x \leq 0 \end{aligned} \tag{6.31}$$

In the resulting LP problem, $\Delta x$ are the variables to be solved. The values of

$\Delta x$ can be either positive or negative. However, negative values for $\Delta x$ are not acceptable for use with the Simplex algorithm. Therefore, the variables are replaced by a difference between two positive variables (i.e., $\Delta x$=$\Delta x^+$-$\Delta x^-$). Thereby, the new form of LP problem to be solved using the Simplex method can be represented as,

$$\begin{aligned} \text{optimize} \quad & f(x_0) + \left.\frac{\partial f}{\partial x}\right|_{x_0} \Delta x^+ - \left.\frac{\partial f}{\partial x}\right|_{x_0} \Delta x^- \\ \text{subject to} \quad & g(x_0) + \left.\frac{\partial g}{\partial x}\right|_{x_0} \Delta x^+ - \left.\frac{\partial g}{\partial x}\right|_{x_0} \Delta x^- = 0 \\ & h(x_0) + \left.\frac{\partial h}{\partial x}\right|_{x_0} \Delta x^+ - \left.\frac{\partial h}{\partial x}\right|_{x_0} \Delta x^- \leq 0 \end{aligned} \tag{6.32}$$

The next point around which the problem is linearized, $x_1$=$x_0$+$\Delta x$, is determined by solving (6.32) for $\Delta x$ (i.e., $\Delta x^+$ and $\Delta x^-$). Likewise, in each step an LP problem is solved to obtain the new point until the stopping criteria is met.

### 6.2.2 Calculation of Marginal Prices, Components of LMP, Components of Network Rental

#### Marginal Prices

For a given LP problem there exists another LP problem called the dual problem, which is related to the original or the primal problem. For the primal problem given in (6.33), where $A$ is a matrix and $b$ and $c$ are vectors, the dual problem can be formulated as given in (6.34).

$$\begin{aligned} \text{minimize} \quad & c^T x \\ \text{subject to} \quad & Ax \geq b \\ & x \geq 0 \end{aligned} \tag{6.33}$$

$$\begin{aligned} \text{maximize} \quad & b^T y \\ \text{subject to} \quad & A^T y \leq c \\ & y \geq 0 \end{aligned} \tag{6.34}$$

It can be proved that the dual variables $y$ in (6.34) are the sensitivity of the objective function to the constraints in the primal problem [9]. In other words, dual variables are the changes in the objective function per unit change in the right hand side value of the constraints, which essentially are the marginal prices. Since the dual problem given in (6.34) is also an LP problem, it can be solved using the Simplex method to find the marginal prices.

### Components of LMP

Since the Hessian matrix is not available in the SLP algorithm, in order to calculate the components of LMP, the Hessian matrix has to be formulated separately (note that part of the H matrix consist of the Jacobian terms, which are already available from the SLP algorithm. Thus, only the remaining terms need to be evaluated).

### Components of Network Rental

The Jacobian matrix required in determining the components of network rental is available in (6.31). Thus, by passing this matrix to the power flow tracing algorithm, the components of network rental are calculated (this is previously discussed under the Newton approach in Section 6.1.3).

## 6.2.3 Algorithm and Implementation Issues of the SLP Method

The algorithm of the SLP method is summarized in the flow chart shown in figure 6.3. As discussed in Section 6.1.4, an initial starting point is chosen based on the solution of the dc power flow.

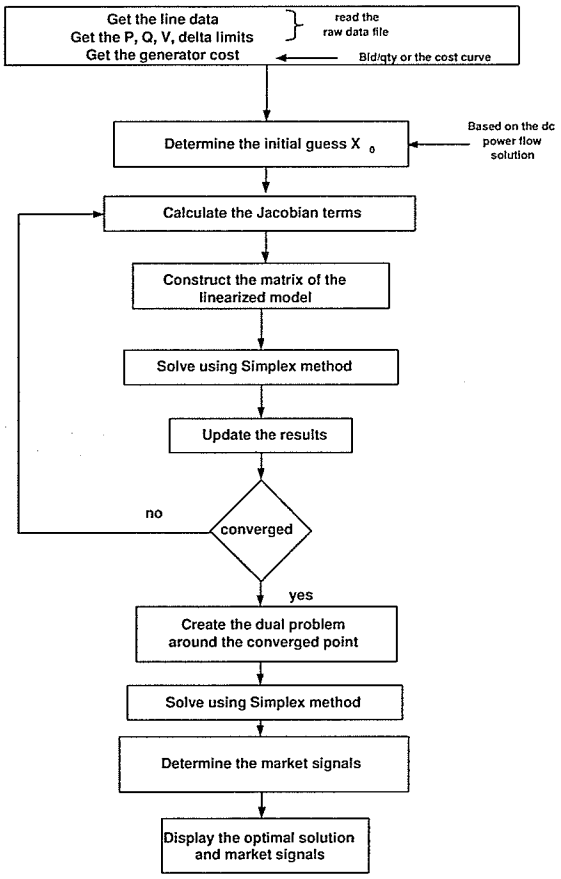


Figure 6.3: Algorithm of the SLP method

Then, the NLP problem is linearized around that starting point and the LP problem is solved to find the next point to be linearized. An efficient variable step is required to maintain the accuracy and the convergence of the SLP approach. This is essential, especially when the starting point is far from the optimal point. If the step length is too small, a large number of iterations is required for the convergence, which effectively increases the execution time. On the other hand, if the step length is too large, the solution can be infeasible or sometimes the solution can bounce between two points during the iterative process.

This problem can be tackled by allowing large steps for the first few iterations and then gradually reducing the step length afterwards [71]. This allows extra freedom for the solution process during the first few iterations to find the desired direction. On

the other hand, efficient step length control reduces the number of iterations required and hence, reduces the execution time for the convergence.

The stopping criteria is met, once the power balance equations are satisfied within a pre-specified tolerance. Therefore, once this condition is met, the control is exit from the iterative loop. Then, the dual problem around the solution is created and the market signals are determined as discussed in Section 6.2.2.

## 6.3 Performance of the Developed Software Tool

In this section, the performance of the $C^{++}$ Newton based and SLP based algorithms are discussed. Tables 6.1 and 6.2 show the execution time (including the raw data file reading and the subsequent market signal analysis) and the number of iterations of the two algorithms for various test systems for the generator quadratic cost function and bid/quantity pairs respectively (the detail on the 30 and 39 bus systems are given in Appendix A and the detail on the remaining test systems can be found in [2], [30]). A Pentium 111 machine with the CPU speed of 2.8 GHz and 512 MB of memory is used to execute the program. The execution times of the OPF modeled in GAMS (excluding the raw data file reading and the subsequent market signal analysis) are also shown in tables 6.1 and 6.2.

Table 6.1: For quadratic cost function

| System | $C^{++}$ Newton based | | $C^{++}$ SLP based | | GAMS |
|---|---|---|---|---|---|
| | time (s) | no of iterations | time (s) | no of iterations | time (s) |
| 3 | 0.09 | 28 | 0.11 | 61 | 0.02 |
| 9 | 0.12 | 16 | 0.40 | 74 | 0.03 |
| 14 | 0.41 | 23 | 0.86 | 71 | 0.09 |
| 30 | 1.56 | 26 | 5.18 | 64 | 0.18 |
| 39 | 2.86 | 24 | 24.00 | 61 | 0.33 |
| 118 | 89.23 | 25 | 716.00 | 48 | 15.23 |

It can be seen that the execution times of the two developed programs are considerably larger than that of models using GAMS. The execution time can be further reduced by exploring the sparsity techniques in matrix manipulations of the two meth-

Table 6.2: For bid/quantity pairs

| System | $C^{++}$ Newton based | | $C^{++}$ SLP based | | GAMS |
|---|---|---|---|---|---|
| | time (s) | no of iterations | time (s) | no of iterations | time (s) |
| 3 | 0.14 | 23 | 0.08 | 40 | 0.03 |
| 9 | 0.21 | 21 | 0.31 | 52 | 0.06 |
| 14 | 0.48 | 24 | 0.89 | 51 | 0.09 |
| 30 | 2.89 | 25 | 3.55 | 58 | 0.14 |
| 39 | 4.58 | 30 | 17.25 | 54 | 0.32 |

ods. Furthermore, a Quasi-Newton approach can be incorporated to speed up the process of the Newton method. The basic idea behind the Quasi-Newton method is to retain the fast convergence speed of the Newton method without evaluating the Hessian at each iteration.

It is identified that for quadratic or any polynomial cost function, Newton method has a good convergence. This is because diagonal terms corresponding to $\frac{\partial^2 f(x)}{\partial P_{gi}^2}$ are always non-zero, giving rise to a conditioned Hessian matrix all the time during the iterative process. On the other hand, for bids and offers, the SLP method has a good convergence due to the fact that normally only few bids are marginal at the optimal solution and the remaining bids are non-marginal (note that in the LP the optimal point is always at the vertex of the feasible region).

During simulations, it is understood that fixed penalty factors for the hard constraints cause some difficulties in finding the optimal solution using the Newton method. Instead, an increasing penalty factor which is a function of the number of iterations is used to tackle this problem. This allows an additional freedom to the variable during the first few iterations, which makes the solution process robust.

## 6.4 Concluding Remarks

This chapter discussed the implemented algorithms of the developed software tool. The inclusion of OPF in the software tool enabled determining the optimal dispatch together with the market signals, while taking the advantage of re-using the same matrices, and eliminating the necessity of a separate OPF solver.

Based on the literature survey of the available OPF solving algorithms, it has been chosen the SLP and the Newton method to implement the OPF. The algorithms, implementation issues, and how to include the market signal analyzing methods for each of the two methods have been discussed. The performances of the developed algorithms have also been demonstrated using various test systems up to 118 buses. A good convergence was obtained by dynamically changing the penalty factors in the Newton algorithm and efficient step length handling in the SLP algorithm. It was also revealed that the Newton method has a good convergence for quadratic or any polynomial cost function, whereas the SLP method has a good convergence for bids and offers. Finally, different methods to improve the performance of the developed software tool have been presented, such as exploring the sparsity techniques in matrix manipulation and adopting the Quasi-Newton approach.

# Chapter 7

# Case Studies and Results

This chapter presents a case study to analyze the market signals using the developed software tool. Since the reactive power and dynamic security related constraints are incorporated in the OPF, more accurate market signals can be analyzed. This investigation study is presented in Section 7.1, where the resulting LMPs, LMP components, and network rental components are analyzed.

## 7.1 Market Signal Analysis using the IEEE New-England 39 Bus System

This section presents a case study using the IEEE New-England 39 bus system shown in Appendix A to analyze the market signals produced by the different methods explained in Chapter 5. A competitive electricity market is modeled using price-quantity bids for the generators as given in table 7.1. The reactive power details given in table 7.2 are as per the reactive power model explained in Chapter 3. The same DSC used in Chapter 4 is considered.

In the presentation of results, all the real and reactive power values are in MW or MVAr, voltages are in pu, prices are in \$/h, and marginal prices are in \$/MWh, \$/MVArh or \$/pu.h depending on the quantity considered.

Table 7.3 shows the real and reactive power dispatch obtained from the developed

Table 7.1: Generator bid data

| Bus | Offer 1 | | Offer 2 | |
|---|---|---|---|---|
| | $P_{ik}^{B}$ | $S_{ik}^{B}$ | $P_{ik}^{B}$ | $S_{ik}^{B}$ |
| 30 | 250 | 3.6 | 750 | 5.2 |
| 31 | 500 | 3.2 | 500 | 4.2 |
| 32 | 600 | 4.0 | 400 | 5.4 |
| 33 | 550 | 3.8 | 450 | 7.25 |
| 34 | 500 | 3.75 | 500 | 4.9 |
| 35 | 650 | 3.7 | 350 | 5.05 |
| 36 | 500 | 3.8 | 500 | 7.4 |
| 37 | 550 | 2.9 | 450 | 5.0 |
| 38 | 900 | 3.8 | 100 | 8.2 |
| 39 | 500 | 3.9 | 500 | 4.1 |

Table 7.2: Reactive power generation data

| Bus | $K_{i,0}^{max}$ | $K_{i,1}^{max}$ | $K_{i,0}^{min}$ | $K_{i,1}^{min}$ | $K_{i}^{Q}$ | $S_{i}^{Q}$ |
|---|---|---|---|---|---|---|
| 30 | 500 | -0.3 | -500 | 0.3 | 0.3 | 0.51 |
| 31 | 500 | -0.3 | -500 | 0.3 | 0.3 | 0.30 |
| 32 | 500 | -0.3 | -500 | 0.3 | 0.3 | 0.74 |
| 33 | 500 | -0.3 | -500 | 0.3 | 0.3 | 0.32 |
| 34 | 500 | -0.3 | -500 | 0.3 | 0.3 | 0.35 |
| 35 | 500 | -0.3 | -500 | 0.3 | 0.3 | 0.28 |
| 36 | 500 | -0.3 | -500 | 0.3 | 0.3 | 0.41 |
| 37 | 500 | -0.3 | -500 | 0.3 | 0.3 | 0.55 |
| 38 | 500 | -0.3 | -500 | 0.3 | 0.3 | 0.64 |
| 39 | 500 | -0.3 | -500 | 0.3 | 0.3 | 0.42 |

software for the case considered. Columns 3, 4 and 5 show the real power dispatch details, whereas the last five columns show the reactive power dispatch details.

It can be seen in table 7.3 and the generator bids given in table 7.1 that the generation dispatch deviates from the merit order significantly. The cheaper generation at buses 34 (i.e., $1^{st}$ bid) and 38 (i.e., $1^{st}$ bid) are not fully dispatched, while the expensive generation at buses 30 (i.e., $2^{nd}$ bid), 31 (i.e., $2^{nd}$ offer), and 37 (i.e., $2^{nd}$ offer) are partly dispatched. Thus, the real power generation at buses 30, 31, 34, 37 and 38 are marginal. This is expected because the power system operates on several binding constraints as evident from the non-zero marginal costs given in table 7.4. The DSC, six voltages (i.e., $V_{33}$, $V_{34}$, $V_{35}$, $V_{36}$, $V_{37}$, $V_{38}$), and one line flow (i.e., $PF_{38\ 29}$) are the binding constraints (i.e., altogether 8 binding constraints). The total real power

Table 7.3: Generation dispatch

| Bus | Real power | | | Reactive power | | | | |
|---|---|---|---|---|---|---|---|---|
| | bid 1 | bid 2 | Total | $Q_{g1}$ | $Q_{g2}$ | Total | $Q_{g1}^{max}$ | $Q_{g}^{max}$ |
| 30 | 250.00 | 425.82 | 675.82 | 202.75 | 94.51 | 297.25 | 127.75 | 297.25 |
| 31 | 500.00 | 9.57 | 509.57 | 152.87 | 194.26 | 347.13 | 152.87 | 347.13 |
| 32 | 600.00 | 0.00 | 600.00 | 180.00 | 140.00 | 320.00 | 180.00 | 320.00 |
| 33 | 550.00 | 0.00 | 550.00 | 165.00 | 47.90 | 212.90 | 165.00 | 335.00 |
| 34 | 128.82 | 0.00 | 128.82 | 38.65 | 122.57 | 161.21 | 38.65 | 461.35 |
| 35 | 650.00 | 0.00 | 650.00 | 195.00 | 88.10 | 283.10 | 195.00 | 305.00 |
| 36 | 500.00 | 0.00 | 500.00 | 150.00 | 19.99 | 169.99 | 150.00 | 350.00 |
| 37 | 550.00 | 179.23 | 729.23 | 218.77 | 0.09 | 218.86 | 218.77 | 281.23 |
| 38 | 800.00 | 0.00 | 800.00 | 229.93 | 0.00 | 229.93 | 240.00 | 260.00 |
| 39 | 500.00 | 500.00 | 1000.00 | 200.00 | 0.00 | 200.00 | 200.00 | 200.00 |

dispatch is 6143.44 MW, which includes an associated real power loss of 46.34 MW.

In regard to the reactive power dispatch, with the exception of bus 38, the free reactive power (i.e Block 1 Reactive Power) from all generators is fully utilized. The voltage limit at bus 38, doesn't allow the use of the remaining amount of Block 1 Reactive Power (note that the shadow cost of the binding $V_{38}$ is comparably large). The Block 2 Reactive Power of generators at buses 30, 31, 32, and 39 are fully utilized and those generators operate at their respective capability limits. Close examination of Block 2 Reactive Power prices given in table 7.2, however, reveal that those generators have higher Block 2 Reactive Power prices. This is because, the binding voltage constraints restrict the cheaper reactive power being dispatched.

Table 7.4: Binding constraints

| constraint | quantity | shadow cost |
|---|---|---|
| $V_{33}$ | 1.10 pu | 1383.61 |
| $V_{34}$ | 1.10 pu | 98.48 |
| $V_{35}$ | 1.10 pu | 1593.07 |
| $V_{36}$ | 1.10 pu | 74.35 |
| $V_{37}$ | 1.10 pu | 1003.34 |
| $V_{38}$ | 1.10 pu | 1766.88 |
| $PF_{38\ 29}$ | 800 MW | 0.53 |
| $DSC$ | 10 cy | 99.40 |

### 7.1.1 LMPs

Based on the generation dispatch, the total network rental paid by all the consumers is calculated and presented in table 7.5 together with the LMPs. This shows that the accumulated real and reactive power network rental with the ISO are 3357.87 and 868.70 respectively.

As pointed out in Chapter 5, other than indicating the price at a given node, the LMP does not show the effects of the contributing components explicitly. Thus, by looking at LMPs, participants only see the relative price at each node. For example, consumer at bus 39 sees a relatively higher LMP for real and reactive power at its node, whereas the generator at bus 38 sees its real and reactive power LMP as relatively low.

At real power marginal buses except at bus 38, the resulting real power LMPs (i.e., $\lambda_{30}$, $\lambda_{31}$, $\lambda_{34}$, and $\lambda_{37}$) are slightly less than the bid price of the corresponding generator. This slight reduction is due to the free reactive power availability when increasing the real power dispatch. The $\lambda_{38}$, however, is equal to the bid price of the generator at bus 38. This is because at bus 38 Block 1 Reactive Power is not fully dispatched. The reactive power generation at buses 33, 34, 35, 36, 37, and 38 are marginal, and hence the resulting reactive power LMPs (i.e., $\sigma_{33}$, $\sigma_{34}$, $\sigma_{35}$, $\sigma_{36}$, and $\sigma_{37}$) are equal to the corresponding Block 2 Reactive Power price of the generator. However, the reactive power LMP at bus 38, $\sigma_{38}$, is zero due to the fact that the Block 1 Reactive Power is not fully dispatched.

### 7.1.2 LMP Components

The LMP components due to binding constraints (i.e., $V_{33}$, $V_{34}$, $V_{35}$, $V_{36}$, $V_{37}$, $V_{38}$, $PF_{38\ 29}$, and $DSC$) are calculated as explained in Chapter 5 and shown in table 7.6. Please note that only the components of real power LMPs are presented to clearly explain the subsequent analysis. However, the components of reactive power LMPs can also be analyzed in the same way.

Table 7.5: Network rental for the 39 bus system

| Bus | LMP | | Generator Receipt | | Consumer Payment | |
|---|---|---|---|---|---|---|
| | $\lambda$ | $\sigma$ | P | Q | P | Q |
| 1 | 5.89 | 1.08 | 0.00 | 0.00 | 0.00 | 0.00 |
| 2 | 5.34 | 0.91 | 0.00 | 0.00 | 0.00 | 0.00 |
| 3 | 5.44 | 0.98 | 0.00 | 0.00 | 1751.36 | 2.36 |
| 4 | 5.49 | 1.29 | 0.00 | 0.00 | 2747.00 | 237.36 |
| 5 | 5.39 | 1.34 | 0.00 | 0.00 | 0.00 | 0.00 |
| 6 | 5.32 | 1.35 | 0.00 | 0.00 | 0.00 | 0.00 |
| 7 | 5.51 | 1.34 | 0.00 | 0.00 | 1288.94 | 112.81 |
| 8 | 5.59 | 1.34 | 0.00 | 0.00 | 2919.02 | 236.19 |
| 9 | 5.98 | 1.21 | 0.00 | 0.00 | 0.00 | 0.00 |
| 10 | 5.19 | 1.31 | 0.00 | 0.00 | 0.00 | 0.00 |
| 11 | 5.24 | 1.31 | 0.00 | 0.00 | 0.00 | 0.00 |
| 12 | 5.29 | 1.07 | 0.00 | 0.00 | 39.67 | 94.16 |
| 13 | 5.24 | 1.29 | 0.00 | 0.00 | 0.00 | 0.00 |
| 14 | 5.36 | 1.28 | 0.00 | 0.00 | 0.00 | 0.00 |
| 15 | 5.27 | 1.08 | 0.00 | 0.00 | 1686.08 | 165.55 |
| 16 | 5.10 | 0.81 | 0.00 | 0.00 | 1678.23 | 26.20 |
| 17 | 5.18 | 0.76 | 0.00 | 0.00 | 0.00 | 0.00 |
| 18 | 5.30 | 0.83 | 0.00 | 0.00 | 836.61 | 25.02 |
| 19 | 4.96 | 0.63 | 0.00 | 0.00 | 0.00 | 0.00 |
| 20 | 5.08 | 0.66 | 0.00 | 0.00 | 3192.12 | 67.77 |
| 21 | 4.90 | 0.68 | 0.00 | 0.00 | 1342.05 | 78.32 |
| 22 | 4.63 | 0.51 | 0.00 | 0.00 | 0.00 | 0.00 |
| 23 | 4.64 | 0.54 | 0.00 | 0.00 | 1149.39 | 45.60 |
| 24 | 5.06 | 0.76 | 0.00 | 0.00 | 1559.97 | 0.00 |
| 25 | 5.07 | 0.84 | 0.00 | 0.00 | 1134.78 | 39.55 |
| 26 | 5.02 | 0.55 | 0.00 | 0.00 | 698.34 | 9.28 |
| 27 | 5.10 | 0.54 | 0.00 | 0.00 | 1433.10 | 41.00 |
| 28 | 4.82 | 0.40 | 0.00 | 0.00 | 992.51 | 11.12 |
| 29 | 4.76 | 0.29 | 0.00 | 0.00 | 1350.31 | 7.83 |
| 30 | 5.15 | 0.85 | 3480.49 | 80.61 | 0.00 | 0.00 |
| 31 | 4.45 | 1.42 | 2265.54 | 276.24 | 40.90 | 6.54 |
| 32 | 4.79 | 1.29 | 2871.00 | 180.46 | 0.00 | 0.00 |
| 33 | 4.44 | 0.32 | 2442.00 | 15.33 | 0.00 | 0.00 |
| 34 | 3.65 | 0.35 | 469.56 | 42.90 | 0.00 | 0.00 |
| 35 | 4.44 | 0.28 | 2884.70 | 24.67 | 0.00 | 0.00 |
| 36 | 4.29 | 0.41 | 2142.50 | 8.20 | 0.00 | 0.00 |
| 37 | 4.84 | 0.55 | 3525.82 | 0.05 | 0.00 | 0.00 |
| 38 | 3.80 | 0.00 | 3040.00 | 0.00 | 0.00 | 0.00 |
| 39 | 6.15 | 1.16 | 6145.00 | 0.00 | 6784.08 | 290.50 |
| | Total | | 29266.60 | 628.45 | 32624.47 | 1497.15 |
| | **Network Rental** | | | | **3357.87** | **868.70** |

Table 7.6: LMP components

| | LMP | LMP component | | | | | | | |
|---|---|---|---|---|---|---|---|---|---|
| | | $V_{33}$ | $V_{34}$ | $V_{35}$ | $V_{36}$ | $V_{37}$ | $V_{38}$ | $PF_{38\ 29}$ | $DSC$ |
| 1 | 5.89 | 0.28 | 0.05 | -0.01 | 0.00 | -0.03 | -0.34 | 0.04 | 0.26 |
| 2 | 5.34 | 0.09 | 0.02 | -0.01 | 0.00 | -0.01 | -0.12 | 0.05 | 0.24 |
| 3 | 5.44 | 0.21 | 0.04 | -0.02 | 0.00 | -0.04 | -0.28 | 0.06 | 0.08 |
| 4 | 5.49 | 0.26 | -0.05 | -0.02 | -0.01 | -0.15 | -0.34 | 0.03 | 0.29 |
| 5 | 5.39 | 0.22 | 0.04 | -0.01 | 0.00 | -0.04 | -0.29 | 0.00 | 0.24 |
| 6 | 5.32 | 0.21 | 0.04 | -0.01 | 0.00 | -0.04 | -0.27 | -0.01 | 0.22 |
| 7 | 5.51 | 0.25 | 0.05 | -0.01 | 0.00 | -0.04 | -0.32 | 0.01 | 0.24 |
| 8 | 5.59 | 0.06 | 0.05 | -0.11 | 0.00 | -0.14 | -0.34 | 0.02 | 0.06 |
| 9 | 5.98 | 0.26 | 0.05 | 0.00 | 0.00 | -0.04 | -0.32 | 0.03 | 0.24 |
| 10 | 5.19 | 0.19 | 0.04 | -0.02 | 0.00 | -0.04 | -0.27 | -0.01 | 0.24 |
| 11 | 5.24 | 0.20 | 0.04 | -0.01 | 0.00 | -0.04 | -0.27 | -0.01 | 0.24 |
| 12 | 5.29 | 0.21 | 0.04 | -0.02 | 0.00 | -0.04 | -0.29 | -0.01 | 0.26 |
| 13 | 5.24 | 0.21 | 0.04 | -0.02 | 0.00 | -0.04 | -0.29 | 0.00 | 0.27 |
| 14 | 5.36 | 0.26 | 0.05 | -0.02 | 0.00 | -0.05 | -0.36 | 0.02 | 0.33 |
| 15 | 5.27 | 0.35 | 0.07 | -0.04 | 0.00 | -0.08 | -0.51 | 0.07 | 0.44 |
| 16 | 5.10 | 0.36 | 0.07 | -0.05 | 0.00 | -0.09 | -0.53 | 0.07 | 0.47 |
| 17 | 5.18 | 0.27 | 0.05 | -0.03 | 0.00 | -0.06 | -0.38 | 0.09 | 0.35 |
| 18 | 5.30 | 0.26 | 0.05 | -0.03 | 0.00 | -0.05 | -0.35 | 0.08 | 0.03 |
| 19 | 4.96 | 0.56 | 0.11 | -0.08 | 0.00 | -0.14 | -0.87 | 0.03 | 0.78 |
| 20 | 5.08 | 0.05 | 0.15 | -0.11 | -0.01 | -0.19 | -1.18 | 0.04 | 1.04 |
| 21 | 4.90 | 0.33 | 0.06 | -0.05 | 0.00 | -0.08 | -0.49 | 0.05 | 0.49 |
| 22 | 4.63 | 0.30 | 0.06 | -0.06 | 0.00 | -0.08 | -0.46 | 0.02 | 0.47 |
| 23 | 4.64 | 0.30 | 0.06 | -0.06 | 0.00 | -0.08 | -0.46 | 0.02 | 0.50 |
| 24 | 5.06 | 0.35 | 0.07 | -0.05 | 0.00 | -0.08 | -0.52 | 0.06 | 0.48 |
| 25 | 5.07 | 0.02 | 0.00 | 0.00 | 0.00 | 0.00 | -0.01 | 0.09 | -0.01 |
| 26 | 5.02 | 0.04 | 0.01 | 0.00 | 0.00 | 0.00 | -0.01 | 0.16 | 0.05 |
| 27 | 5.10 | 0.05 | 0.03 | -0.02 | 0.00 | -0.13 | -0.18 | 0.14 | 0.18 |
| 28 | 4.82 | -0.06 | -0.01 | 0.01 | 0.00 | 0.02 | 0.17 | 0.23 | 0.07 |
| 29 | 4.76 | -0.08 | -0.02 | 0.01 | 0.00 | 0.02 | 0.20 | 0.23 | 0.11 |
| 30 | 5.15 | 0.00 | 0.00 | 0.00 | 0.00 | 0.00 | 0.00 | 0.00 | 0.00 |
| 31 | 4.45 | 0.00 | 0.00 | 0.00 | 0.00 | 0.00 | 0.00 | 0.00 | 0.00 |
| 32 | 4.79 | 0.38 | 0.08 | -0.06 | 0.00 | -0.10 | -0.62 | -0.02 | 0.58 |
| 33 | 4.44 | 0.38 | 0.08 | -0.06 | 0.00 | -0.10 | -0.62 | 0.02 | 0.58 |
| 34 | 3.65 | 0.00 | 0.00 | 0.00 | 0.00 | 0.00 | 0.00 | 0.00 | 0.00 |
| 35 | 4.44 | 0.30 | 0.06 | -0.08 | 0.00 | -0.08 | -0.46 | 0.02 | 0.49 |
| 36 | 4.29 | 0.30 | 0.06 | -0.07 | 0.00 | -0.08 | -0.45 | 0.02 | 0.49 |
| 37 | 4.84 | 0.00 | 0.00 | 0.00 | 0.00 | 0.00 | 0.00 | 0.00 | 0.00 |
| 38 | 3.80 | 0.00 | 0.00 | 0.00 | 0.00 | 0.00 | 0.00 | 0.00 | 0.00 |
| 39 | 6.15 | -0.25 | -0.05 | -0.10 | -0.01 | -0.03 | -0.30 | 0.04 | 0.20 |

These components of LMPs show the contribution of each LMP due to each binding constraint. For example, component due to binding constraints $PF_{38\ 29}$ and DSC

on $\lambda_{20}$ are 0.04 and 1.04 respectively. This provides the consumer at bus 20 with an additional information about the price in the form of contributing components. Similar information is available for the other consumers as well.

The table 7.6 reveals that higher contributions on LMPs due to binding $PF_{38\ 29}$ and DSC are resulted at bus 29 and bus 20 respectively. Furthermore, it can be seen that the effects of the binding line flow $PF_{38\ 29}$ is localized around bus 29, whereas the effects of the binding DSC are significant throughout the system. However, consumers have no information about the effects of transmission losses on their respective LMPs, instead are embedded in the explicitly expressed components.

### 7.1.3 Network Rental Components

The power flow tracing is used to determine how each load and the apportioned losses supplied by each generator. The resulting generator contributions are shown in table 7.7. For example, there is 4.70 MW of associated losses in catering 322 MW at bus 3 and generators at bus 30 and 38 supply this load and the losses in part by 237.61 MW and 89.09 MW respectively. The important point to note is that the load at bus 31 and part of the load at bus 39 are locally provided by the respective generators and hence are automatically ignored during the power flow tracing (also note that due to these loads no network rental is accumulated as the generation and the load are at the same bus). The remaining portion of the load, however, causes an accumulation of network rental which is already considered in power flow tracing as shown in table 7.7.

Once the tracing is done, the power system can be viewed as several independent networks (18 in number for this case), each having a single load. Thus, based on the proposed method explained in Chapter 5, the network rental components paid by each consumer are calculated and presented in table 7.8. The real power loss rental and reactive power loss rental are given in columns 2 and 3 respectively, and constraint rental due to binding constraints (i.e., $V_{33}$, $V_{34}$, $V_{35}$, $V_{36}$, $V_{37}$, $V_{38}$, $PF_{38\ 29}$,

Table 7.7: Generator contributions and apportioned losses to each load

| | Generator | | | | | | | | | $P^{L\_app}$ |
|---|---|---|---|---|---|---|---|---|---|---|
| | 30 | 31 | 32 | 33 | 34 | 35 | 36 | 37 | 38 | |
| 3 | 237.61 | 0.00 | 0.00 | 0.00 | 0.0 | 0.00 | 0.00 | 89.09 | 0.00 | 4.70 |
| 4 | 165.20 | 83.74 | 203.56 | 0.00 | 0.0 | 0.00 | 0.00 | 61.94 | 0.00 | 5.24 |
| 7 | 0.00 | 147.28 | 87.45 | 0.00 | 0.0 | 0.00 | 0.00 | 0.00 | 0.00 | 0.94 |
| 8 | 59.34 | 278.55 | 165.39 | 0.00 | 0.0 | 0.00 | 0.00 | 22.25 | 0.00 | 3.53 |
| 12 | 0.00 | 0.00 | 7.57 | 0.00 | 0.0 | 0.00 | 0.00 | 0.00 | 0.00 | 0.07 |
| 15 | 7.25 | 0.00 | 136.03 | 16.99 | 0.0 | 108.94 | 4.78 | 23.87 | 25.86 | 3.72 |
| 16 | 12.87 | 0.00 | 0.00 | 30.14 | 0.0 | 193.28 | 8.48 | 42.36 | 45.89 | 4.02 |
| 18 | 116.82 | 0.00 | 0.00 | 0.00 | 0.0 | 0.00 | 0.00 | 43.80 | 0.00 | 2.63 |
| 20 | 0.00 | 0.00 | 0.00 | 502.87 | 128.8 | 0.00 | 0.00 | 0.00 | 0.00 | 3.69 |
| 21 | 0.00 | 0.00 | 0.00 | 0.00 | 0.0 | 275.23 | 0.00 | 0.00 | 0.00 | 1.23 |
| 23 | 0.00 | 0.00 | 0.00 | 0.00 | 0.0 | 32.17 | 215.84 | 0.00 | 0.00 | 0.51 |
| 24 | 0.00 | 0.00 | 0.00 | 0.00 | 0.0 | 40.38 | 270.90 | 0.00 | 0.00 | 2.68 |
| 25 | 0.00 | 0.00 | 0.00 | 0.00 | 0.0 | 0.00 | 0.00 | 224.89 | 0.00 | 0.89 |
| 26 | 0.00 | 0.00 | 0.00 | 0.00 | 0.0 | 0.00 | 0.00 | 63.39 | 77.50 | 1.89 |
| 27 | 0.00 | 0.00 | 0.00 | 0.00 | 0.0 | 0.00 | 0.00 | 128.86 | 157.54 | 5.40 |
| 28 | 0.00 | 0.00 | 0.00 | 0.00 | 0.0 | 0.00 | 0.00 | 0.00 | 208.08 | 2.08 |
| 29 | 0.00 | 0.00 | 0.00 | 0.00 | 0.0 | 0.00 | 0.00 | 0.00 | 285.13 | 1.63 |
| 39 | 76.73 | 0.00 | 0.00 | 0.00 | 0.0 | 0.00 | 0.00 | 28.77 | 0.00 | 1.50 |
| | 675.82 | 509.57 | 600.00 | 550.00 | 128.8 | 650.00 | 500.00 | 729.23 | 800.00 | 46.34 |

and $DSC$) are given in the next eight columns in the same order.

At a glance, table 7.8 shows the overpayment made by all the consumers due to the losses and the binding constraints separately. A closer look reveals that the bulk of the network rental collected by the ISO is due to the binding DSC for the case considered. Further, a significant network rental is accumulated in the form of reactive power loss rental (note that unlike the case study discussed in Chapter 5, the reactive power loss rental in this case is higher due to reactive power pricing). The binding line flow $PF_{38\ 29}$ accumulated a rental from consumers at buses 15, 16, 26, 27, 28, and 29. The generator contributions based on power flow tracing given in table 7.7 confirms that the generator at bus 38 (which is the constrained-off generator due to the binding line flow $PF_{38\ 29}$) supplies only to the above loads. This is in agreement with the LMP components calculated previously, where a higher component is resulted due to binding $PF_{38\ 29}$ at bus 29 . Thus, these figures give a good insight to what leads them to overpay due to the binding line flow $PF_{38\ 29}$.

Table 7.8: Components of network rental

| | Network Rental | | | | | | | | | | |
|---|---|---|---|---|---|---|---|---|---|---|---|
| | total | loss rental | | constraint rental | | | | | | | |
| | | P | Q | $V_{33}$ | $V_{34}$ | $V_{35}$ | $V_{36}$ | $V_{37}$ | $V_{38}$ | $PF_{38\ 29}$ | $DSC$ |
| $NR_{P3}$ | 97.03 | 18.41 | 151.11 | -4.95 | -0.35 | -5.85 | -0.28 | -12.14 | -15.79 | 0.00 | -33.12 |
| $NR_{P4}$ | 163.15 | 24.35 | 163.35 | -20.50 | -1.46 | -24.21 | -1.14 | -24.65 | -40.40 | 0.00 | 87.82 |
| $NR_{P7}$ | 220.77 | 10.13 | 104.78 | -6.19 | -0.44 | -7.31 | -0.34 | -4.16 | -8.11 | 0.00 | 132.41 |
| $NR_{P8}$ | 475.86 | 19.90 | 286.43 | -24.86 | -1.77 | -29.36 | -1.38 | -20.77 | -37.83 | 0.00 | 285.48 |
| $NR_{P12}$ | 3.81 | 0.43 | 3.38 | -1.14 | -0.08 | -1.34 | -0.06 | -0.86 | -1.63 | 0.00 | 5.12 |
| $NR_{P15}$ | 204.60 | 17.83 | 161.52 | -8.93 | -0.63 | -18.44 | -0.77 | -14.00 | -28.60 | 13.82 | 82.81 |
| $NR_{P16}$ | 204.69 | 21.49 | 122.25 | -0.48 | -0.03 | -14.57 | -0.51 | -10.37 | -24.45 | 24.52 | 86.84 |
| $NR_{P18}$ | 37.14 | 23.91 | 75.40 | -4.18 | -0.30 | -4.94 | -0.23 | -11.41 | -14.25 | 0.00 | -26.87 |
| $NR_{P20}$ | 508.25 | 52.01 | 136.28 | -26.91 | 0.06 | -52.44 | -2.47 | -40.98 | -73.51 | 0.00 | 516.20 |
| $NR_{P21}$ | 126.64 | 11.72 | 57.88 | -2.58 | -0.18 | -12.76 | -0.38 | -2.38 | -4.27 | 0.00 | 79.58 |
| $NR_{P23}$ | 84.07 | 4.43 | 29.70 | -0.38 | -0.03 | -1.01 | -0.38 | -0.36 | -0.64 | 0.00 | 52.74 |
| $NR_{P24}$ | 233.56 | 26.76 | 106.51 | -4.61 | -0.33 | -21.67 | -1.57 | -4.26 | -7.64 | 0.00 | 140.38 |
| $NR_{P25}$ | 51.89 | 8.40 | 53.63 | 0.00 | 0.00 | 0.00 | 0.00 | -5.55 | 0.00 | 0.00 | -4.59 |
| $NR_{P26}$ | 106.91 | 21.59 | 35.94 | -5.51 | -0.39 | -6.51 | -0.31 | -6.20 | -10.21 | 41.41 | 37.09 |
| $NR_{P27}$ | 238.88 | 66.84 | 95.26 | -15.15 | -1.08 | -17.89 | -0.84 | -20.29 | -42.33 | 84.18 | 90.18 |
| $NR_{P28}$ | 211.92 | 22.63 | 32.27 | -14.75 | -1.05 | -17.42 | -0.82 | -9.58 | -12.16 | 111.19 | 101.62 |
| $NR_{P29}$ | 274.65 | 14.44 | 17.20 | 0.00 | 0.00 | 0.00 | 0.00 | 0.00 | -3.77 | 152.36 | 94.42 |
| $NR_{P39}$ | 114.06 | 30.80 | 121.13 | -47.51 | -3.39 | -56.12 | -2.64 | -33.33 | -65.13 | 0.00 | 170.24 |
| | **3357.87** | **396.07** | **1754.03** | **-188.63** | **-11.45** | **-291.85** | **-14.13** | **-221.27** | **-390.72** | **427.49** | **1898.34** |

A higher rental is accumulated due to DSC from the consumer at bus 20, which is also in agreement with the previously calculated LMP components at bus 20. Further, the rental due to DSC is distributed throughout the system, which is also similar to that of LMP components.

### 7.1.4 Discussion

An important point to note is that the resulting LMP component and the network rental component due to a given binding constraint cannot be directly compared. This is because the effects of the losses are embedded in the LMP component, whereas they are explicit in the network rental component. This situation is clearly observed in the LMP components and network rental components of the binding voltage constraints. Due to this reason, for a given binding voltage constraint, while the resulting LMP component is positive, the resulting network rental component could be negative and

vice-versa. In fact, a closer look reveals that the components of network rental are shifted relatively downwards with respect to the LMP components and the effects of this shift is seen as positive contributions to the reactive power loss rental.

Another point to note is that the components of network rental shown in table 7.8 are for the total load, whereas LMP components presented in table 7.6 are for unit MW or MVAr. In general, LMP components can be calculated for all the buses, whereas network rental components can only be calculated for load buses. Thus, these rental components can be considered as consumer-oriented market signals.

## 7.2 Concluding Remarks

The case study performed using the IEEE New England 39 bus system demonstrated the application of network rental components in market signal analysis. It has been shown that these individual components provide supplementary information for the consumers, in terms of the amounts they overpaid due to marginal losses and binding constraints.

The results of the case study revealed that even though LMPs provide valuable information at each location, they failed to provide the effects of the contributing factors explicitly. On the other hand, the calculated LMP components showed a detailed description due to all binding constraints. However, the effects of the losses were implicit to the explicitly available components.

The calculated components of network rental showed the effects of the losses and the binding constraints explicitly. It has also been shown that LMP components and network rental components are in good agreement, even though the results of the two methods cannot be directly compared.

# Chapter 8

# Conclusions

## 8.1 General Conclusions

A new approach to analyze the market signals has been presented by means of components of network rental in this thesis. A mathematical analysis has been proposed to determine these network rental components, by combining the KKT optimality conditions and the power flow tracing. Network rental is the accumulated revenue with the ISO after settling the transactions. This accumulated revenue is solely paid by the consumers due to the effects of marginal losses and binding constraints imposed by the OPF. As the network rental is determined by the above factors, it has been argued that supplementary market signals are provided by components of network rental showing the decomposition due to each of the above factors to each consumer. A case study has also been presented to demonstrate this.

This thesis also highlights the fact that the correct market signals can only be analyzed, if the operating constraints are correctly modeled in the OPF. Thus, an effort has been made to mathematically model two such important constraints (i.e., reactive power and the dynamic security) in the OPF. The competitive electricity market has also been modeled using generator bid/quantity pairs for the mathematical analysis and case studies presented in this thesis.

Chapter 2 investigated the operation of the current electricity markets to de-

termine a common market framework for the work presented in this thesis. After reviewing the common features to most of the existing electricity markets, the pool-based market model has been chosen for the research work presented in this thesis, due to its competitive framework. Chapter 2 also presented the concept of Locational Marginal Pricing, which is currently used in most electricity markets together with some examples to demonstrate how these LMPs are calculated.

Chapters 3 and 4 dealt with incorporating reactive power and dynamic security related constraints into the OPF respectively. Chapter 3 started with investigating the present reactive power procurement methods and explaining the different ways of modeling reactive power in market dispatch. The limitations and the drawbacks of these methods have been discussed. A new reactive power model considering both the capability of the synchronous generator and the fairness of reactive power supply obligation in a competitive market environment has been presented thereafter. The main features of this model are, (a) generators are not required to supply reactive power free of charge when they are not supplying real power, (b) generators are required to make a minimum amount of reactive power available to the system and this amount is proportional to the real power, (c) the maximum limit of the reactive power is determined by the capability curve of the generator and is dependent on the real power generation. A case study with the proposed reactive power model has been presented to demonstrate that, (a) real power LMP has a reactive power component, (b) LMP for reactive power can also be defined, and (c) sequential approach may give rise to an unfair advantage to some participants while the overall solution is inferior to the simultaneous dispatch.

A brief summary about the system security including both static security and dynamic security has been presented at the beginning of Chapter 4. The inclusion of the DSC in the OPF and its effects on nodal pricing have been presented thereafter. The function to represent the DSC proposed in [51] is differentiable, and thus suitable for optimization algorithms such as sequential linear programming (SLP) and Newton

type algorithms. It has been shown that any number of DSCs, each representing a credible contingency, can be incorporated in the OPF to ensure security of the system in the event of the contingencies represented by the respective DSCs. A case study has also been presented to demonstrate the effects of DSC on dispatch as well as on LMPs.

Having incorporated reactive power and dynamic security issues into market dispatch, analyzing the market signals has been discussed in Chapter 5. It has been mentioned that LMPs provide crucial market signals for the participants in the present electricity market. A recently proposed method of LMP components has then been presented. It has been shown that the decomposed components provide additional information at each location due to marginal generators and binding constraints, even though the effects of the losses are not explicitly shown.

A new method to analyze market signals has been proposed later in Chapter 5 by means of components of network rental. In this regard, a method to decompose the network rental among the consumers into loss rental and constraint rental due to each binding constraint has been proposed by combining the power flow tracing and KKT optimality conditions of the NLP-OPF. The rental components for a single load bus has been calculated by mathematically expressing the network rental in terms of LMP differences, and substituting those with the implicitly calculated values based on post processed KKT optimality conditions. The proposed method utilized an efficient way to calculate the LMP difference between two buses by implicitly calculating the individual components using the post processed KKT optimality conditions of the NLP-OPF. This has then been extended to a general case of multiple load buses by tracing the power flow to identify how each load and the associated losses are supplied by the generators in the system. Some case studies have been presented to demonstrate the proposed method of analyzing market signals.

In Chapter 6, the software tool developed in $C^{++}$ to incorporate the market signal analyzing methods has been discussed. It has been decided to implement the OPF in

the software tool to take the advantage of re-using the matrices created in solving the OPF. This made determining the market signal together with the optimal dispatch possible, while taking advantage of re-using the same matrices.

Based on the literature survey of the available OPF solving algorithms, the SLP and the Newton method were chosen to implement the OPF. The algorithms, implementation issues, and how to include the market signal analyzing methods for the above two methods, have been discussed. A good convergence was obtained by dynamically changing the penalty factors in the Newton algorithm and efficient step length handling in the SLP algorithm. Two algorithms revealed that the Newton method has a good convergence for quadratic or any polynomial cost functions whereas the SLP method has a good convergence for bids and offers. The performance of the implemented algorithms has also been presented using various test systems.

Chapter 7 presented a case study to demonstrate the application of the components of network rental in analyzing the market signals using the developed software tool. The IEEE New-England 39 bus system has been chosen with reactive power and dynamic security related constraints modeled in the OPF. It has been shown that the components of network rental provide consumer oriented market signals, which can be considered as supplementary information, in addition to LMPs and LMP components.

## 8.2 Contributions

The main contributions of the work presented in this thesis are as follows:

- Proposed a new method to be used in market signal analysis, by determining the components of network rental. Since network rental is the overpayment made by all the consumers due to marginal losses and binding constraints, these individual components show how much each consumer has actually overpaid due to each of the above factors.

- Proposed a new reactive power model for a simultaneous dispatch of real and reactive power, considering both the capability of the synchronous generator and the fairness of reactive power supply obligation in a competitive market environment; and incorporated in the OPF.

- Incorporated the dynamic security constraint in the OPF, so that the dynamic security has been considered simultaneously with the optimal dispatch.

- Implemented a software tool written in $C^{++}$ language to incorporate the OPF and the market signal analysis methods using two OPF solution algorithms: Successive Linear Programming method and the Newton method. This enabled determining the market signals together with the OPF results.

- Demonstrated the suitability of the proposed method of components of network rental in market signal analysis using a case study.

These contributions have led to the following publications;

- L. Y. C. Amarasinghe, and U. D. Annakkage, "Determination of Network Rental Components in a Competitive Electricity Market", Accepted to be published in IEEE Transactions on Power Systems.

- L. Y. C. Amarasinghe, and U. D. Annakkage, "Analysis of Market Signals in a Competitive Electricity Market using Components of Network Rental", Submitted to the Electrical Power System Research Journal.

- L. Y. C. Amarasinghe, and U. D. Annakkage, "Analysis of Network Rental in the Competitive Electricity Market", *In proceedings of IEEE Power Engineering Society General Meeting*, Tampa, FL, USA, June 2007.

- L. Y. C. Amarasinghe, U. D. Annakkage, and R. A. S. K. Ranatunga, "A Reactive Power Model for a Simultaneous Real and Reactive Power Dispatch", *In proceedings of IEEE Power Engineering Society General Meeting*, Tampa, FL, USA, June 2007.

- U. D. Annakkage, B. Jayasekara, and L. Y. C. Amarasinghe, "Determination of an Accurate Dynamic Security Constraint with Applications in Market Dispatch", *Invited paper, In proceedings of PES Power System Conference and Exposition*, Atlanta, GA, USA, October 2006.

- L. Y. C. Amarasinghe, B. Jayasekara, and U. D. Annakkage, "The Effect of Dynamic Security Constraints on the Locational Marginal Prices", *In proceedings of IEEE Power Engineering Society General Meeting*, San Francisco, CA, USA, June 2005.

## 8.3 Suggestions for Future Research

The work presented in this thesis has focused on developing an effective software tool to determine market signals by calculating LMPs, LMP components, and network rental components, after solving the NLP-OPF. The reactive power and dynamic security constraints were incorporated in this OPF. This software tool uses two algorithms to solve the OPF: the SLP based algorithm and the Newton based algorithm.

The speed of execution and the convergence issues can be further improved to make the software tool a reliable one. Theoretically attractive methods have been proposed in the literature in achieving those objectives. Some of these techniques such as (a) incorporating sparsity techniques in matrix manipulation; (b) application of Quasi-Newton methods in the Newton algorithm; (c) improving the effective step length handling in both algorithms; and (d) combining these two algorithm at different stages of the solution process, can be incorporated to the software tool to make it a reliable one.

The availability of the OPF within the software tool allows performing computational experiments to gain further insight into the operation of the electricity market. One such analysis is to determine the associated risk due to ignoring the dynamic security of the system. In fact, the contribution in LMP due to each incorporated DSC can be separately calculated using this software tool, which in turn can be used

to determine the additional cost to ensure the dynamic security against a considered contingency. This could be then compared with the risk associated with the occurrence of that contingency which depends on the probability of the occurrence of the contingency and the cost of exposing the power system to that contingency. Thereby, a decision can be made based on quantitative information, whether or not to ignore the corresponding contingency represented by the DSC in market dispatch from the economical and reliability point of view.

Currently, in most electricity markets, the collected network rental is redistributed among the market participants through a Financial Tradable Right (FTR) auction. The FTR holder (does not necessarily have to be a consumer) has the right to receive the LMP difference between two buses for a contracted amount of real power. In fact, the proposed method determines how each consumer has actually contributed to the network rental using the general NLP-OPF. Thus, it would be interesting to look at how these proposed network rental components could be used in redistributing the collected network rental.

The reactive power model proposed in this thesis is for a synchronous generator. This model was used in the OPF for a simultaneous dispatch of real and reactive power, assuming that the synchronous generators are the only source in providing reactive power. However, in reality, there are some other reactive power sources such as synchronous condensers, capacitor banks, and static var compensators connected to different locations of the system. Thus, the effects of these reactive power sources have to be incorporated in the OPF for an economical utilization of the reactive power, while compensating for their services.

# Appendix A

# Test Systems Data

All per-unit quantities are given with respect to a per-unit base defined by 100 MVA and 500 kV.

## A.1 IEEE 39 bus system

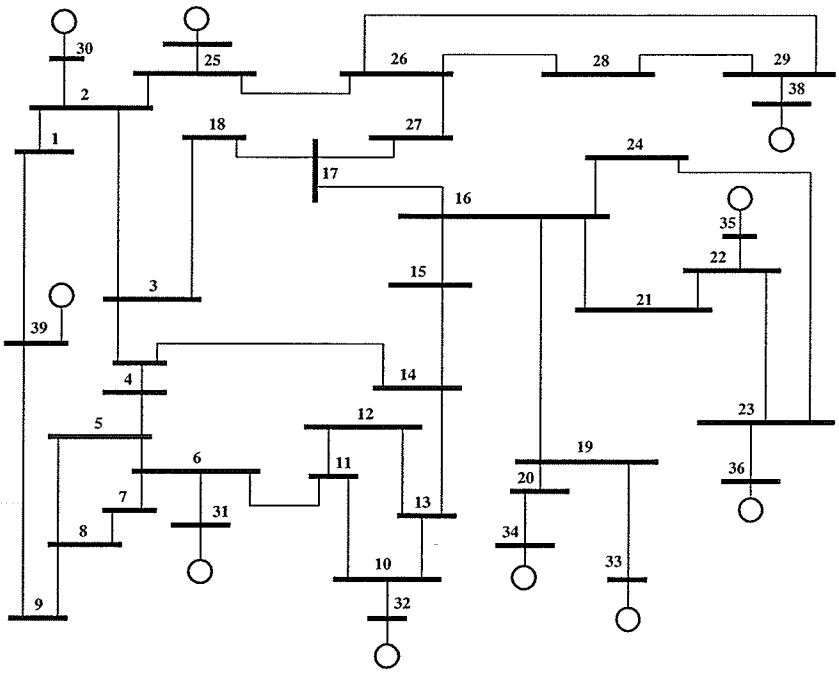


Figure A.1: Single line diagram of IEEE New England 39 bus system

Table A.1: Real and reactive power loads for IEEE New England 39 bus system

| $i$ | $P_{Di}$ (MW) | $Q_{Di}$ (MVAr) |
|---|---|---|
| 3 | 322.00 | 2.40 |
| 4 | 500.00 | 184.00 |
| 7 | 233.80 | 84.00 |
| 8 | 522.00 | 176.00 |
| 12 | 7.50 | 88.00 |
| 15 | 320.00 | 153.00 |
| 16 | 329.00 | 32.30 |
| 18 | 158.00 | 30.00 |
| 20 | 628.00 | 103.00 |
| 21 | 274.00 | 115.00 |
| 23 | 247.50 | 84.60 |
| 24 | 308.60 | -92.20 |
| 25 | 224.00 | 47.20 |
| 26 | 139.00 | 17.00 |
| 27 | 281.00 | 75.50 |
| 28 | 206.00 | 27.60 |
| 29 | 283.50 | 26.90 |
| 31 | 9.20 | 4.60 |
| 39 | 1104.00 | 250.00 |

Table A.2: Transmission line data for IEEE New England 39 bus system

| $i$ | $j$ | $r_{ij}$ (pu) | $x_{ij}$ (pu) | $b_{ij}$ (pu) |
|---|---|---|---|---|
| 1 | 2 | 0.00350 | 0.04110 | 0.69870 |
| 1 | 39 | 0.00100 | 0.02500 | 0.75000 |
| 2 | 3 | 0.00130 | 0.01510 | 0.25720 |
| 2 | 25 | 0.00700 | 0.00860 | 0.14600 |
| 2 | 30 | 0.00000 | 0.01810 | 0.00000 |
| 3 | 4 | 0.00130 | 0.02130 | 0.22140 |
| 3 | 18 | 0.00110 | 0.01330 | 0.21380 |
| 4 | 5 | 0.00080 | 0.01280 | 0.13420 |
| 4 | 14 | 0.00080 | 0.01290 | 0.13820 |
| 5 | 6 | 0.00020 | 0.00260 | 0.04340 |
| 5 | 8 | 0.00080 | 0.01120 | 0.14760 |

Table A.3: Transmission line data for IEEE New England 39 bus system Contd.

| $i$ | $j$ | $r_{ij}$ (pu) | $x_{ij}$ (pu) | $b_{ij}$ (pu) |
|---|---|---|---|---|
| 6 | 7 | 0.00060 | 0.00920 | 0.11300 |
| 6 | 11 | 0.00070 | 0.00820 | 0.13890 |
| 6 | 31 | 0.00000 | 0.02500 | 0.00000 |
| 7 | 8 | 0.00040 | 0.00460 | 0.07800 |
| 8 | 9 | 0.00230 | 0.03630 | 0.38040 |
| 9 | 39 | 0.00100 | 0.02500 | 1.20000 |
| 10 | 11 | 0.00040 | 0.00430 | 0.07290 |
| 10 | 13 | 0.00040 | 0.00430 | 0.07290 |
| 10 | 32 | 0.00000 | 0.02000 | 0.00000 |
| 11 | 12 | 0.00160 | 0.04350 | 0.00000 |
| 12 | 13 | 0.00160 | 0.04350 | 0.00000 |
| 13 | 14 | 0.00090 | 0.01010 | 0.17230 |
| 14 | 15 | 0.00018 | 0.02170 | 0.36600 |
| 15 | 16 | 0.00090 | 0.00940 | 0.17100 |
| 16 | 17 | 0.00070 | 0.00890 | 0.13420 |
| 16 | 19 | 0.00160 | 0.01950 | 0.30400 |
| 16 | 21 | 0.00080 | 0.01350 | 0.25480 |
| 16 | 24 | 0.00030 | 0.00590 | 0.06800 |
| 17 | 18 | 0.00070 | 0.00820 | 0.13190 |
| 17 | 27 | 0.00130 | 0.01730 | 0.32160 |
| 19 | 20 | 0.00070 | 0.01380 | 0.00000 |
| 19 | 33 | 0.00070 | 0.01420 | 0.00000 |
| 20 | 34 | 0.00090 | 0.01800 | 0.00000 |
| 21 | 22 | 0.00080 | 0.01400 | 0.25650 |
| 22 | 23 | 0.00060 | 0.00960 | 0.18460 |
| 22 | 35 | 0.00000 | 0.01430 | 0.00000 |
| 23 | 24 | 0.00220 | 0.03500 | 0.36100 |
| 23 | 36 | 0.00050 | 0.02720 | 0.00000 |
| 25 | 26 | 0.00320 | 0.03230 | 0.51300 |
| 25 | 37 | 0.00060 | 0.02320 | 0.00000 |
| 26 | 27 | 0.00140 | 0.01470 | 0.23960 |
| 26 | 28 | 0.00430 | 0.04740 | 0.78020 |
| 26 | 29 | 0.00570 | 0.06250 | 1.02900 |
| 28 | 29 | 0.00140 | 0.01510 | 0.24900 |
| 29 | 38 | 0.00080 | 0.01560 | 0.00000 |

## A.2 IEEE 30 bus system

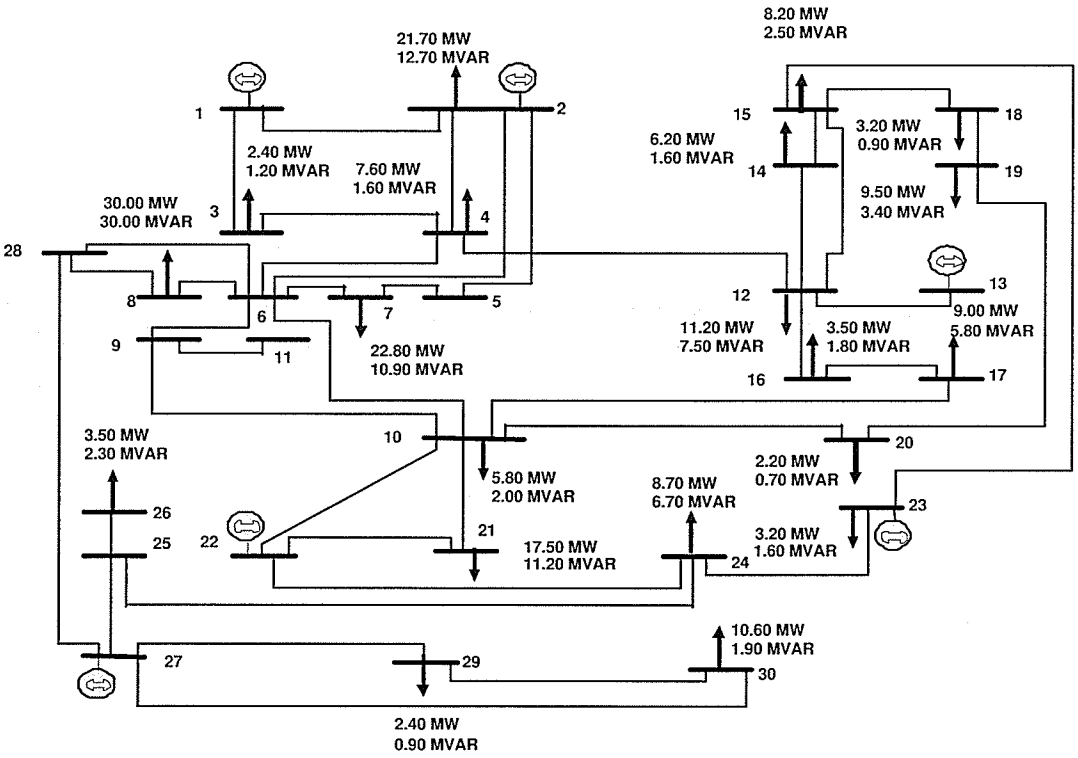


Figure A.2: Single line diagram of IEEE 30 bus system

Table A.4: Real and reactive power loads for IEEE 30 bus system

| $i$ | $P_{Di}$ (MW) | $Q_{Di}$ (MVAr) | $i$ | $P_{Di}$ (MW) | $Q_{Di}$ (MVAr) |
|---|---|---|---|---|---|
| 2 | 21.7 | 12.7 | 17 | 9.0 | 5.8 |
| 3 | 2.4 | 1.2 | 18 | 3.2 | 0.9 |
| 4 | 7.6 | 1.6 | 19 | 9.5 | 3.4 |
| 7 | 22.8 | 10.9 | 20 | 2.2 | 0.7 |
| 8 | 30.0 | 30.0 | 21 | 17.5 | 11.2 |
| 10 | 5.8 | 2.0 | 23 | 3.2 | 1.6 |
| 12 | 11.2 | 7.5 | 24 | 8.7 | 6.7 |
| 14 | 6.2 | 1.6 | 26 | 3.5 | 2.3 |
| 15 | 8.2 | 2.5 | 29 | 2.4 | 0.9 |
| 16 | 3.5 | 1.8 | 30 | 10.6 | 1.9 |

Table A.5: Transmission line data for IEEE 30 bus system

| $i$ | $j$ | $r_{ij}$ (pu) | $x_{ij}$ (pu) | $b_{ij}$ (pu) |
|---|---|---|---|---|
| 1 | 2 | 0.01920 | 0.05750 | 0.05280 |
| 1 | 3 | 0.04520 | 0.18520 | 0.04080 |
| 2 | 4 | 0.05700 | 0.17370 | 0.03680 |
| 3 | 4 | 0.01320 | 0.03790 | 0.00840 |
| 2 | 5 | 0.04720 | 0.19830 | 0.04180 |
| 2 | 6 | 0.05810 | 0.17630 | 0.03740 |
| 4 | 6 | 0.01190 | 0.04140 | 0.00900 |
| 5 | 7 | 0.04600 | 0.11600 | 0.02040 |
| 6 | 7 | 0.02670 | 0.08200 | 0.01700 |
| 6 | 8 | 0.01200 | 0.04200 | 0.00900 |
| 6 | 9 | 0.00000 | 0.20800 | 0.00000 |
| 6 | 10 | 0.00000 | 0.55600 | 0.00000 |
| 9 | 11 | 0.00000 | 0.20800 | 0.00000 |
| 9 | 10 | 0.00000 | 0.11000 | 0.00000 |
| 4 | 12 | 0.00000 | 0.25600 | 0.00000 |
| 12 | 13 | 0.00000 | 0.14000 | 0.00000 |
| 12 | 14 | 0.12310 | 0.25590 | 0.00000 |
| 12 | 15 | 0.06620 | 0.13040 | 0.00000 |
| 12 | 16 | 0.09450 | 0.19870 | 0.00000 |
| 14 | 15 | 0.22100 | 0.19970 | 0.00000 |
| 16 | 17 | 0.08240 | 0.19230 | 0.00000 |
| 15 | 18 | 0.10730 | 0.21850 | 0.00000 |
| 18 | 19 | 0.06390 | 0.12920 | 0.00000 |
| 19 | 20 | 0.03400 | 0.06800 | 0.00000 |
| 10 | 20 | 0.09360 | 0.20900 | 0.00000 |
| 10 | 17 | 0.03240 | 0.08450 | 0.00000 |
| 10 | 21 | 0.03480 | 0.07490 | 0.00000 |
| 10 | 22 | 0.07270 | 0.14990 | 0.00000 |
| 21 | 22 | 0.01160 | 0.02360 | 0.00000 |
| 15 | 23 | 0.10000 | 0.20200 | 0.00000 |
| 22 | 24 | 0.11500 | 0.17900 | 0.00000 |
| 23 | 24 | 0.13200 | 0.27000 | 0.00000 |
| 24 | 25 | 0.18850 | 0.32920 | 0.00000 |
| 25 | 26 | 0.25440 | 0.38000 | 0.00000 |
| 25 | 27 | 0.10930 | 0.20870 | 0.00000 |
| 28 | 27 | 0.00000 | 0.39600 | 0.00000 |
| 27 | 29 | 0.21980 | 0.41530 | 0.00000 |
| 27 | 30 | 0.32020 | 0.60270 | 0.00000 |
| 29 | 30 | 0.23990 | 0.45330 | 0.00000 |
| 8 | 28 | 0.06360 | 0.20000 | 0.04280 |
| 6 | 28 | 0.01690 | 0.05990 | 0.01300 |

# Appendix B

# Constrained Optimization

In this appendix, some fundamental concepts related to the constrained optimization are presented. This includes the formulation of the Optimal Power Flow (OPF) program, formulation of the Lagrange equation and the presentation of necessary conditions for optimality.

The OPF program determines the optimal generation dispatch subjected to a given set of constraints which basically represent the physical and operating capabilities of the power system [20]. Mathematically, the OPF problem can be written as,

$$\begin{aligned} \text{optimize} \quad & f(x) \\ \text{subject to} \quad & g(x) = 0 \\ & h(x) \leq 0 \end{aligned} \tag{B.1}$$

where $x$ represents the decision variables for which the OPF being solved; $f(x)$ is the objective function that being optimized; $g(x)$ are the equality constraints that include the active and reactive power balance equations at each bus; and $h(x)$ are the device limits due to the physical and operating capabilities of the power system.

This OPF can be written in the expanded form by considering that there are $N$

equality constraints, $R$ inequality constraints and $M$ decision variables, as:

$$\begin{aligned} \text{optimize} \quad & f(x) \\ \text{subject to} \quad & g_n(x) = 0 \qquad \forall n \\ & h_r(x) \leq 0 \qquad \forall r \\ & x_m \leq x_m^{max} \qquad \forall m \\ & x_m^{min} \leq x_m \qquad \forall m \end{aligned} \tag{B.2}$$

Note that for the sake of clear explanation, inequality constraints representing the lower and upper bound of a variable are explicitly shown separate from the remaining inequality constraints.

The constrained optimizing problem given in (B.2) can be written as an unconstrained optimization problem using the Lagrangian function, L [1], [21] as given in (B.3).

$$\begin{aligned} L = f(x) + \sum_{n=1}^{N} \lambda_n^T g_n(x) + \sum_{r=1}^{R} \mu_r^T h_r(x) \\ + \sum_{m=1}^{M} \gamma_m^{+T}(x_m - x_m^{max}) + \sum_{m=1}^{M} \gamma_m^{-T}(x_m^{min} - x_m) \end{aligned} \tag{B.3}$$

The elements of vector $\lambda$ are the Lagrange multipliers associated with equality constraints. The elements of vectors $\mu$, $\gamma^+$, $\gamma^-$ are the Lagrange multipliers associated with inequality constraints. These Lagrange multipliers indicate the sensitivity of the Lagrangian function to a change in the corresponding constraint.

The Karush-Kuhn-Tucker conditions or the KKT conditions are the most important theoretical results governing the necessary condition for the optimality conditions [21]. The KKT conditions for the Lagrangian equation given in (B.3) can be written as,

$$\frac{\partial L}{\partial x_m} = \frac{\partial f(x)}{\partial x_m} + \sum_{n=1}^{N} \lambda_n^T \frac{\partial g_n(x)}{\partial x_m} + \sum_{r=1}^{R} \mu_r^T \frac{\partial h_r(x)}{\partial x_r} + \gamma_m^+ - \gamma_m^- = 0; \quad m = 1, \ldots, M \tag{B.4}$$

$$\frac{\partial L}{\partial \lambda_n} = g_n(x) = 0; \qquad n = 1, \ldots, N \tag{B.5}$$

$$\lambda_n \neq 0; \qquad n = 1, \ldots, N \tag{B.6}$$

$$\mu_r h_r(x) = 0; \qquad r = 1, \ldots, R \tag{B.7}$$

$$\gamma_m^+(x_m - x_m^{max}) = 0; \qquad m = 1, \ldots, M \tag{B.8}$$

$$\gamma_m^-(x_m^{min} - x_m) = 0; \qquad m = 1, \ldots, M \tag{B.9}$$

$$\mu_r, \gamma_m^+, \gamma_m^- \geq 0 \tag{B.10}$$

The Lagrange multipliers associated with the equality constraints (i.e., $\lambda$'s) are always non-zero. Further, the multipliers associated with all inequality constraints (i.e., $\mu$'s, $\gamma^+$'s and $\gamma^-$'s) are always nonnegative (this is due to the fact that the inequality constraints in the OPF formulation in (B.1) are written as 'less than or equal' type constraints).

If a particular inequality constraint is binding at the solution, then the corresponding Lagrange multiplier is non-zero, and if the inequality constraint is non-binding at the solution, then the corresponding Lagrange multiplier is zero. Equations (B.7), (B.8) and (B.9), which are known as 'complimentary slackness conditions', ensure that the above condition is met.

The variables $x_m$'s are constrained by an upper limit and a lower limit as given in (B.2). As the upper and lower limits are different, the respective variables can't be on both limits at the same time. Therefore, at least one of the multipliers must always be zero. Hence, a single multiplier can be used to represent the shadow cost of a lower and upper bound variable.

$$\gamma_m^+ \gamma_m^- = 0 \Longrightarrow \gamma_m = \gamma_m^+ - \gamma_m^-$$

Based on the value of the shadow cost, the following conclusions can be made.

$if,$

$$\gamma_m > 0 \implies \gamma_m^+ > 0,\ \gamma_m^- = 0 \implies x_m = x_m^{max}$$

$$\gamma_m < 0 \implies \gamma_m^+ = 0,\ \gamma_m^- > 0 \implies x_m = x_m^{min}$$

$$\gamma_m = 0 \implies \gamma_m^+ = 0,\ \gamma_m^- = 0 \implies x_m^{min} < x_m < x_m^{max}$$

# Appendix C

# LMP Relationships

In this appendix, the mathematical derivation to obtain the LMP relationships is presented. For a 3 bus system, (5.72) can be written in the expanded form as,

$$\begin{bmatrix} \frac{\partial G_1(x)}{\partial V_1} & \frac{\partial G_2(x)}{\partial V_1} & \frac{\partial G_3(x)}{\partial V_1} & \frac{\partial \overline{G}_1(x)}{\partial V_1} & \frac{\partial \overline{G}_2(x)}{\partial V_1} & \frac{\partial \overline{G}_3(x)}{\partial V_1} \\ \frac{\partial G_1(x)}{\partial V_2} & \frac{\partial G_2(x)}{\partial V_2} & \frac{\partial G_3(x)}{\partial V_2} & \frac{\partial \overline{G}_1(x)}{\partial V_2} & \frac{\partial \overline{G}_2(x)}{\partial V_2} & \frac{\partial \overline{G}_3(x)}{\partial V_2} \\ \frac{\partial G_1(x)}{\partial V_3} & \frac{\partial G_2(x)}{\partial V_3} & \frac{\partial G_3(x)}{\partial V_3} & \frac{\partial \overline{G}_1(x)}{\partial V_3} & \frac{\partial \overline{G}_2(x)}{\partial V_3} & \frac{\partial \overline{G}_3(x)}{\partial V_3} \\ \frac{\partial G_1(x)}{\partial \theta_1} & \frac{\partial G_2(x)}{\partial \theta_1} & \frac{\partial G_3(x)}{\partial \theta_1} & \frac{\partial \overline{G}_1(x)}{\partial \theta_1} & \frac{\partial \overline{G}_2(x)}{\partial \theta_1} & \frac{\partial \overline{G}_3(x)}{\partial \theta_1} \\ \frac{\partial G_1(x)}{\partial \theta_2} & \frac{\partial G_2(x)}{\partial \theta_2} & \frac{\partial G_3(x)}{\partial \theta_2} & \frac{\partial \overline{G}_1(x)}{\partial \theta_2} & \frac{\partial \overline{G}_2(x)}{\partial \theta_2} & \frac{\partial \overline{G}_3(x)}{\partial \theta_2} \\ \frac{\partial G_1(x)}{\partial \theta_3} & \frac{\partial G_2(x)}{\partial \theta_3} & \frac{\partial G_3(x)}{\partial \theta_3} & \frac{\partial \overline{G}_1(x)}{\partial \theta_3} & \frac{\partial \overline{G}_2(x)}{\partial \theta_3} & \frac{\partial \overline{G}_3(x)}{\partial \theta_3} \end{bmatrix} \begin{bmatrix} \lambda_1 \\ \lambda_2 \\ \lambda_3 \\ \sigma_1 \\ \sigma_2 \\ \sigma_3 \end{bmatrix} = \begin{bmatrix} c_1 \\ c_2 \\ c_3 \\ d_1 \\ d_2 \\ d_3 \end{bmatrix}$$

If real and reactive power LMPs at bus 1 are known, then the rows corresponding to real and reactive power balance equations at bus 1 (i.e., rows 1 and 4) are deleted. To make the matrix square, columns corresponding to real and reactive power price at bus 1 (i.e., $\lambda_1$ and $\sigma_1$) are taken out as,

$$\lambda_1 \begin{bmatrix} \frac{\partial G_1(x)}{\partial V_2} \\ \frac{\partial G_1(x)}{\partial V_3} \\ \frac{\partial G_1(x)}{\partial \theta_2} \\ \frac{\partial G_1(x)}{\partial \theta_3} \end{bmatrix} + \sigma_1 \begin{bmatrix} \frac{\partial \overline{G}_1(x)}{\partial V_2} \\ \frac{\partial \overline{G}_1(x)}{\partial V_3} \\ \frac{\partial \overline{G}_1(x)}{\partial \theta_2} \\ \frac{\partial \overline{G}_1(x)}{\partial \theta_3} \end{bmatrix} + \begin{bmatrix} \frac{\partial G_2(x)}{\partial V_2} & \frac{\partial G_3(x)}{\partial V_2} & \frac{\partial \overline{G}_2(x)}{\partial V_2} & \frac{\partial \overline{G}_3(x)}{\partial V_2} \\ \frac{\partial G_2(x)}{\partial V_3} & \frac{\partial G_3(x)}{\partial V_3} & \frac{\partial \overline{G}_2(x)}{\partial V_3} & \frac{\partial \overline{G}_3(x)}{\partial V_3} \\ \frac{\partial G_2(x)}{\partial \theta_2} & \frac{\partial G_3(x)}{\partial \theta_2} & \frac{\partial \overline{G}_2(x)}{\partial \theta_2} & \frac{\partial \overline{G}_3(x)}{\partial \theta_2} \\ \frac{\partial G_2(x)}{\partial \theta_3} & \frac{\partial G_3(x)}{\partial \theta_3} & \frac{\partial \overline{G}_2(x)}{\partial \theta_3} & \frac{\partial \overline{G}_3(x)}{\partial \theta_3} \end{bmatrix} \begin{bmatrix} \lambda_2 \\ \lambda_3 \\ \sigma_2 \\ \sigma_3 \end{bmatrix} = \begin{bmatrix} c_2 \\ c_3 \\ d_2 \\ d_3 \end{bmatrix}$$

Therefore, the remaining LMPs can be expressed as,

$$\begin{bmatrix} \lambda_2 \\ \lambda_3 \\ \sigma_2 \\ \sigma_3 \end{bmatrix} = -\lambda_1.U. \begin{bmatrix} \frac{\partial G_1(x)}{\partial V_2} \\ \frac{\partial G_1(x)}{\partial V_3} \\ \frac{\partial G_1(x)}{\partial \theta_2} \\ \frac{\partial G_1(x)}{\partial \theta_3} \end{bmatrix} - \sigma_1.U. \begin{bmatrix} \frac{\partial \overline{G}_1(x)}{\partial V_2} \\ \frac{\partial \overline{G}_1(x)}{\partial V_3} \\ \frac{\partial \overline{G}_1(x)}{\partial \theta_2} \\ \frac{\partial \overline{G}_1(x)}{\partial \theta_3} \end{bmatrix} + U. \begin{bmatrix} c_2 \\ c_3 \\ d_2 \\ d_3 \end{bmatrix}$$

where,

$$U = \begin{bmatrix} \frac{\partial G_2(x)}{\partial V_2} & \frac{\partial G_3(x)}{\partial V_2} & \frac{\partial \overline{G}_2(x)}{\partial V_2} & \frac{\partial \overline{G}_3(x)}{\partial V_2} \\ \frac{\partial G_2(x)}{\partial V_3} & \frac{\partial G_3(x)}{\partial V_3} & \frac{\partial \overline{G}_2(x)}{\partial V_3} & \frac{\partial \overline{G}_3(x)}{\partial V_3} \\ \frac{\partial G_2(x)}{\partial \theta_2} & \frac{\partial G_3(x)}{\partial \theta_2} & \frac{\partial \overline{G}_2(x)}{\partial \theta_2} & \frac{\partial \overline{G}_3(x)}{\partial \theta_2} \\ \frac{\partial G_2(x)}{\partial \theta_3} & \frac{\partial G_3(x)}{\partial \theta_3} & \frac{\partial \overline{G}_2(x)}{\partial \theta_3} & \frac{\partial \overline{G}_3(x)}{\partial \theta_3} \end{bmatrix}^{-1}$$

# Appendix D

# Power Flow Tracing using Bialek Method

In this appendix, the theoretical background behind the Bialek power flow tracing method is presented.

Let $P_i^{gross}$ be the unknown gross nodal power flow through bus $i$ and $PF_{ij}^{gross}$ be the unknown gross line flow in line connected to bus $i$ and $j$, both of which would flow in lossless system that was fed with the actual generation. Consequently the gross line flows at either ends are same (i.e., $PF_{ij}^{gross} = PF_{ji}^{gross}$).

The gross power flow through bus $i$, $P_i^{gross}$ can be written as,

$$P_i^{gross} = \sum_{j \in \alpha^{in}} PF_{ij}^{gross} + P_{gi} \qquad \forall i$$

where $\alpha^{in}$ is the set of buses supplying directly to bus $i$ and $P_{gi}$ is the actual generation at bus $i$ (i.e., $\sum_k P_{ik}$). Now assuming that the transmission losses are small compared to that of line flow,

$$PF_{ij}^{gross} = PF_{ji}^{gross} = \frac{PF_{ji}^{gross}}{P_j^{gross}} P_j^{gross} \simeq \frac{PF_{ji}}{P_j}$$

This corresponds to the assumption that the distribution of gross flows at any node

is same as that of the actual flows.

$$P_i^{gross} - \sum_{j \in \alpha^{in}} \frac{PF_{ji}}{P_j} P_j^{gross} = P_{gi} \qquad \forall i$$

$$A_u P^{gross} = P_g$$

where $P^{gross}$ is the unknown vector of gross nodal flows, $P_g$ is the vector of actual nodal generation and $A_u$ is the upstream distribution matrix having $ij^{th}$ element of

$$[A_u]_{ij} = \begin{cases} 1, & \text{for } i{=}j; \\ -\frac{PF_{ji}}{P_j}, & \text{for } j \in \alpha^{in}\ ; \\ 0, & \text{otherwise.} \end{cases}$$

$$P^{gross} = A_u^{-1} P_g$$

This shows how each gross nodal power is supplied by generators in the system. Hence, the gross line flow, $PF_{ij}^{gross}$ can be calculated using the proportional sharing principle as,

$$PF_{ij}^{gross} = \frac{PF_{ij}^{gross}}{P_i^{gross}} P_i^{gross} = \frac{PF_{ij}}{P_i} \sum_t [A_u]_{it}^{-1} P_{gt}$$

This shows the contribution of generation in each gross line flows. Similarly, the gross demand at bus $i$, $P_{Di}^{gross}$ can be calculated as,

$$P_{Di}^{gross} = \frac{P_{Di}^{gross}}{P_i^{gross}} P_i^{gross} = \frac{P_{Di}}{P_i} \sum_t [A_u]_{it}^{-1} P_{gt}$$

Therefore, the losses apportioned to each load, $P^{L\_app}$ can be calculated as,

$$P^{L\_app} = P_D^{gross} - P_D$$

# Acronyms

| | |
|---|---|
| CAISO | California Independent System Operator |
| CCT | Critical Clearing Time |
| DSC | Dynamic Security Constraint |
| DSCOPF | Dynamic Security Constraint Optimal Power Flow |
| ERCOT | Electric Reliability Council of Texas |
| FERC | Federal Energy Regulatory Commission |
| FTR | Financial Tradable Right |
| IEEE | Institution of Electrical and Electronics Engineers |
| ISO | Independent System Operator |
| KKT | Karush-Khun-Tucker |
| LF | Loss Factor |
| LMP | Locational Marginal Price |
| LP | Linear Programming |
| LP-OPF | Linear Programming based Optimal Power Flow |
| LRMC | Long Run Marginal Cost |
| MCP | Market Clearing Price |
| MISO | Midwest Independent System Operator |
| NE | New England |
| NLP | Nonlinear Programming |
| NLP-OPF | Nonlinear Programming based Optimal Power Flow |
| NYISO | New-York Independent System Operator |
| OPF | Optimal Power Flow |
| PJM | Pennsylvania-New Jersey-Maryland |
| SF | Shift Factor |
| SLP | Successive Linear Programming |
| SMD | Standard Market Design |
| SRMC | Short Run Marginal Cost |

# Reference


[1] IEEE Tutorial Course, "Optimal power flow: Solution techniques, requirements, and challenges", IEEE Power Engineering Society, 1996.

[2] M. Shahidehpour, Hatim Yamin, Zuyi Li, "Market operations in electric power systems", *John Wiley and Sons, Inc, New York*, 2002.

[3] R.A.S.K. Ranatunga, U.D. Annakkage, *Optimal power dispatch in multi-node electricity markets: Electricity industry reform*, Auckland Universities Limited, 1997.

[4] William W. Hogan, *Restructuring the electricity market: Institutions for network systems*, John F. Kennedy School of Government, Harvard University, Cambridge, Massachusette, April 1999.

[5] Federal Energy Regulatory Commission, "Remedying undue discrimination through open access transmission service and standard electricity market design: Notice of proposed rulemaking", FERC, Docket No. RM01-12-000, July 1996.

[6] Federal Energy Regulatory Commission, "Commission proposes new foundation for bulk power markets with clear, standardized rules and vigilant oversight", Docket No. RM01-12-000, July 31, 2002, [online]. Available: http://www.ferc.gov/news/news-releases/2002/2002-3/july31-02smdx.pdf.

[7] Federal Energy Regulatory Commission, "State of the markets report - 2004", June 2005.

[8] F.C. Schweppe, M.C. Caramanis, R.D. Tabors, R. Bohn, "Spot pricing of electricity", *Kluwer Academic Publishers, Boston, MA*, 1988.

[9] Enrique Castillo, Antonio Conejo, Pablo Pedregal, Ricardo Garcia, Natalia Alguacil, "Building and solving mathematical programming models in engineering and science", *John Wiley and Sons, Inc, New York*, 2002.

[10] Eugene Litvinov, Tongxin Zheng, Gary Rosenwald, Payman Shamsollahi, "Marginal loss modelling in LMP calculation", *IEEE Transactions on Power Systems*, Vol. 19, No. 2, pp. 880-888, May 2004.

[11] T. Alvy, D. Goodwin, X. Ma, Streiffert, D. Sun, "A security constraint bid clearing system for the New Zealand wholesale electricity marlet", *IEEE Transactions on Power Systems*, Vol. 13, No. 2, May 1998.

[12] Andrew L. Ott, "Experience with PJM market operations, system design and implementation", *IEEE Transactions on Power Systems*, Vol. 18, No. 2, pp. 528-534, May 2003.

[13] R.A.S.K. Ranatunga, *Extensions for nodal pricing and dispatch algorithms to include ancillary services*, Ph.D Thesis, Department of Electrical and Electronics Engineering, University of Auckland, New Zealand, December 2002.

[14] D. Gan, R. J. Thomas, R. D. Zimmerman, "Stability-constrained optimal power flow", *IEEE Transactions on Power Systems*, vol. 15, pp. 535-540, May 2000.

[15] M. L. Scala, M. Trovato, C. Antonelli, "On-line dynamic preventive control: An algorithum for transient security dispatch", *IEEE Transactions on Power Systems*, vol. 13, pp. 601-610, May 1998.

[16] B. Jayasekara, U.D. Annakkage, "Derivation of an accurate polynomial representation of the transient stability boundary", *IEEE Transactions on Power Systems*, Vol. 21, No. 4, pp. 1856 - 1863, November 2006.

[17] M.I. Alomoush, S.M. Shahidehpour, "Fixed transmission rights for zonal congestion management", *IEE Proceedings-Generation, Transmission and Distribution*, Vol. 146, Issue 5, pp. 471-476, September 1999.

[18] H.Y. Yamin, K. Al-Tallaq, S.M Shahidehpour, "FERC order 2000",*Proceedings of Power Engineering 2002 Large Engineering Systems Conference - LESCOPE 02*, pp. 13 - 17, 26-28 June 2002.

[19] P.S. Li, "Experience with electric industry deregulation in North America: a system operator's perspective", *International Conference on Advances in Power System Control, Operation and Management, 2000. APSCOM-00*, pp. 41 - 48, November 2000.

[20] S.A. Soman, S.A. Khaparde, Shubha Pandit, "Computational methods for large sparce power systems analysis", *Kluwer Academic Publishers, Boston, MA*, 2002.

[21] Narayan S Rau, "Optimization principles", *John Wiley Sons Inc.*, 2003.

[22] Youfei Liu, Felix F. Wu, "Generator strategic bidding in electricity markets", *IEEE Transactions on Automatic Control*, Vol. 52, No. 6, pp. 11143-1149, June 2007.

[23] Vasileios P. Gountis, Anastasios G. Bakirtzis, "Bidding strategies for electricity producers in a competitive electricity marketplace", *IEEE Transactions on Power Systems*, Vol. 19, No. 4, pp. 356-365, February 2004.

[24] J. Lima, "Allocation of transmission fixed charges; an overview", *IEEE Transactions on Power Systems*, Vol. 9, No. 3, pp. 1409-1418, 1996.

[25] Yong Fu, Zuyi Li, "Different models and properties on LMP calculations", *IEEE Power Engineering Society, General Meeting*, June 2006.

[26] US-Canada power system outage task force, *Final report on the August 14,2003 blackout in the United States and Canada: Causes and recomandations*, April 2004.

[27] W. Hogan, Markets in real electric networks require reactive prices, *The Energy Journal*, 14(3), pp.171-200, 1993.

[28] M.L. Baughman , S.N. Siddiqi, J.W. Zarnikau, "Advanced pricing in electrical systems Part I: Theory", *IEEE Transactions on Power Systems*, vol 12, no 1, pp. 489 - 495, February 1997.

[29] M.L. Baughman, S.N. Siddiqi, J.W. Zarnikau, "Advanced pricing in electrical systems Part II: Implications", *IEEE Transactions on Power Systems*, vol 12, no 1, pp. 496 - 502, February 1997.

[30] B.J. Ring, "Dispatch based pricing in decentralised power systems", Ph.D Thesis, Department of Management,University of Canterbury, New Zealand, 1995.

[31] Andrew Ward, "The behaviour of reactive power marginal prices in an electricity spot market", Masters Thesis, University of Canterbury, New Zealand, 1995.

[32] M.L. Baughman, S.N. Siddiqi, "Real time pricing of reactive power: Theory and case study results", *IEEE Transactions on Power Systems*, pp. 23-29, 1991.

[33] E. Kahn, R. Baldick, Reactive power is a cheap constraint *The Energy Journal*, pp. 191-201, 1994.

[34] FERC Staff Report, *Principles for efficient and reliable reactive power supply and consumption*, Docket No. AD05-1-000, February 2005.

[35] New York Independent System Operator Corporation, *Ancillary service manual*, 1999.

[36] PJM Interconnection, *PJM open access transmission tariff: schedule 2*, February 2002.

[37] California Independent System Operator Corporation, *Ancillary services requirement protocol*, FERC Electricity Tariff, October 2000.

[38] The national Grid Company, *Ancillary services - An introduction*, 1995.

[39] National Electricity Market Management Company, *Ntional electricity market ancillary services*, November 1999.

[40] A.G. Ward, C.P. Arnold, N.R. Watson, "Reactive power generation costs and their effect on real and reactive power spot prices", *Proc. International Power Engineering Conference*, pp. 264-269, May 1999.

[41] Jin Zhong, Kankar Bhattacharya, "Toward a competitive market for reactive power", *IEEE Transactions on Power Systems*, vol. 17, no. 4, pp. 1206 - 1215, November 2002.

[42] G. Chicco, G. Gross, Shu Tao, "Allocation of the reactive power support requirements in multitransaction networks (Republished)", *IEEE Transactions on Power Systems*, vol. 17, no 4, pp. 1283 - 1289, November 2002.

[43] S. Hao, A. Papalexopoulos, "Reactive power pricing and management", *IEEE Transactions on Power Systems*, vol. 12, pp. 95-104, February 1997.

[44] P. Kundur, *Power system stability and control*, McGrew-Hill, Inc, 1993.

[45] A.J. Wood, B.F. Wollenberg, "Power generation operations and control",*John Wiley and Sons, Inc, New York*, 1984.

[46] D. Gan, R. J. Thomas, R. D. Zimmerman, "Stability-constrained optimal power flow", *IEEE Trans. Power Syst.*, vol. 15, pp. 535-540, May 2000.

[47] M. L. Scala, M. Trovato, C. Antonelli, "On-line dynamic preventive control: An algorithum for transient security dispatch", *IEEE Transactions on Power Systems*, vol. 13, pp. 601-610, May 1998.

[48] J.D. McCalley, S. Wang, R.T. Treinen, A.D. Papalexopoulos, "Security boundary visualization for system operation", *IEEE Transactions on Power Systems*, vol. 12, pp. 940-947, May 1997.

[49] A. Berizzi, G. Demartini, M. Delfanti, P. Marannino, G. Rizzi, "Security constrained OPF for optimal transaction scheduling in an open access environment", *in Proc. 13th Power Systems Computational Conf.*, pp. 1214-1219, 1999.

[50] L. Chen, Y. Tada, H. Okamoto, R. Tanabe, "Optimal operation solutions of power systems with transient stability constraints", *IEEE Transactions on Circuits System I*, vol. 48, pp. 327-339, March 2001.

[51] B. Jayasekara, U.D. Annakkage, "Derivation of an accurate polynomial representation of the transient stability boundary", *IEEE Transactions on Power Systems*, vol. 21, no. 4, pp. 1856 - 1863, November 2006.

[52] B. Jayasekara, *Determination of transient stability boundary in functional form with applications in optimal power flow and security control*, Ph.D Thesis, Department of Electrical and Computer Engineering, University of Manitoba, Canada, December 2006.

[53] Xu Cheng, Thomas J. Overbye, "An energy reference bus independent LMP decomposition algorithm", *IEEE Transactions on Power Systems*, vol. 21, no. 3, pp. 1041-1049, August 2006.

[54] Luonan Chen, Hideki Suzuki, Tsunehisa Wachi, Yukihiro Shimura, "Components of nodal prices for electric power systems", *IEEE Transactions on Power Systems*, vol. 17, no. 1, pp. 41-49, February 2002.

[55] A.J. Conejo, Enrique Castillo, Roberto Minguez, Federico Milano, "Locational marginal price sensitivities", *IEEE Transactions on Power Systems*, vol. 20, no. 4, pp. 2026-2033, November 2005.

[56] Fangxing Li, Jiuping Pan, Henry Chao, "Marginal loss calculation in competitive electrical energy markets", *IEEE International Conference on Electric Utility Deregulation, Restructuring and Power Technologies*, April 2004.

[57] A.J. Conejo, M. Arroyo, N. Alguacil, A.L. Guijarro, "Transmission loss allocation: A comparison of different practical algorithms", *IEEE Transactions on Power Systems*, vol. 17, no. 3, pp. 571-576, August 2002.

[58] J. Bialek, "Tracing the flow of electricity", *IEE Procedings on Generation, transmission and Distribution*, vol. 143, no. 4, pp. 313-320, 1996.

[59] D. Kirschen, R. Allan, G. Strbac, "Contributions of individual generators to loads and flows", *IEEE Transactions on Power Systems*, vol. 2, no. 1, pp. 52-60, 1997.

[60] Francisco D. Galiana, Antonio J. Conejo, Hugo A. Gil, "Transmission network cost allocation based on equivalent bilateral exchanges", *IEEE Transactions on Power Systems*, vol. 18, no. 4, pp. 1425-1431, November 2003.

[61] Jiuping Pan, Yonael Teklu, Saifur Rahman, "Review of usage based transmission cost allocation methods under open acess", *IEEE Transactions on Power Systems*, vol. 15, no. 4, pp. 1218-1224, November 2000.

[62] GAMS Release 2.50, *A user's guide*, GAMS Development Corporation: 1998.

[63] Power World Corporation: Website, "http://www.powerworld.com/products/opf.html".

[64] ETAP Corporation: Website, "http://www.etap.com/powerstation.htm".

[65] Power Technologies Inc: Website, "http://www.shawgrp.com/PTI/software/psse/opf.cfm".

[66] David I. Sun, Bruce Ashley, Brian Brewer, Art Hughes, William Tinney, "Optimal power flow by Newton approach", *IEEE Transactions on Power Apparatus and Systems*, vol. 1, no. 2, pp. 2864-2875, 1984.

[67] J.D. Weber, "Implementation of a Newton based optimal power flow into a power system simulation environment", MSc Thesis, University of Illinois at Urbana Champaign, IL, USA, 1997.

[68] M. Huneault, F.D. Galiana, "A survey of the optimal power flow literature", *IEEE Transactions on Power Systems*, vol. 6, no. 2, pp. 762-770, 1991.

[69] R.C. Burchett, H.H. Happ and D.R. Vierath and K.A. Wirgau, "Development in optimal power flow", *IEEE Transactions on Power Systems*, vol. 101, no. 2, pp. 406-414, 1982.

[70] H.H. Happ, "Optimal power dispatch", *IEEE Transactions on Power Systems*, vol. 93, no. 1, pp. 820-830, 1974.

[71] Geraldo L. Torres, Victor H. Quintana, "Optimal power flow via interior point method: An educational tool in Matlab", *CCECE*, 1996.